Analysis of Wt1 Expression in Neural Crest Cells

Thesis submitted in accordance with the requirements of the University of Liverpool for the degree of Doctor in Philosophy

by

JOANNA MARIE ALLARDYCE

January 2012

Declaration

This thesis is the result of my own work. The material contained in this thesis has not been presented, nor is currently being presented, either wholly or in part for any other degree or qualification.

The research was carried out at the Department of
Human Anatomy and Cell Biology
University of Liverpool

For our Trevor

Acknowledgements

I would like to thank my supervisors Bettina Wilm and David Edgar. You have given me so much time, help and support over the course of this project for which I am very grateful. Bettina, I hope I haven't been too much of a pain as your very first PhD student!

Thanks also to Trish Murray and the members of the stem cell group for all your help over the years. No more days spent sat at the cryostat!

I am very lucky to have had the support from my lovely family and friends. Mum, you are amazing for putting up with me through my write up! And Brian thanks so much for letting me rant on when I've needed to and for keeping on at me to get finished!

Abstract

The neural crest is a transient collection of cell, termed neural crest cells (NCCs), which develop during neurulation at the outer extremities of the neural folds between surface ectoderm and the developing neural tube. NCCs delaminate from the crest and migrate throughout the developing embryo and differentiate into many cell types such as melanocytes, peripheral neurons, osteocytes, muscle cells and enteric neurons and glia.

With the use of a lineage tracing system (Wt1-Cre X Rosa26R mouse line) it was previously found that cells derived from Wt1-expressing cells have contributed to the post-natal enteric nervous system (ENS), indicating that Wt1 must have been expressed in progenitor cells of the ENS during embryonic development. The goal of this project was therefore to identify when and where Wt1 is expressed during this process.

Data from immunofluorescence studies revealed that Wt1 is transiently expressed in Sox10-expressing NCCs when they first begin their migration from the neural crest, at E8.5 in the mouse. Wt1 is then down-regulated in NCCs before they enter the foregut at E9.5. This data has been supported by in situ hybridisation studies, where Wt1 has been found in cells of the neural crest at the same time point (E8.5) but Wt1 mRNA was not shown to be present at any embryonic stage later than this.

In vitro investigations were carried out in order to characterise Wt1 in vagal level NCCs, as it is NCCs from this region (opposite somites 1-7) and the sacral neural crest (caudal to somite 28) which have been established as the origin of the ENS. NCCs were characterised by morphology and marker expression over a time-period of 7 days. The results from immunofluorescence experiments revealed co-expression of Wt1 and NCC markers, Sox10, up to 96 hours in culture. After this time-point it was no longer possible to detect these proteins in cultured explants. The neuronal marker βIII Tubulin was detected from 48 hours and was still found to be expressed at high levels after 96 hours when Wt1 and NCC markers had ceased to be expressed, suggesting differentiation of NCCs.

Migration assays whereby the rate of migration was determined in NCCs in culture over a period of 48 hours revealed a mean migration rate of 6μm/hour. These data are relevant for future siRNA Wt1 knock-down experiments in NCCs in vitro to investigate the effect of loss of Wt1 function on migration rates, cell morphology, and expression patterns following preliminary experiments carried out on kidney stem cells.

Abbreviation List

+/- KTS	Wt1 isoform with addition (+KTS) or omission (-KTS) of 3 amino acids: lysine, threonine, serine
µg	microgram
µl	microlitre
µm	micrometre
Amh	Müllarian inhibiting substance
ANS	autonomic nervous system
aw	abdominal wall
bHLH	basic helix-loop-helix
BSA	bovine serum albumin
cc	coelomic cavity
cDNA	complimentary DNA
CO_2	carbon dioxide
C-terminal	carboxyl-terminal
d	duodenum
da	dorsal aorta
DEPC	diethylpyrocarbonate
DMEM	Dulbecco's modified eagle medium
E	embryonic day
ECM	extra-cellular matrix
ee	embryonic endoderm
EMT	epithelial-mesenchymal transition
ENS	enteric nervous system
ET-3	endothelin-3
fb	forelimb bud
FCS	foetal calf serum
fg	foregut
g	gonad
GDNF	glial-derived neurotrophic factor
GFRα	GDNF receptor alpha
gl	developing nephron
gr	genital ridge
h	heart
H_2O	water
H_2O_2	hydrogen peroxide
hb	hindlimb bud
HCl	hydrochloric acid
HRP	horse radish peroxidase
ic	intraembryonic coelom
IM	intermediate mesoderm
kb	kilobase
KSC	kidney stem cells
L	lumen
l	liver
LB	Luria broth
lu	lung
m	mesentery

MET	mesenchymal-epithelial transition
Mg	midgut
mg	milligram
ml	millilitre
mm	millimetre
mRNA	messenger RNA
mt	mesonephric tubules
n	notochord
NaAc	sodium acetate
NaCl	sodium chloride
NCC(s)	neural crest cell(s)
NCS	neonatal calf serum
ne	neuroepithelium
nf	neural folds
ng	neural groove
$NiCl_2$	nickel chloride
np	neural plate
nt	neural tube
N-terminal	amino-terminal
NTMT	alkaline phosphatase buffer
o	omentum
op	optic pit
ov	otic vesicle
p (11p13)	petit – position on short arm of chromosome
PBS	phosphate buffered saline
PBSMT	PBST + skimmed milk
PBST	PBS + Triton
PBT	PBS + Tween
PFA	paraformaldehyde
ps	primitive streak
s	stomach
SDS	sodium dodecyl sulfate
siRNA	small interfering RNA
so	somite
Sry	sex determining gene
SSC	sodium chloride, sodium citrate
st	septum transversum
ua	umbilical artery
Wt1/Wt1	Wilms' tumour gene/protein
YAC	yeast artificial chromosome
β	beta
β-Gal	beta-galactosidase – bacterial enzyme

Table of Contents

Chapter 1

Introduction

The following chapter will describe the background to the work I have carried out during this project looking at the expression of the Wilms' tumour gene (*Wt1*) and its unexpected detection in the developing enteric nervous system (ENS) using lineage tracing techniques. I will discuss the development of the ENS from its origin in the neural crest and specific markers that are expressed during ENS development. While these markers have important functions, they can also be used as a tool for visualising cells of the neural crest and developing ENS and so have been employed for this purpose throughout my studies. I will also discuss the multifaceted Wt1 protein, its discovery, structure and function, and will attempt to establish the link between *Wt1* and the ENS which serves as the basis for my research.

1.1 The enteric nervous system and its origin

The enteric nervous system (ENS) is unique in its ability to control gut behaviour without the direct control of the central nervous system (brain and spinal cord). It is therefore regarded as a branch of the autonomic nervous system (ANS). The ENS consists of enteric ganglia, which contain both neurons and supporting cells, known as glia. There are two major types of enteric ganglia found in different locations within the intestinal tract. These are the myenteric plexus (of Auerbach) and the submucosal plexus (of Meissner) (Furness 2006). Axons originating in these plexuses innervate all aspects of the digestive tract, controlling the processes involved in digestion, such as peristalsis and secretion of enzymes and hormones needed for the breakdown and uptake of ingested foodstuff from accessory organs such as the biliary system and the pancreas (Furness 2006).

The significance of studying the enteric nervous system (ENS) stems from congenital disorders of the intestinal tract, which occur due to malformations of the ENS. One such disorder is Hirschsprung's disease, which is found in 1 in 5000 live births. This is a congenital disorder usually restricted to the hindgut where it is characterised by an absence of enteric ganglia in this area (Whitehouse and Kernohan 1948; Amiel and Lyonnet 2001; Heanue and Pachnis 2006). The absence of enteric ganglia leads to a condition known as megacolon, which was first described by Harald Hirschsprung in 1888. Megacolon arises from the tonic contraction of the aganglionic portion of colon, which results in obstruction and distension of the more rostral bowel (Amiel and Lyonnet 2001; Heanue and Pachnis 2006). The following section describes the ENS and its development from the neural crest during embryogenesis thus serving as a foundation for my investigation into the embryonic ENS.

Development of the neural crest

The neural crest is a transient collection of cells, termed neural crest cells (NCCs), which develop during neurulation at the outer extremity of the neural folds, between the surface ectoderm and the developing neural tube (Figure 1.1). These cells undergo epithelial-mesenchymal transition (EMT), transforming from static epithelial cells into motile mesenchymal cells. After delamination NCCs migrate away from the neural crest as neural tube closure ensues (Kalcheim and Burstyn-Cohen 2005; Young, Cane et al. 2010). The NCCs migrate, originating along the entire length of the neural tube, throughout the developing embryo. NCCs from varying levels within the embryo differentiate into a vast number of cell types, including the sympathetic and parasympathetic nervous system (ANS) and

specifically the ENS. They also develop into the pigment cells of the skin, known as melanocytes (Stanchina, Baral et al. 2006) and form the craniofacial skeleton. The neural crest-derived bones of the skull vault, face and neck differ from the rest of the skeleton, which are derived from mesoderm forming from a cartilaginous model through the process of endochondrial ossification (Erlebacher, Filvaroff et al. 1995; Abzhanov, Rodda et al. 2007). Interestingly, Gans and Northcutt hypothesised that the neural crest-derived portion of the head and neck evolved to support and protect the ever increasing brain capacity found throughout the evolution of vertebrates, from primitive organisms such as lampreys to modern man and our relatively large brain (Gans and Northcutt 1983; Kalcheim and Burstyn-Cohen 2005).

The neural crest and the development of the enteric nervous system

Many different cell lineages including the ENS are derived from NCCs. In 1954, Yntema and Hammond undertook a study to determine the region of neural crest specific to the development of the ENS. They ablated specific regions along the rostro-caudal axis of neural tube in the chick embryo revealing that removal of the neural crest in the vagal region, i.e. opposite somites 1-7, lead to a complete deficiency of enteric ganglia along the whole gastrointestinal tract. The conclusion from their study was that the vagal region of the neural crest is solely responsible for ENS formation (Yntema and Hammond 1954). Interestingly, some twenty years later Le Douarin and Teillet conducted chick/quail experiments whereby they placed regional quail neural tube grafts into the corresponding region in chick embryos. Their work confirmed that vagal level neural crest does indeed contribute to ENS development. They further demonstrated that the sacral neural crest also

contributes to ENS development in the distal portion of the intestinal tract. The sacral neural crest lies caudal to somite 28 in the chick, and NCCs from this region contribute to enteric ganglia in the hindgut (Le Douarin and Teillet 1973) (Figure 1.2).

The vagal neural crest is described as the area of the dorsal neural tube laying opposite somites 1-7 of the developing embryo i.e. the site of emergence of the tenth cranial nerve, Vagus nerve (Le Douarin 2004). Although the vagal neural crest has been described as the major contributor to the formation of the ENS, and this will be discussed in detail, it is important to note that the cells emigrating from this level of the neural crest also differentiate into multiple other neural crest-derived lineages (Le Douarin 2004; Kuo and Erickson 2010). An overview can be seen in (Figure 1.3). The normal development of the embryonic heart relies on the correct migration of NCCs derived from the cardiac neural crest region around somites 1-3. This is a direct overlap with the path of the vagal neural crest (opposite somites 1-7) (Le Lievre and Le Douarin 1975; Kirby, Gale et al. 1983; Kirby, Turnage et al. 1985; Kirby and Waldo 1995; Le Douarin 2004; Kuo and Erickson 2010). The cells in this region migrate to the heart and form the aorticopulmonary septum, separating the truncus arteriosus of the developing cardiac outflow tract in to the primitive ascending aorta and the pulmonary trunk (Kirby, Gale et al. 1983). Cells from the rostral most vagal neural crest also develop into bones and musculature of the jaw and neck e.g. Hyoid bone, due to their contribution to the caudal most pharyngeal arches (Kuratani and Kirby 1991; Couly, Grapin-Botton et al. 1996; Le Douarin 2004; Rupp and Kulesa 2007; Kuo and Erickson 2010). The vagal neural crest also contributes to the dermis and

melanocytes of the skin, sensory and sympathetic ganglia, and peripheral nerves and glia (Le Lievre and Le Douarin 1975; Le Douarin 2004; Kuo and Erickson 2010). With this in mind the contribution of vagal neural crest to the ENS will now be discussed in more detail.

Several techniques have been employed to visualise neural crest cells in order to track their migratory pathways within the gastrointestinal tract. The DβH-nLacZ transgene utilises the human dopamine β-hydroxylase gene promoter to drive β-Galactosidase expression in NCCs. Dopamine β-hydroxylase was chosen due to its early expression in gastrointestinal development, before differentiation into enteric neurons (Kapur, Yost et al. 1992). Immunohistochemistry techniques were applied to studies, which aimed to show NCC migratory dynamics in mouse (Kapur, Yost et al. 1992; Young, Hearn et al. 1998). The results from these studies revealed the migratory pathways of the vagal population of NCCs were unidirectional along the rostro-caudal axis of the gastrointestinal tract (Figure 1.4). However, individual NCCs within the vagal population display unique and complicated migratory behaviours, changing both direction and speed as they move along the gut (Young, Bergner et al. 2004). NCCs were shown to enter the foregut of the mouse at E9.5. They progress along the gut mesenchyme and by E12 were found throughout the foregut and the majority of the midgut, completely colonising the caecum. At E13 the neural crest cells had migrated as far as the caudal-most one third of the hindgut and by E14.5 the entire length of the gastrointestinal tract had been colonised with NCCs (Kapur, Yost et al. 1992; Young, Hearn et al. 1998). However, these studies did not discuss the sacral neural crest contribution during ENS development.

In order to follow the migration of sacral NCCs in the mouse DβH-nLacZ embryos were once again used. At E11.5 β-Gal positive NCCs resided in a dorsal position to the hindgut (Anderson, Stewart et al. 2006). Between E12.5 and E14.5 the position of β-Gal positive NCCs had moved ventrally and NCCs were found close to the urogenital sinus (Kapur 2000) but before E14.5 NCCs were not found within the hindgut mesenchyme. By E14.5 vagal level NCCs had colonised the entire hindgut and it was at this time point that β-Gal positive sacral NCCs were shown to migrate in a caudo-rostral manner within the hindgut (Anderson, Stewart et al. 2006). Studies conducted in avian embryos used chick/quail chimeras to distinguish sacral level from vagal level NCCs (Pomeranz and Gershon 1990; Burns and Douarin 1998; Burns, Champeval et al. 2000; Burns and Le Douarin 2001). The findings from these studies revealed that sacral NCCs colonise the hindgut once vagal NCCs have arrived there. It was also discovered that ablation of the vagal neural crest did not impede sacral NCC colonisation of the hindgut, suggesting that sacral NCCs are independent of vagal NCCs and do not require the presence of vagal NCCs in order to form enteric ganglia within the hindgut. However, sacral NCCs were shown to be insufficient to colonise the entire gastrointestinal tract alone and so cannot compensate and produce a complete ENS in the absence of vagal NCCs. Therefore the ENS does not develop fully in the absence of vagal NCCs and aganglionosis occurs (Pomeranz and Gershon 1990; Burns and Douarin 1998; Burns, Champeval et al. 2000; Burns and Le Douarin 2001).

Determination of NCCs along the ENS lineage

The previous sections described the structure and function of the ENS and how the origin of ENS was experimentally established i.e. predominantly from the vagal and sacral neural crest. It is also important to discuss the determining factors which are essential for the proper development of the ENS and what happens when this complex system of signalling goes wrong or is altered.

Specific genes are expressed when the neural crest forms and as enteric neurons and glia mature. There are many different proteins encoded for by these genes such as transcription factors, growth factors and receptors. Each gene/protein has a specific function during the development of the ENS. A comprehensive list of genes and molecules expressed during ENS development can be found in table 1.1. However, they can also be utilised as tools for visualising cells histologically and are therefore useful markers when studying ENS development. Thus, several of these proteins have been used in immunofluorescence experiments in order to locate NCCs, enteric neurons and glia at specific time-points during mouse embryonic development throughout this project.

The sequence of events and associated molecular signalling mechanisms involved in ENS development have been unravelled by several labs resulting in a good general understanding of the process. A general theme running throughout the literature shows that the genes and protein expressed earliest in ENS development have the most devastating effects if they are inactivated or mutated. As mentioned previously the neural crest develops during the process of neurulation, very early on in embryonic development. In mouse the neural crest can be detected at

embryonic day (E) 8 by the expression of Sox10, a very early marker for uncommitted NCCs (Anderson, Stewart et al. 2006). Sox10 belongs to a family of transcription factors known as Sry-HMG-box (Wegner 1999; Schepers, Teasdale et al. 2002). The Sox family of proteins is subdivided into Sox A-H groups and they function by binding to DNA via the HMG (high-mobility group) domain. Sox10 is part of the SoxE group (Hong and Saint-Jeannet 2005). Development progresses rapidly and within half a day in the mouse (E8.5) NCCs have already begun their migration away from the neural crest (Anderson, Stewart et al. 2006). Important molecules expressed at this stage include Sox10, p75 and Phox2b (Young and Newgreen 2001; Anderson, Stewart et al. 2006). Deletion of Phox2b or Sox10 show the most dramatic ENS phenotypes as complete aganglionosis along the entire gastrointestinal tract is observed (Herbarth, Pingault et al. 1998; Southard-Smith, Kos et al. 1998; Kapur 1999; Pattyn, Morin et al. 1999; Young and Newgreen 2001; Anderson, Stewart et al. 2006) (Figure 1.5, A). As vagal NCCs migrate towards the foregut, where they reach the oesophagus at E9.5, in order to begin their rostro-caudal journey along the gut tube molecules are expressed in a specific sequence, ensuring the correct NCCs end up in the correct place. For example, Mash 1, a transcription factor in the bHLH family, is expressed by NCCs which form the ENS of the oesophagus (Lo, Guillemot et al. 1994; Young and Newgreen 2001; Gershon 2010). When Mash1 is knocked out aganglionosis is restricted to the oesophagus, while enteric ganglia are present throughout the rest of the gut (Lo, Guillemot et al. 1994; Young and Newgreen 2001) (Figure 1.5, B). In contrast, the vagal NCCs which will go on to innervate the gut caudal to the stomach are highly dependent on GDNF/GFRα/Ret signalling (Chalazonitis, Rothman et al. 1998; Hearn, Murphy et al. 1998; Taraviras, Marcos-Gutierrez et al.

1999; Gershon 2010). Therefore the deletion of any of these molecules produces a phenotype whereby aganglionosis occurs caudal to the stomach (Figure 1.5, C) (Schuchardt, D'Agati et al. 1994; Moore, Klein et al. 1996; Young and Newgreen 2001). NCCs migrate and form enteric plexuses readily up to the proximal colon, i.e. the caecum, if the aforementioned molecules are expressed, they arrive at the proximal colon around E11.5 in the mouse (Young and Newgreen 2001). Past this point NCCs critically require the expression of endothelin-3 (ET-3), a 21 amino acid peptide, and its G-protein-coupled seven-transmembrane endothelin-B receptor (Ednrb), in order to reach the most distal portions of the large bowel (E11.5-E14.5 in mouse) (Baynash, Hosoda et al. 1994; Hosoda, Hammer et al. 1994; Young, Hearn et al. 2000; Young and Newgreen 2001; Gershon 2010). Deletion of either ET-3 or Ednrb leads to aganglionosis of the distal-most large intestine (Figure 1.5, D) (Baynash, Hosoda et al. 1994). This is similar to the phenotype present in Hirschsprung's disease (Baynash, Hosoda et al. 1994; Gershon 2010).

1.2 Epithelial to mesenchymal transition, EMT

Epithelial to mesenchymal transition (EMT) is crucial for neural crest cell development. EMT is a process by which epithelial cells become motile by transforming into mesenchymal cells (Figure 1.6). Conversely, motile mesenchymal cells can also transform into epithelial cells. This is known as mesenchymal to epithelial transition (MET) (Figure 1.6) (Chaffer, Thompson et al. 2007). These processes are controlled by transcription factors of the Snail family (Nieto, Sargent et al. 1994). Snail transcription factors function by repressing the expression of cell adhesion molecules, which are vital in maintaining the structural integrity of epithelial cells. E-cadherin has been particularly well described as a cell adhesion molecule controlled by Snail transcription factors, such as Slug, in the process of all EMTs (Cano, Perez-Moreno et al. 2000). In the following part I will delineate why EMT is considered on of the most important processes throughout embryonic development (Hay 1995).

The earliest role for EMT is during gastrulation when the primitive streak is formed (Duband, Monier et al. 1995; Murray and Gridley 2006; Chaffer, Thompson et al. 2007; Hugo, Ackland et al. 2007). As mentioned above, EMT is also essential for neural crest development (Figure 1.1). Neural crest cells originate as part of the neural plate, which is epithelial in structure. In order to be able to migrate as extensively as NCCs are known to do, they have to lose their epithelial properties and become motile mesenchymal cells. Immediately after delamination, NCC-derived cells migrate away from the dorsal neural tube (Duband, Monier et al. 1995; Sakai and Wakamatsu 2005).

EMT and/or MET occur in various tissues during development of the mammalian embryo, including the kidneys and mesothelium. Interestingly, the Wilms' tumour gene (*Wt1*) is expressed in both tissues/organs. Therefore, it has been proposed that Wt1 actively plays a role in EMT and MET processes (Pritchard-Jones, Fleming et al. 1990; Armstrong, Pritchard-Jones et al. 1993; Moore, McInnes et al. 1999; Carmona, Gonzalez-Iriarte et al. 2001; Wilm, Ipenberg et al. 2005; Martinez-Estrada, Lettice et al. 2010).

MET is an important process in kidney formation, which involves the two main tissues of the developing kidney, the ureteric bud and the metanephric mesenchyme. When the ureteric bud invades the metanephric mesenchyme, which expresses Wt1, the mesenchymal cells to undergo MET as a consequence. The resulting metanephric mesenchyme-derives cells then form epithelial structures which give rise to the nephrons (Figure 1.7) (Vainio and Lin 2002; Chaffer, Thompson et al. 2007).

The mesothelium expresses Wt1 and is also known to undergo EMT. The mesothelium consists of mesothelial cells which form an epithelial monolayer that gives a covering to the body cavities of mammals. There are three cavities in the developing embryo and these divide the mesothelium into three specific parts. The peritoneum surrounds the abdominal cavity and the organs housed within it. The pericardium surrounds the heart and mediastinum. The pleura lines the lungs and the thoracic cavity. These serosal mesothelial coverings provide protection and allow movement of organs against one another without friction (Mutsaers 2002; Mutsaers 2004). Investigation into coronary blood vessel development had shown

that mesothelial cells from an area of the septum transversum, the proepicardium, migrate to the heart and undergo EMT, subsequently differentiating into coronary blood vessels (Mikawa and Gourdie 1996; Dettman, Denetclaw et al. 1998). A similar phenomenon occurs during development of the gut and lung vasculature, whereby mesothelial cells of the peritoneum undergo EMT and contribute to the smooth muscle component of these vessels (Wilm, Ipenberg et al. 2005; Que, Wilm et al. 2008). In order to identify the role of the serosal mesothelium in the development of intestinal vasculature, the Cre-LoxP system was employed. Specifically, a transgenic mouse line was used in which Cre recombinase was placed under control of the human *Wt1* promoter, to study the lineage of embryonic mesothelial cells which express Wt1 protein (Wilm, Ipenberg et al. 2005). Cells marked by Cre activity were found in the vascular smooth muscle of the intestine, the heart and the lungs (Wilm, Ipenberg et al. 2005; Que, Wilm et al. 2008). However, unexpectedly, marked cells were also discovered in the ENS along the intestinal tract of adult mice (Figure 1.8) (Wilm, Ipenberg et al. 2005). This was a novel finding since the ENS has never before been described as developing from Wt1-expressing cells and Wt1 is not expressed in the ENS of adult mice. In the adult Wt1 is restricted to podocytes of the kidney and the mesothelium (Rivera and Haber 2005; Wilm, Ipenberg et al. 2005).

1.3 Wilms' tumour gene, *Wt1*

Wt1 encodes a four C-terminal Cys_2-His_2 zinc fingered protein with a proline/glutamine rich N-terminal (Call, Glaser et al. 1990; Gessler, Poustka et al. 1990) (Figure 1.9). The structure of the protein encoded for by *Wt1*, and its localisation in the nucleus indicated that Wt1 protein functions as a transcription

factor (Rauscher, Morris et al. 1990; Morris, Madden et al. 1991; Pelletier, Schalling et al. 1991; Bickmore, Oghene et al. 1992). However, it has since been discovered that Wt1 is also expressed in the cytoplasm (Niksic, Slight et al. 2004). Staining observed using immunohistological techniques had at first been disregarded as an artefact (Hohenstein and Hastie 2006) but *Wt1* has since been shown to actively shuttle between the nucleus and cytoplasm (Niksic, Slight et al. 2004). Further work into cytoplasmic *Wt1* revealed an interaction with actin (Jomgeow, Oji et al. 2006). Actin is part of the cell cytoskeleton and is vital for cell movement (Dudnakova, Spraggon et al. 2010). The results from these investigations suggest there is also a role for Wt1 in the cytoplasm. Although further investigation is needed in order to confirm the role of cytoplasmic *Wt1*, the data suggests that *Wt1* could be an adaptor protein which aids in the transport of actin mRNA to its target area (Dudnakova, Spraggon et al. 2010). *Wt1* has 10 exons and has been found to have many different isoforms. The resulting isoforms are the result of alternative splicing, alternative start sites and RNA editing events (Hohenstein and Hastie 2006). Alternative slicing and its significance for Wt1 function will be discussed in subsequent sections.

The discovery of *Wt1*

Wt1 was discovered by examining the genetic properties of Wilms' tumour (Call, Glaser et al. 1990). Wilms' tumour, also known as nephroblastoma, is a malignant tumour found in the neonatal kidney. Wilms' tumours arise due to a continuing presence of renal stem cells, which remain in a proliferative state instead of either becoming terminally differentiating thus ceasing to divide, or dying (Hastie 1994). The incidence of this tumour is around 1 in 10,000 children (Matsunaga 1981). A

deletion in chromosome 11 on the short arm at position p13 (11p13) demonstrated a genetic predisposition to the development of Wilms' tumour (Riccardi, Sujansky et al. 1978; Francke, Holmes et al. 1979). A proportion of children with Wilms' tumours also suffered from other problems, including aniridia, an abnormality found in the eye, genitourinary irregularities, particularly pseudohermaphroditism in males, and mental retardation. Due to these corresponding conditions resulting from mutations at 11p13, it was termed WAGR syndrome (Wilms' tumour, Aniridia, Genitourinary abnormalities, mental Retardation) (Francke, Holmes et al. 1979; Hastie 1994). By cloning a sequence of cDNA located at chromosome 11p13 both Call and Gessler were able to delineate one candidate gene likely to be responsible for the development of Wilms' tumour. This was the Wilms' tumour gene, *Wt1* (Call, Glaser et al. 1990; Gessler, Poustka et al. 1990). The following section describes the published *Wt1* expression pattern and function during development.

Expression pattern of *Wt1* in embryonic development

Following the discovery of the Wilms' tumour gene, *Wt1*, work began to establish an animal model that could be used in the study of Wilms' tumour, associated disorders, and *Wt1* function. The expression pattern of *Wt1* was initially investigated using in situ hybridisation. Within a few years of its discovery quite a comprehensive catalogue of tissues expressing *Wt1* had been assembled. Early work using Northern blot analysis and in situ hybridisation showed Wt1 expression in the foetal kidney, the stromal cells and splenic capsule of the spleen, gonads (primitive testis and ovaries), and foetal brain of the mouse (Pritchard-Jones, Fleming et al. 1990; Park, Schalling et al. 1993). Pritchard-Jones also reported the

expression of Wt1 in the developing human kidney. In situ hybridisation data on 18 week human embryonic kidney showed human WT1 expression becoming more restricted as development progressed. The results revealed weak expression in the early condensing mesenchyme, stronger expression in the renal vesicle, and restriction to podocytes in the maturing glomeruli, where it remains into adulthood (Figure 1.6) (Pritchard-Jones, Fleming et al. 1990). Expression of Wt1 in the developing genitourinary system was found to become specified to the granulosa cells of the ovaries, the sertoli cells of the testis, and the myometrium of the uterus (Pelletier, Schalling et al. 1991). Armstrong and colleagues made a comprehensive investigation using in situ hybridisation. The results revealed *Wt1* expression in all the tissues listed above but also additional tissues including the mesothelial cells covering the coelomic cavity, particularly in the region of the heart and gut, the spinal cord, roof of the fourth ventricle and body wall musculature. RNA-PCR at E12.5 showed low levels of *Wt1* in the eye and tongue. They also reported that *Wt1* is not expressed prior to E9.0 in the mouse (Armstrong, Pritchard-Jones et al. 1993). Since these findings in the early nineties several other regions have also been found to express *Wt1*. In 1998 with the use of a LacZ reporter gene inserted into exon 1 of the *Wt1* locus using yeast artificial chromosomes (YACs), *Wt1* was found to be expressed in the septum transversum, which is the primitive diaphragm (Moore, Schedl et al. 1998). Although the expression of *Wt1* has been investigated in depth, these analyses could not elucidate its specific function within these tissues. Further investigations were needed in order to determine the role for Wt1 in development.

The function of *Wt1* in the developing embryo

In order to determine a function for *Wt1* Kreidberg and colleagues in 1993 used a targeted mutation of the *Wt1* gene. Their targeting strategy deleted the first exon of *Wt1* and an upstream sequence of 0.5kb. Mice heterozygous for the mutated *Wt1* did not appear to have any developmental problems. At the age of 10 months the mice had not developed any tumours. In contrast, the death of homozygous mutant mice occurred between E13 and E15. No kidney developed in the mutants due to induction failure of the metanephric mesenchyme, and there was no ureteric bud (Figure 1.7). The conclusion drawn from the resulting lack of kidneys was that *Wt1* must play a critical role in kidney development from an early stage. However, they also noted that kidney agenesis was not a valid reason for embryonic lethality at E13 to E15. This lead to investigations into finding other tissues affected in the mutant. There was immense oedema throughout the embryo from E12 due to haemodynamic problems. Examination of the mutant heart found it to be significantly smaller than that of wild-type embryo. Mutants had a smaller left ventricle, which was dilated and had a very thin muscular wall. The functional quality of the mutant heart was not tested but from its structure, oedema and circulatory problems, it was assumed that death occurred due to the abnormal development of the heart. Other phenotypes noted in mutants were abnormal formation of the septum transversum, which lead to the thoracic contents herniating into the abdominal cavity, a reduction in size of the lungs as well as incomplete development of the mesothelial lining, the pleura (Kreidberg, Sariola et al. 1993). As mesothelial cells have been reported to undergo EMT and renal tissue undergoes MET during development, it was put forward that Wt1 plays a role in

these processes (Armstrong, Pritchard-Jones et al. 1993; Kreidberg, Sariola et al. 1993).

Wt1 as a tumour suppressor gene and a potential oncogene

Wt1 was first identified as a tumour suppressor gene due to mutations detected in the *Wt1* gene that lead to an inactive form of Wt1 protein (Coppes, Campbell et al. 1993). Mutations in the *Wt1* gene account for 10% of sporadic Wilms' tumours (Park, Schalling et al. 1993). Wilms' tumours correspond to the Knudson two-hit statistical model which states that two mutational events must happen in order for tumorigenesis to occur (Knudson 1971). One mutation is inherited and the other occurs randomly in somatic cells. This model was first described after investigation into retinoblastoma, a malignancy of the eye (Knudson 1971). It was then found that Wilms' tumour development follows the two-hit model (Knudson and Strong 1972). *Wt1* was, therefore, considered a tumour suppressor gene suppressing the transcription of genes by binding to DNA via the proline/glutamine rich region of the Wt1 protein (Figure 1.9) (Rauscher 1993; Hastie 1994) and promoting apoptosis and suppressing growth signals (Essafi and Hastie 2010). Over expression of *Wt1* in a Wilms' tumour cell line (RM1) revealed tumour cell growth was suppressed in vitro (Haber, Park et al. 1993). This finding further indicated a role for Wt1 in tumour suppression. However, a mutated version of *Wt1* where zinc finger 3 is missing was thought to be associated with a known oncogene (*EIA*) and so it was concluded that *Wt1* may also function as an oncogene causing the development of tumours (Haber, Timmers et al. 1992). *Wt1* expression has since been detected in several adult tumours such as breast (Loeb, Evron et al. 2001), colorectal (Koesters, Linnebacher et al. 2004) and leukemic

(Algar, Khromykh et al. 1996; Sugiyama 2005). Treatments for such tumours have shown inhibition of tumour growth when Wt1 is knocked down with the use of Wt1 antisense oligomers and Wt1-specific siRNA (Algar, Khromykh et al. 1996; Sugiyama 2005; Tatsumi, Oji et al. 2008). *Wt1* has been shown to regulate oncogenes by activation as well as repression. Further work is needed in order to understand the process by which *Wt1* functions in activation and repression of tumorigenesis.

Wt1 and MET/EMT

Wt1 had long been hypothesised as having a function in the process of EMT and MET. Investigations were carried out in order in attempt to prove this. One such study employed an in vitro system where kidneys were removed from E11 mouse embryos and placed into culture. The kidney cultures were subjected to small interfering RNAs (siRNAs) in order to investigate *Wt1* function in nephron differentiation (Davies, Ladomery et al. 2004). SiRNA is a technique for 'silencing' a particular gene by means of RNA interference (Elbashir, Harborth et al. 2001; Harborth, Elbashir et al. 2001). Knocking down *Wt1* in kidney cultures resulted in nephrogenic failure. Nephrogenesis relies on the process of MET, whereby metanephric mesenchymal cells are transformed into epithelial nephron precursors. Therefore they concluded that Wt1 is required for the onset of MET in kidney development (Davies, Ladomery et al. 2004; Hohenstein and Hastie 2006).

Alternative splicing of the *Wt1* gene

Alternative splicing allows many different proteins to be generated from a single gene. This occurs by splicing together different parts of exons, creating different

types of mRNA and therefore different protein isoforms are produced. There are several alternative splicing sites on the *Wt1* gene (Hammes, Guo et al. 2001). Two are characterised by the absence or presence of a number of amino acids at these specified sites (Figure 1.9). An alternative splicing domain can be found at exon 5. Exon 5 consists of 17 amino acids and is either present or missing to form two Wt1 isoforms (Hohenstein and Hastie 2006). A second alternative splice site is found between exons 1 and 2 (Dallosso, Hancock et al. 2004). The testis were found to express a smaller Wt1 transcript as well as the original transcript (Pritchard-Jones, Fleming et al. 1990). This finding led to further investigations aiming to locate more alternative splicing domains (Dallosso, Hancock et al. 2004). A truncated version of Wt1 was found and was named AWT1, where alternative splicing was shown to take place at the N-terminal of Wt1 and produced an alternative exon 1. The function of AWT1 is yet to be determined. However, AWT1 has been shown to be confined to the paternal allele (Dallosso, Hancock et al. 2004). There is also an alternative splicing domain which is characterised by the absence or presence of only three amino acids (lysine, threonine and serine) between the third and fourth zinc fingers at exon 9 (Schedl, Larin et al. 1993). This amino acid complex is referred to as KTS. There are two isoforms produced and these are Wt1 +KTS and Wt1 –KTS (Hohenstein and Hastie 2006).

Examples of roles for *Wt1* splice variants

The +KTS and –KTS isoforms of *Wt1* have been conserved in all vertebrates (Hastie 2001; Hohenstein and Hastie 2006) and have, therefore, been the subject of intense study. Gene targeting techniques have allowed the deletion of these specific isoforms in order to determine what role they play in development. Mouse

mutants have been generated, which contain the Wt1 +KTS or Wt1 –KTS isoform exclusively (Hammes, Guo et al. 2001). Both mutants were found to die shortly after they were born due to defects in the kidney, which included haemorrhaging of the kidney and an empty bladder indicting a deficiency in glomerular filtration (Hammes, Guo et al. 2001). Although the outcome of both was death in both the +KTS and –KTS *Wt1* isoform mutants, the phenotypes produced due to the deletion of each of the isoforms was distinct, which suggested they each have a distinct function. +KTS mutants revealed massively reduced levels of the Y-chromosome specific sex determination gene *Sry* and an absence of foot-like processes found in the podocytes of the kidney. These findings indicated the +KTS isoform of *Wt1* was essential for *Sry* expression, which is required for the initiation of testis development in the male (Gubbay, Collignon et al. 1990; Sinclair, Berta et al. 1990; Hammes, Guo et al. 2001). The findings also suggested an important role for the +KTS isoform in the development and maintenance of podocyte structure (Hammes, Guo et al. 2001). The –KTS mutants demonstrated a decrease in size of the kidneys and the gonads. Analysis of this phenotype revealed an increase in apoptosis in cells at the urogenital ridge, which resulted in the failure of proper development of the kidney and gonad. These findings suggested that the –KTS isoform of *Wt1* is crucial for the survival of urogenital progenitors (Hammes, Guo et al. 2001).

Wt1 in sex determination

Sox9 is a member of the Sry-HMG-box group of transcription factors, along with Sox10 (Hong and Saint-Jeannet 2005). Sox10 is a NCC marker for developing ENS precursors and Sox9 is also expressed in the neural crest (Hong and Saint-

Jeannet 2005). Sox10 functions in the neural crest-derived ENS and melanocytes (Hong and Saint-Jeannet 2005). This was shown using Sox10 mutant mice, which had aganglionosis of the gastrointestinal tract (Herbarth, Pingault et al. 1998; Southard-Smith, Kos et al. 1998). Sox9 does not function in the developing ENS but has been shown to have an important role in neural crest-derived chondrocytes, which go on to from parts of the skeletal system (Kent, Wheatley et al. 1996). Sox9 mutants show skeletal malformations and sex reversal. This is analogous to the human condition campomelic dyplasia, which occurs due to a mutation at the Sox9 locus (Foster, Dominguez-Steglich et al. 1994; Wagner, Wirth et al. 1994; Hong and Saint-Jeannet 2005). This suggested that Sox9, like Sry, plays a role in sex determination and bone differentiation.

Sex determination arises via the testis-determining gene, which is specific to the Y-chromosome. It was discovered during genetic analysis of patients presenting with sex reversal. This testis- determining gene was termed the *Sry* gene (Gubbay, Collignon et al. 1990; Sinclair, Berta et al. 1990). The *Sry* gene has been found to be critical for sex determination as expression of *Sry* was shown to lead to testis development even in XX genotypes (females) (Koopman, Gubbay et al. 1991). Sox9 mRNA and protein were shown to be expressed in the gonad of the developing mouse (Kent, Wheatley et al. 1996). Sox9 was found to be testis-specific and up-regulated in the developing gonads of the mouse a short time after the expression of the *Sry* gene had been activated (Kanai, Hiramatsu et al. 2005). These studies suggested Sox9 played a role in the sex determination of the male and not the female phenotype, and it was thought that Sox9 could be activated by *Sry* up-regulation (Kent, Wheatley et al. 1996). A Sox9 conditional null mouse was

generated employing the Flox/Cre-LoxP system (Akiyama, Chaboissier et al. 2002; Kist, Schrewe et al. 2002). The Sox9 null mutant was found to develop gonads. However, embryonic death occurred around E11.5 due to defects in the development of the cardiovascular system (Akiyama, Chaboissier et al. 2002; Kist, Schrewe et al. 2002; Kobayashi, Chang et al. 2005). Due to the early lethality of the Sox9 null mutant embryos at E11.5 the genital ridge was dissected and cultured in an in vitro system for 2-3 days to attempt to determine how they developed. This investigation revealed that testicular cords did not develop in Sox9 null mutants. It was also found that markers for Sertoli cells, such as *Amh* (müllarian inhibiting substance) were not expressed (Kobayashi, Chang et al. 2005). It was concluded from the examination of in vitro cultures that Sox9 is vital for the development of the testis (Kobayashi, Chang et al. 2005).

It has also been shown that Wt1 is related to sex determination and is involved in modulation of *Amh* (Nachtigal, Hirokawa et al. 1998). Wt1 is well documented as being expressed in the developing gonad and sertoli cells of the adult testis (Armstrong, Pritchard-Jones et al. 1993; Kreidberg, Sariola et al. 1993). An investigation was carried out to determine if Wt1 had an effect on Sox9 expression and therefore sex determination. This was achieved by ablating Wt1 in Sertoli cells, in the adult, by using a Wt1 conditional knockout mouse. The Sertoli cell specific knockout was generated by crossing a $Wt1^{flox}$ mouse, which contained a *Wt1* conditional knockout allele, with an *Amh*-Cre mouse. The results of these studies revealed Sox9 was down-regulated in the mutant sertoli cells. These findings suggested Wt1 is required for maintenance of Sox9 expression in sertoli cells (Gao, Maiti et al. 2006). A conserved region 5' of Sox9 has been found,

including a putative Wt1-binding site (Bagheri-Fam, Ferraz et al. 2001). This finding is in support of the idea that Wt1 has a direct involvement in Sox9 expression (Bagheri-Fam, Ferraz et al. 2001; Gao, Maiti et al. 2006).

Lineage tracing of *Wt1*

The Wt1-CreRosa26 reporter mouse was the product of mating Wt1-Cre transgenic mice with the Rosa26 reporter mouse strain (Wilm, Ipenberg et al. 2005) (Figure 1.10). This involved the Cre-LoxP system, which is a way of manipulating DNA and developing mouse strains when looking at gene function or ablation (Rajewsky, Gu et al. 1996; Soriano 1999). A Cre-recombinase enzyme recognises the 34bp sequence of LoxP (Hoess, Ziese et al. 1982; Argos, Landy et al. 1986; Rajewsky, Gu et al. 1996). By using LoxP sites to flank a sequence of DNA the Cre-recombinase can excise that particular sequence. This means genes can be replaced or deleted, or signal sequences removed in order to activate gene expression (Rajewsky, Gu et al. 1996). In the Wt1-Cre mouse line a Cre-recombinase was placed under the control of the human WT1 promoter. This was achieved by using yeast artificial chromosomes (YACs) because they are easy to manipulate (Schedl, Larin et al. 1993; Moore, Schedl et al. 1998; Wilm, Ipenberg et al. 2005). The Rosa26 reporter mouse strain was developed in order to examine Cre-expression. A LacZ gene was placed under the control of the Rosa26 promoter, along with LoxP sites, which flanked a STOP cassette. Rosa26 is ubiquitously expressed (Soriano 1999). When the two mouse strains, Wt1-Cre and Rosa26R, were crossed the Cre-recombinase would excise the STOP cassette. Following recombination, LacZ would be expressed in any cells that were either expressing Wt1 or were derived from Wt1-expressing cells. Therefore, the fate of

Wt1-expressing cells could be followed and when stained for LacZ these cells could be visualised with a blue precipitate (X-Gal staining) (Figure 1.8). LacZ staining, using this system has been shown in many tissues and structures where Wt1 has been reported to be expressed or play a role in their development. Such structures include mesothelial cells and the vascular smooth muscle component of heart, lung and gut musculature (Wilm, Ipenberg et al. 2005; Que, Wilm et al. 2008). LacZ staining has also been demonstrated in the adrenal gland, epicardium, diaphragm, and kidney (Moore, Schedl et al. 1998; Moore, McInnes et al. 1999). As well as the aforementioned tissues LacZ staining was also detected in cells in the region of the ENS of the adult mouse gut (Figure 1.8) (Wilm, Ipenberg et al. 2005) In order to confirm LacZ staining was present in the ENS immunofluorescence co-staining was carried out in newborn Wt1-CreRosa26R mice for the pan-neuronal marker Hu and β-Galactosidase (Figure 1.11). The results revealed β-Galactosidase and Hu co-localised in around half of the enteric neurons (Figure 1.11) (Wilm, unpublished).

1.4 Aims of the project

Therefore, this project aimed to establish the time-point at which *Wt1* was expressed in the developing ENS, since LacZ expression in the adult ENS and β-Galactosidase expression in the newborn ENS of the Wt1-Cre mouse line had been previously and unexpectedly observed (Figure 1.8 and Figure 1.11) (Wilm, Ipenberg et al. 2005). However extensive investigation into the expression pattern of Wt1 has shown that it is not expressed in the ENS of the post-natal mouse as expression becomes highly restricted and is only found in the podocytes of the kidney glomerulus and the mesothelium (Rivera and Haber 2005); (Wilm, Ipenberg et al. 2005). Thus I aim to systematically examine embryonic development of the ENS employing immunohistochemical and in situ hybridisation techniques in order to determine when Wt1 was expressed to explain the results of the lineage tracing experiments.

The establishment of this time point is essential for the experiments described in the second part of this thesis designed to investigate the hypothesis that Wt1 has a function(s) in the developing ENS. I therefore aim to characterise the behaviour of vagal level NCCs in vitro. I also aim to set up a siRNA gene knock down system in kidney stem cells, which once optimised in the future could be adapted for use on NCCs. This will be important in future projects aiming to elucidate the function for Wt1 in NCCs.

The questions that need addressing are:

- Is Wt1 expressed in the developing ENS?
- At what time-point is Wt1 expressed in the developing ENS?
- How do NCCs behave in vitro?
- With the use of siRNA can Wt1 be knocked down in kidney stem cells for eventual use on NCCs?

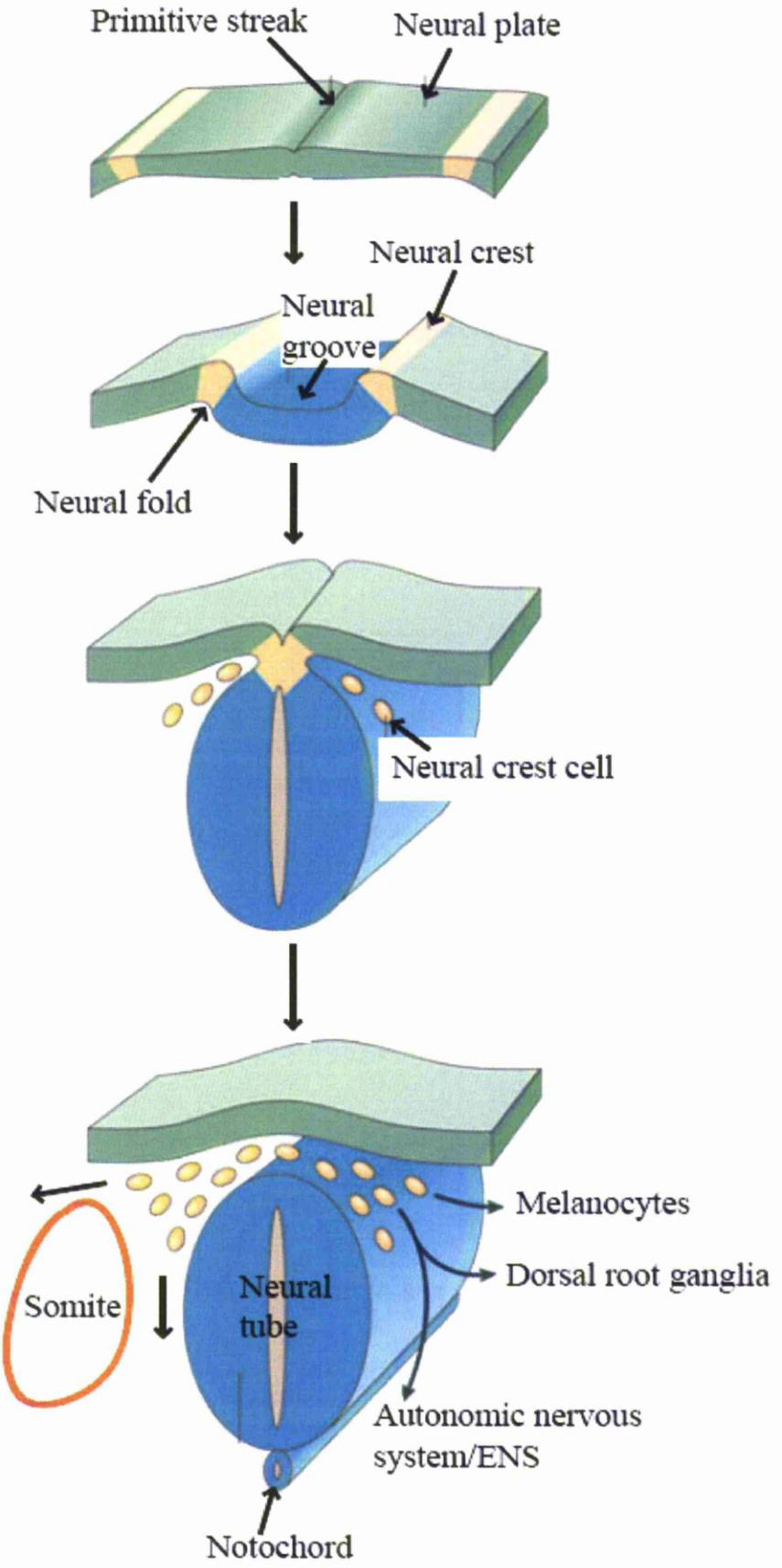
Primitive streak
Neural plate
Neural crest
Neural groove
Neural fold
Neural crest cell
Melanocytes
Dorsal root ganglia
Somite
Neural tube
Autonomic nervous system/ENS
Notochord

Figure 1.1 Neural crest development in the mouse

Figure adapted from Jessen and Mirsky (2005) showing the process of neurulation, which consists of the generation of the neural tube (primitive brain and spinal cord, blue) and the neural crest (yellow) (Jessen and Mirsky 2005). Neurulation commences when the neural plate, derived from ectoderm, begins to invaginate to form the neural groove (Shum and Copp 1996). The neural crest forms at the peak of the neural folds, between the neural and surface ectoderm (green). As the neural folds unite to produce the hollow neural tube, which is a continuous process between the stages of E8.5 and E10.5 in the mouse, the neural tube detaches from the surface ectoderm to produce two distinct structures. During this time cells of the neural crest (NCCs) undergo EMT (Sauka-Spengler and Bronner-Fraser 2008) in order to detach from their epithelial environment of the neural tube, and migrate throughout the embryo.

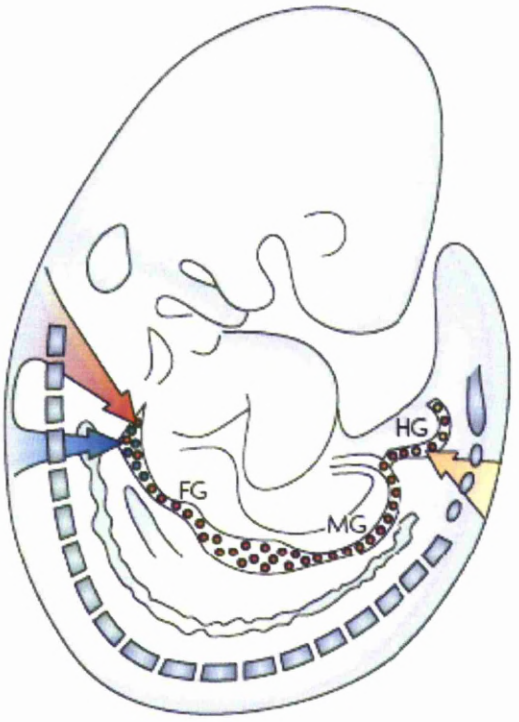

Figure 1.2 Vagal and sacral NCC contribution to the ENS

This figure shows a schematic representation of ENS development in the mouse adapted from Heanue and Pachnis 2007 (Heanue and Pachnis 2007). Vagal NCCs are shown in red and account for the majority of the total cell population of the developing ENS. Sacral NCCs are shown in yellow at the caudal end of the embryo. There is also a small contribution of NCCs from the trunk level neural crest (blue).

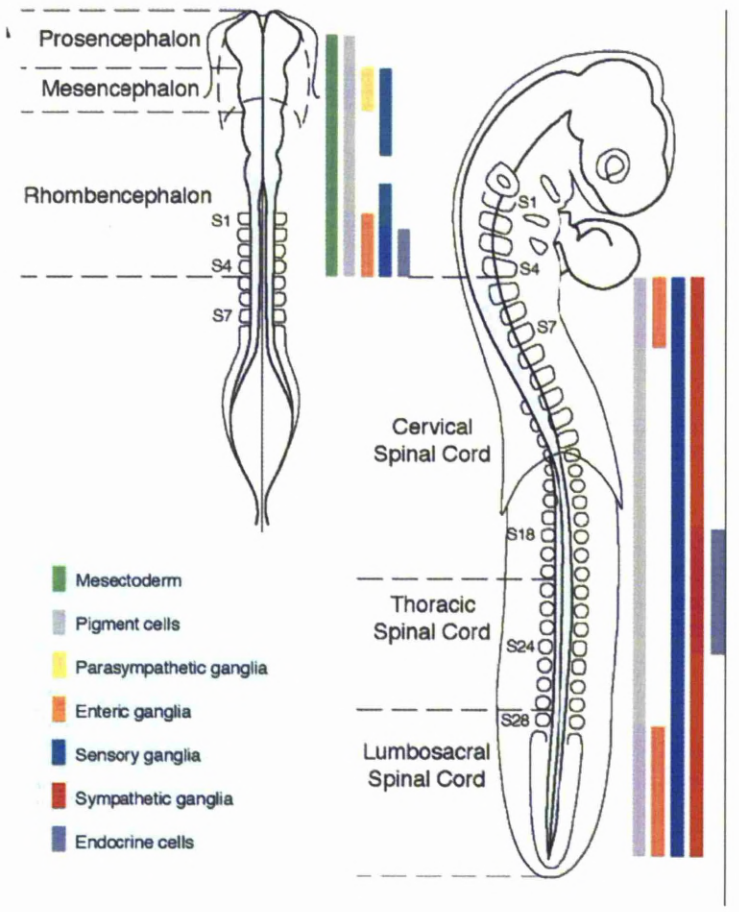

Figure 1.3 Regional differences in neural crest-derived tissues

This figure was adapted from (Le Douarin 2004). It shows the varying tissues which are neural crest-derived in the chick, and the regions of neural crest which contribute to each tissue. Overlap between regions is shown. Mesectoderm (green) is restricted to the head region between prosencephalon and somite (s) 4 (rhombencephalon). Pigment cells (melanocytes, grey) are derived from all levels of the neural crest. Parasympathetic ganglia region (yellow) is confined to mesencephalon. Enteric ganglia (orange) are derived from neural crest in the region of somites 1-7. Sensory ganglia (blue) are essentially formed from all regions of the neural crest. Sympathetic ganglia (red) are derived from the neural crest caudal to somite 4. Endocrine cells (lilac) are formed from neural crest at somites 2-4 and 18-24.

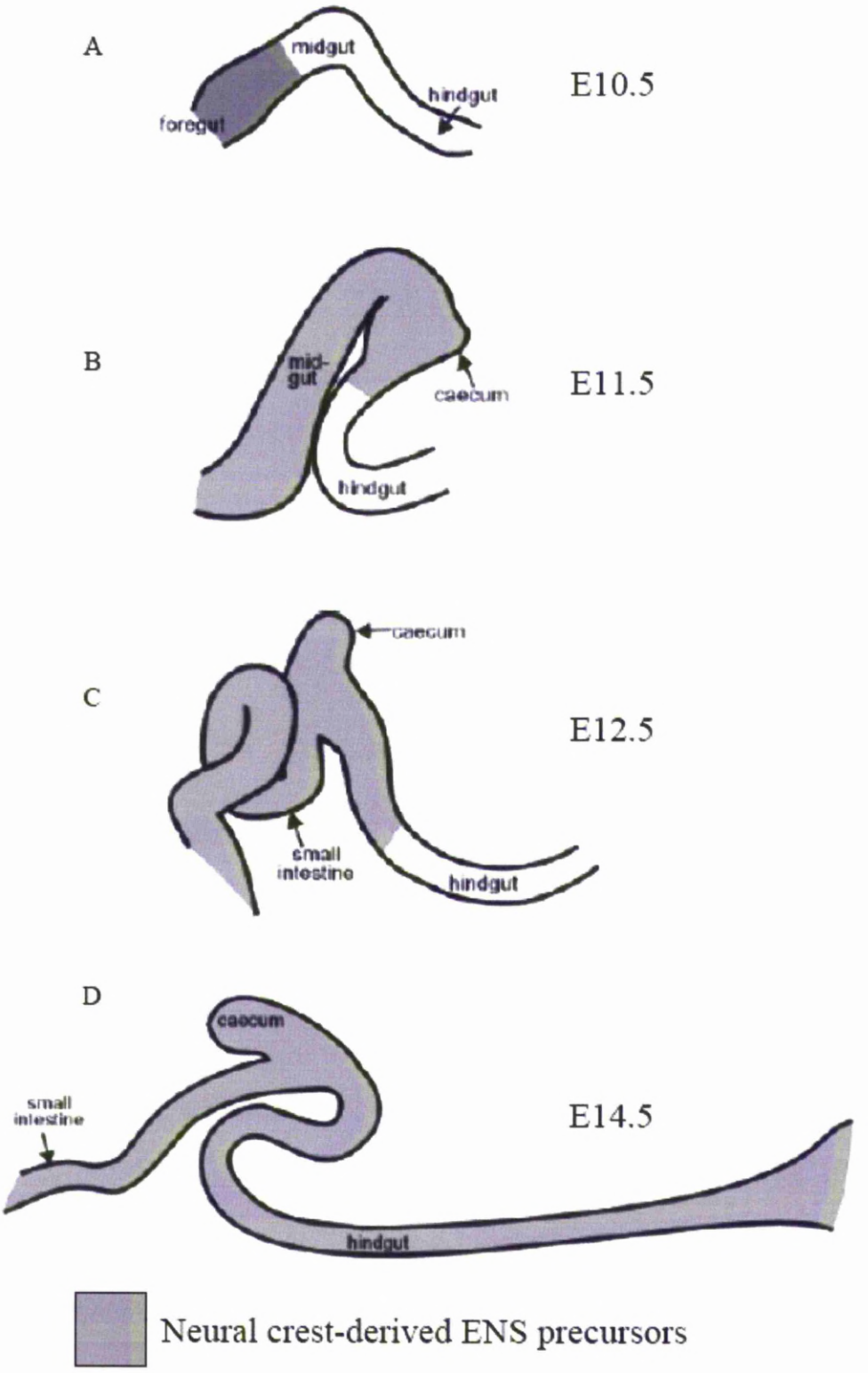
A
midgut
hindgut
foregut
E10.5
B
mid-
gut
caecum
hindgut
E11.5
C
caecum
small
intestine
hindgut
E12.5
D
caecum
small
intestine
hindgut
E14.5
Neural crest-derived ENS precursors

Figure 1.4 Development of the ENS

Figure adapted from Young and Newgreen, 2001 showing the colonisation of vagal NCCs in the mouse embryonic gut between E10.5 and E14.5, during ENS development (Young and Newgreen 2001). The vagal NCCs migrate in a rostro-caudal manner. Following the migration the neural tube at E8.5 and entry into the foregut at E9.5 (Young, Hearn et al. 2000) the NCCs reach the midgut by E10.5 (A). By E11.5 the caecum (proximal colon) has been colonised (B). Between E12.5 and E14.5 the NCCs begin to colonise the hindgut (C) and are found throughout the entire gastrointestinal tract (D).

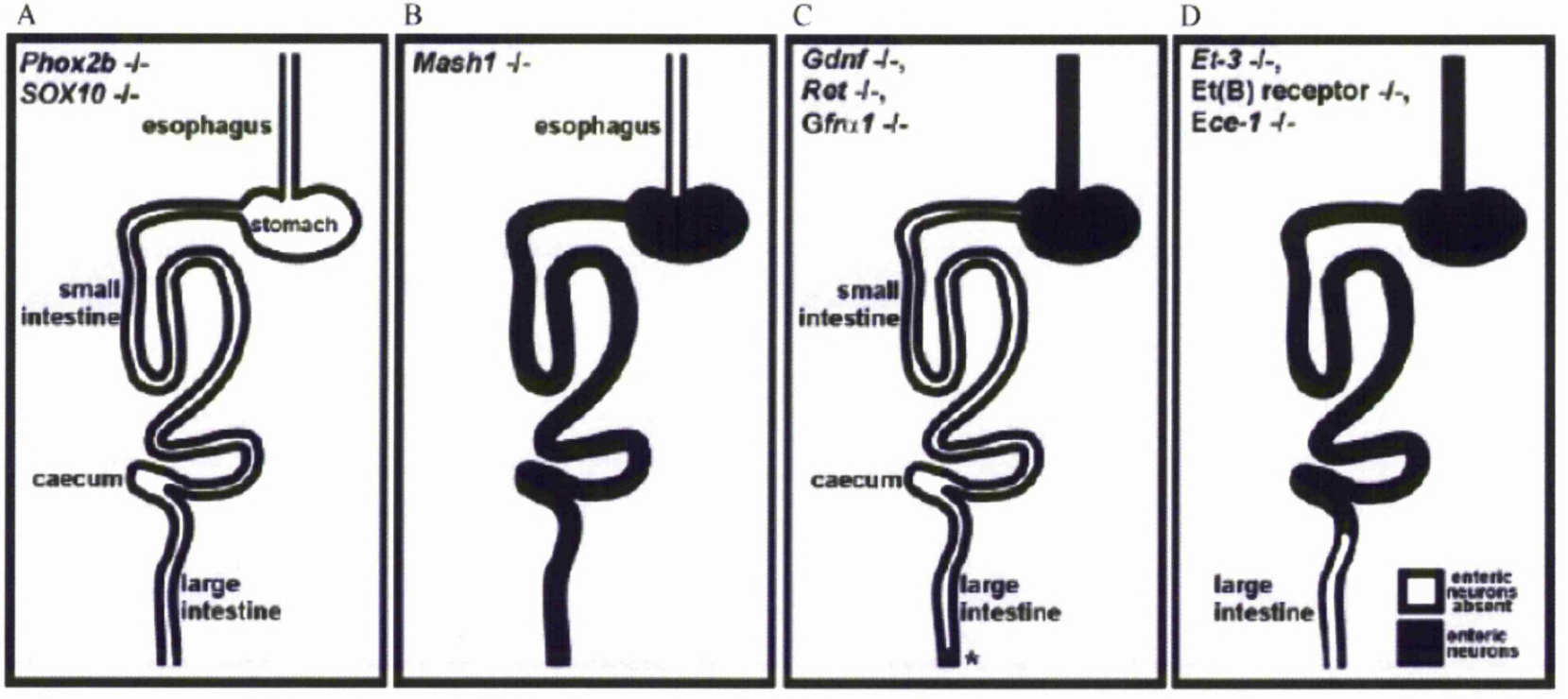
A
Phox2b -/-
SOX10 -/-
esophagus
stomach
small intestine
caecum
large intestine
B
Mash1 -/-
esophagus
C
Gdnf -/-,
Ret -/-,
Gfrα1 -/-
small intestine
caecum
large intestine
*
D
Et-3 -/-,
Et(B) receptor -/-,
Ece-1 -/-
large intestine
enteric neurons absent
enteric neurons

Figure 1.5 Enteric aganglionosis in various knock-out mice

This figure has been adapted from (Young and Newgreen 2001). It shows the varying degrees of enteric aganglionosis in a number of different knock-out mice. Image A shows total aganglionosis in the Sox10 and Phox2b knock-out mice. Image B shows aganglionosis is confined to the oesophageal region in the Mash1 knock-out mouse. The Gdnf, Ret and Gfrα1 knock-out mice show aganglionosis distal to the stomach with a small portion of the most distal bowel retaining enteric ganglia (*, C). Image D shows aganglionosis in the caudal part of the gut, the large intestine, in Et-3, Et(B) receptor and Ece-1 knock-out mice. Gdnf, glial derived neurotrophic factor. Et-3, endothelin-3. Et(B) receptor, endothelin B receptor. Ece-1, endothelin converting enzyme-1.

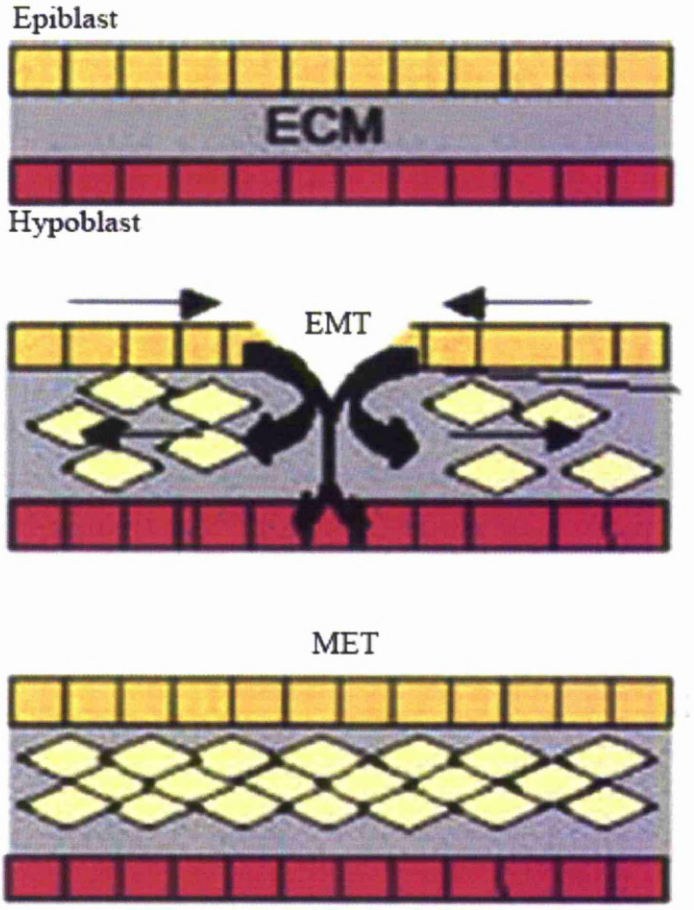

Figure 1.6 EMT and MET at gastrulation

This figure was adapted from (Hugo, Ackland et al. 2007). It shows the earliest occurrence of EMT and MET during embryonic development, during gastrulation. A subset of cells from the epiblast (primitive ectoderm) undergoes EMT to produce motile mesenchymal cells. These cells form the third germ layer, the mesoderm, which lies between the ectoderm and the endoderm (hypoblast prior to gastrulation). ECM, extra-cellular matrix.

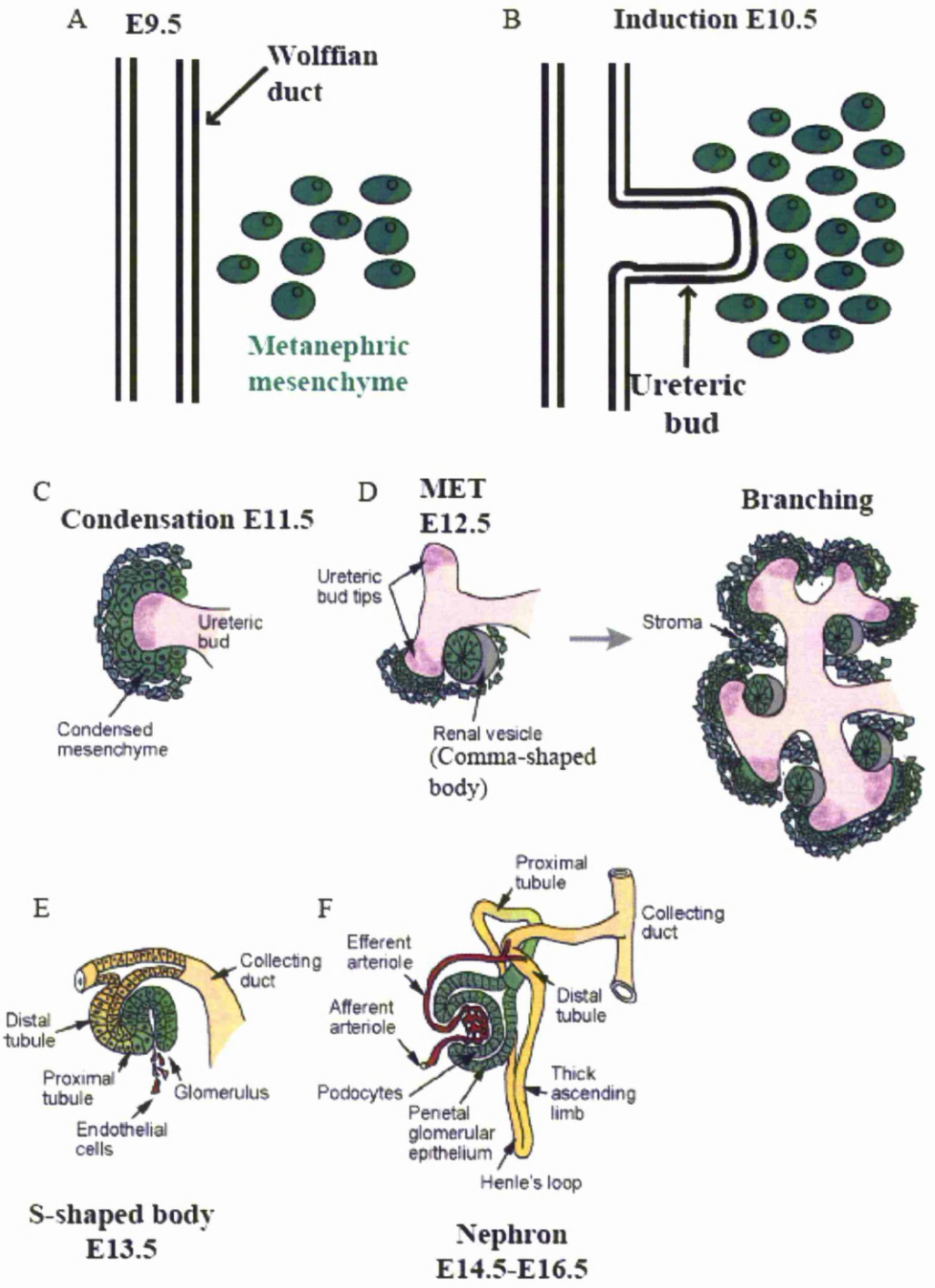
A
E9.5
Wolffian duct
Metanephric mesenchyme
B
Induction E10.5
Ureteric bud
C
Condensation E11.5
Ureteric bud
Condensed mesenchyme
D
MET
E12.5
Ureteric bud tips
Renal vesicle
(Comma-shaped body)
Branching
Stroma
E
Collecting duct
Distal tubule
Proximal tubule
Glomerulus
Endothelial cells
S-shaped body
E13.5
F
Proximal tubule
Collecting duct
Efferent arteriole
Distal tubule
Afferent arteriole
Podocytes
Thick ascending limb
Penetal glomerular epithelium
Henle's loop
Nephron
E14.5-E16.5

Figure 1.7 Kidney development

Figure adapted from Rivera, 2005 and Dressler, 2006 showing the process of nephrogenesis. Wt1-expressing cells are shown in green throughout. At E9.5 the intermediate mesoderm (IM) can be identified in the developing mouse embryo and expresses Wt1 (green). The most caudal end of the IM is the metanephric mesenchyme (MM), which lies next to the Wolffian duct (A). The process of induction begins at E10.5 when the ureteric bud (UB) branches from the Wolffian duct and invades the MM (B). The action of UB invasion causes the condensation of the MM around the tip of the UB at E11.5 (C). The MM undergoes MET and forms epithelial renal vesicles at E12.5, meanwhile further branching of the UB continues (D). At E13.5 tubules (proximal and distal) begin to form and the renal vesicle becomes more complex, producing the S-shaped body. Between E14.5 and E16.5 the nephron matures and endothelial cells invade to form the glomerulus. Wt1 expression becomes restricted to the podocytes of the glomerulus (Rivera and Haber 2005; Dressler 2006).

A

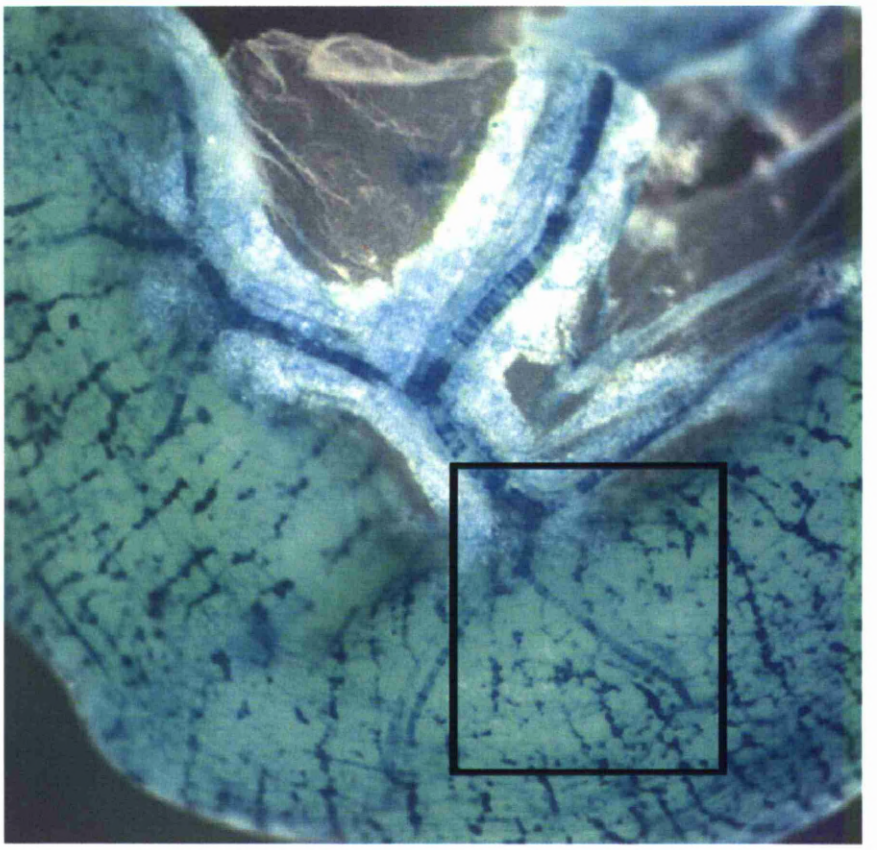

B

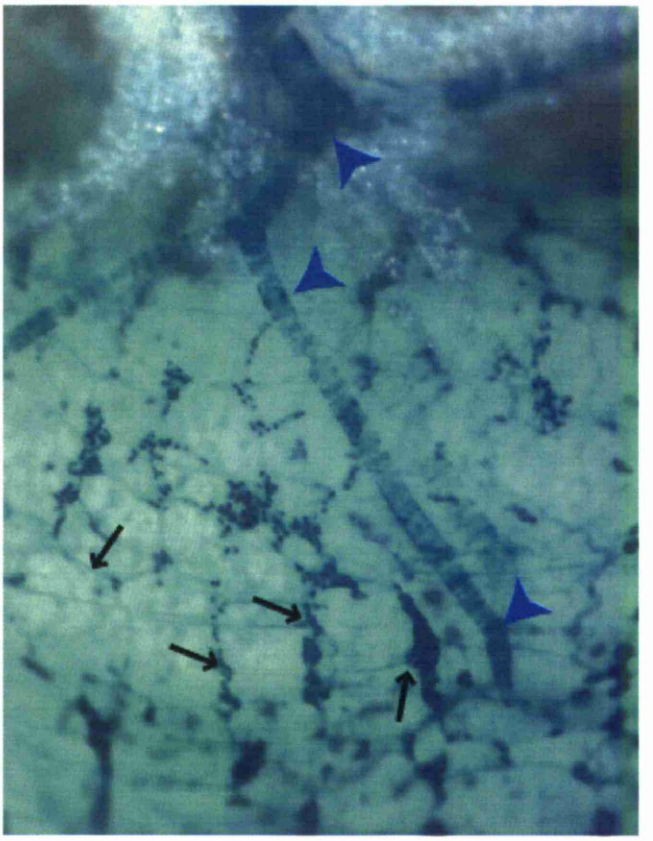

C

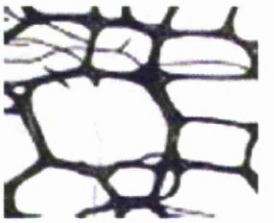

Figure 1.8 Wt1-derived cells in the ENS

Figure adapted from Wilm, 2005 showing whole-mount LacZ staining of an adult mouse intestine (A and B). Image B is a high magnification image of the boxed area in image A. The blue arrowheads indicate Wt1-derived serosal mesothelial cells which contribute to the smooth muscle component of the intestinal vasculature (B) (Wilm, Ipenberg et al. 2005). Black arrows reveal LacZ staining localised in the adult mouse ENS (B). Image C shows a schematic diagram of the myenteric plexus (adapted from (Furness 2006). LacZ staining follows a similar pattern to that seen in the diagram (B and C).

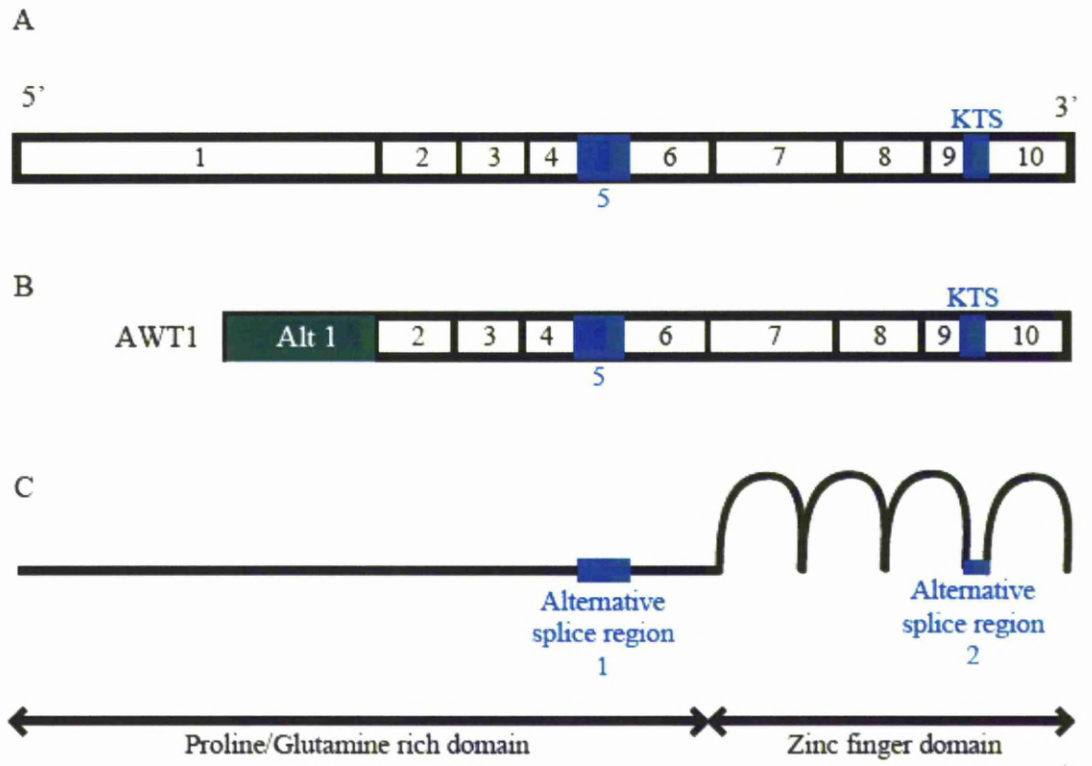

Figure 1.9 *Wt1* gene and protein

Figure adapted from (Vize, Woolf et al. 2003) showing a schematic diagram of the *Wt1* gene consisting of 10 exons (A). *AWT1* consisting of an alternative exon1 is shown in B. *AWT1* encodes a shorter protein than the original *Wt1* transcript. Green box represents the alternative exon 1 (Alt 1). *Wt1* encodes a protein with a proline/glutamine rich domain and four zinc fingers (C). Blue boxes represent two alternative slice sites. The first at exon 5 and the second at the 3' end of exon 9, characterised by the presence or absence of three amino acids, KTS (leucine, threonine, serine).

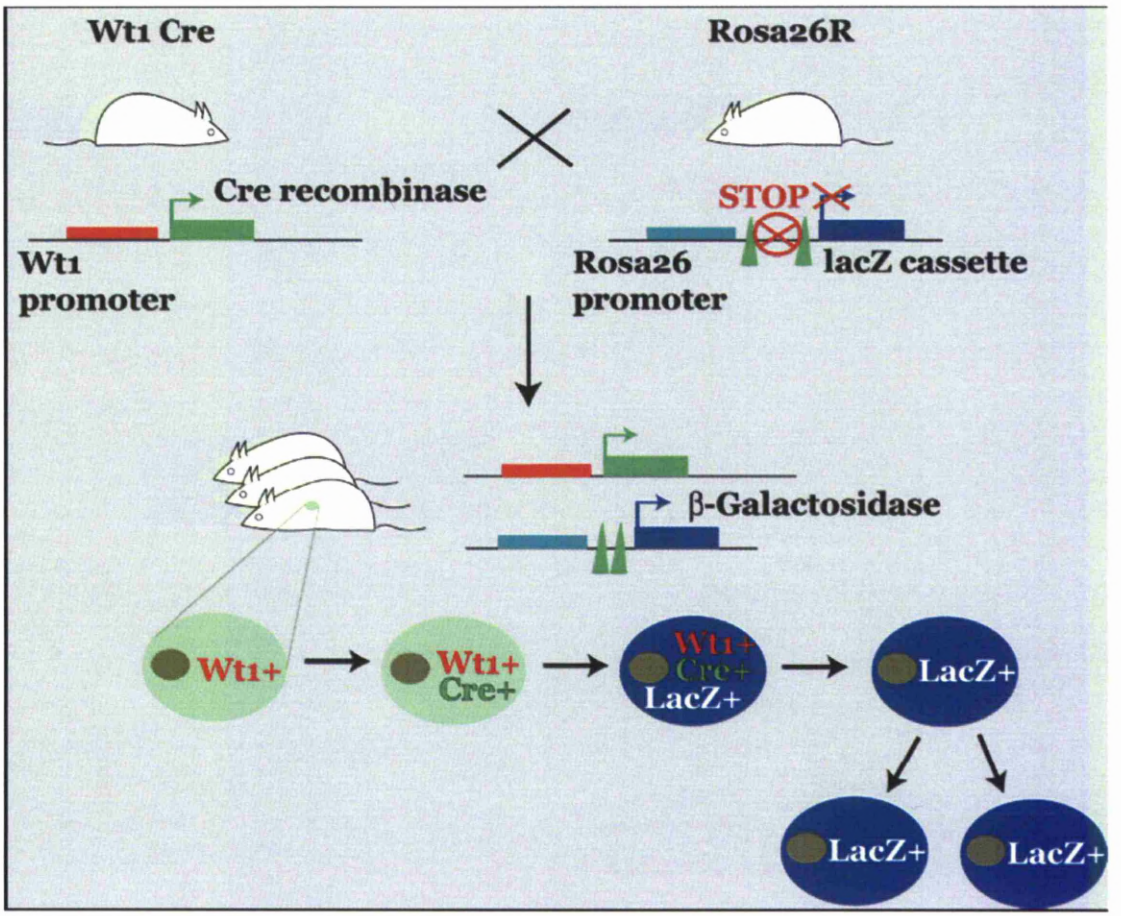

Figure 1.10 Lineage tracing of Wt1-derived cells

The Wt1-Cre mouse (A) carries a Cre recombinase (green) under the control of the human Wt1 promoter (red). This was crossed with the Rosa26 reporter mouse line (B), which has a LacZ cassette (dark blue) under the control of the ubiquitously expressed Rosa26 promoter (light blue). A stop cassette flanked by LoxP sites (green triangles) prevents LacZ expression. The Wt1-expressing cells within the progeny (C) of this Wt1-Cre and Rosa26R crossing contain active Cre recombinase. The Cre acts on the LoxP sites and the stop cassette is excised causing expression of β-Galactosidase. Due to ubiquitous expression of Rosa26 any cell expressing Wt1 or Wt1-derived cell will express LacZ and lineage could be traced by visualising a blue precipitate when X-Gal staining or immunofluorescence for β-Galactosidase is performed.

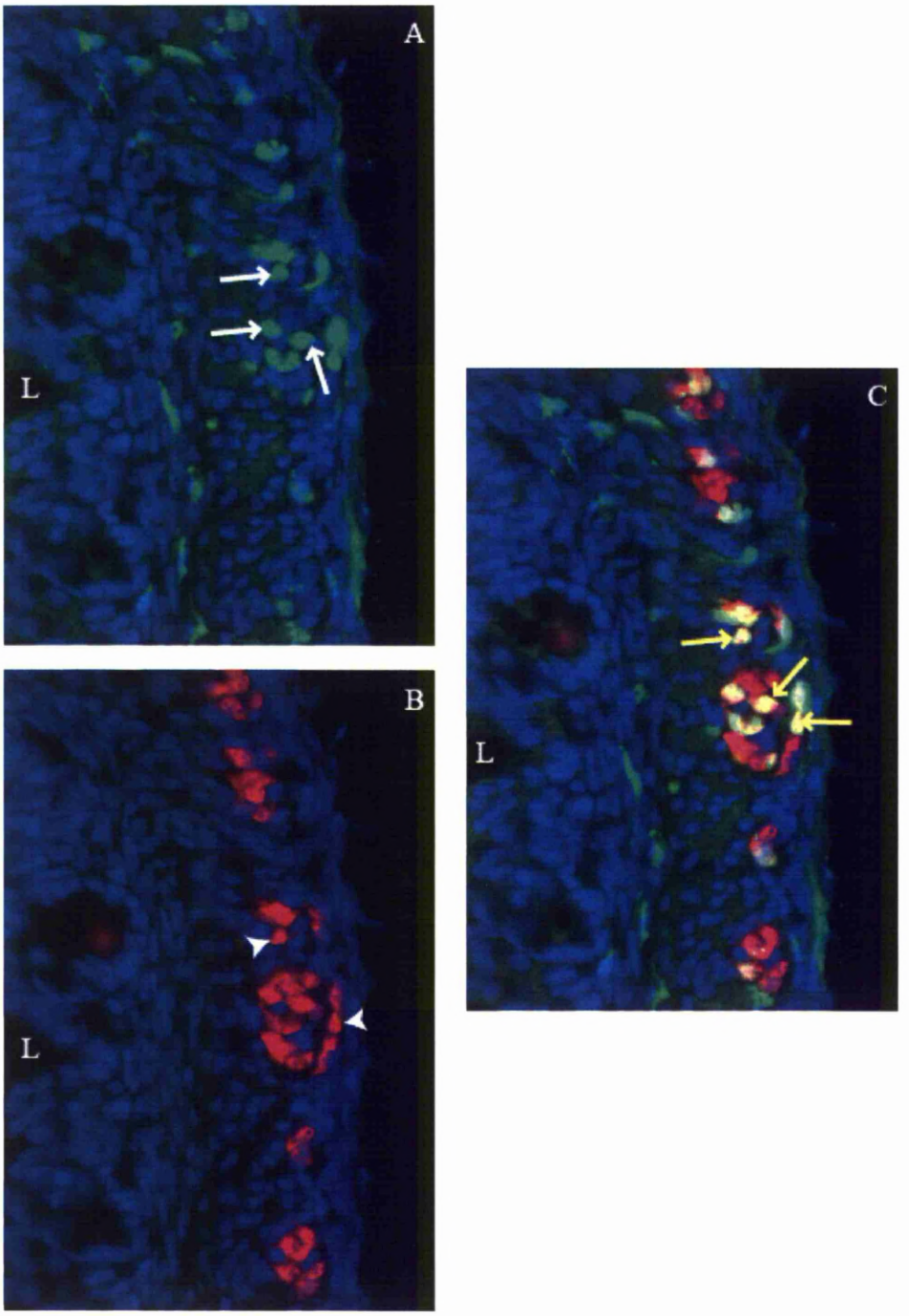
A
L
B
L
C
L

Figure 1.11 β-Gal expression in enteric neurons

Frozen sections taken from newborn mouse intestine showing immunofluorescence co-stained for β-Gal (Wt1-derived cells, A, green) and pan-neuronal marker Hu (enteric neurons, B, red). Image C is a composite showing co-localisation of Hu in around half of enteric neurons (C, yellow arrows). The nuclear stain DAPI is shown in blue (A-C). L, intestinal lumen.

Table 1.1 Adapted from Young and Newgreen, 2001. This table shows the molecules and genes expressed by NCCs during ENS development. Expression shown in orange (e.g. Yes).

Marker	Function	Species	Expression in NCCs prior to entry to gut	Expression in NCCs within the gut	References if differ from Young and Newgreen, 2001
Transgenes					
DBH-lacZ	LacZ expression driven by the promoter of the catecholamine synthetic enzyme, DBH	Mouse	No	Yes	
CCK-LacZ	LacZ expression driven be the promoter of regulatory peptide, CCK	Mouse	Yes	Yes	
P0-Cre	LacZ expression in cells expressing the P0 glycoprotein (cell adhesion molecule)	Mouse	Yes	Yes	
Receptors for neurotrophic factors					
Ret	Receptor tyrosine kinase; forms part of the receptor complex for GDNF. Downstream of Hoxb5	Mouse, chick, rat	Yes	Yes	(Lui, Cheng et al. 2008)
GFRα1	Forms part of the receptor complex for GDNF, along with Ret	Mouse, rat, chick, zebrafish	Reports suggest not	Yes	(Schiltz, Benjamin et al. 1999; Taraviras, Marcos-Gutierrez et al. 1999; Lucini, Facello et al. 2010)
ErbB3	Receptor tyrosine kinase; receptor for neuroregulin-1	Mouse	Yes	Yes	
$p75^{NTR}$	Low-affinity neurotrophin receptor	Rat, Mouse	Yes	Yes	

TrkC	Receptor for NT-3	Rat, mouse	Reports suggest not	Yes	(Chalazonitis 2004; Chalazonitis, D'Autreaux et al. 2004; Levanti, Esteban et al. 2009; Bartkowska, Turlejski et al. 2010)
ET-B receptor	Receptor for Endothelin 3	Mouse, human, chick, quail	Yes	Yes	
CNTFRα	α component of neuropoietic cytokine receptor	Rat	Reports suggest not	Yes	(Masu, Wolf et al. 1993; Rhee and Yang 2010)
Gp130 and LIFRβ	β components of neuropoietic cytokine receptor	Rat	Reports suggest not	Yes	(Masu, Wolf et al. 1993; Rhee and Yang 2010)
Neurotransmitter-related molecules					
5-HT transporter and receptor	Transporter and receptor for serotonin	Rat, mouse	Reports suggest not	Yes	(Vitalis, Alvarez et al. 2003; Li, Caron et al. 2010)
Tyrosine Hydroxylase	Catecholamine synthetic enzyme	Mouse, rat	Yes	Yes	
Transcription factors					
MASH1	Mammalian homologue of *Drosophila* proneural genes	Mouse, rat	No	Yes	(Okamura and Saga 2008)
Phox2a	Involved in cascade involving Ret and MASH1	Mouse	No	Yes	
Phox2b	Essential for expression of Ret and TH	Mouse	Yes	Yes	
Sox10	Activator of regulatory cascade in ENS and melanocyte development. Interacts with Pax3	Mouse	Yes	Yes	(Hong and Saint-Jeannet 2005; Betancur, Bronner-Fraser et al. 2010; Nelms, Pfaltzgraff et al. 2011; Sommer 2011)
Foxd3	Maintains neural crest progenitors. Interacts with Pax3 in cardiac NC	Mouse	Yes	Yes	(Teng, Mundell et al. 2008; Nelms, Pfaltzgraff et al. 2011)

cHox11L2	Activation important pathway in T leukemogenesis. Neurons	Chick, zebrafish	No	Yes	(Andermann and Weinberg 2001; Bernard, Busson-LeConiat et al. 2001)
Hox11L1	Knockout is a mouse model for intestinal neuronal dysplasia	Mouse	No	Yes	(Puig, Champeval et al. 2009)
HoxB5	Regulates angiogenesis via activation of flk1. Ret is a downstream target	Mouse	Yes	Yes	(Wu, Moser et al. 2003; Winnik, Klinkert et al. 2009)
HAND2	Transcriptional regulator. Binds to Ebox proteins. Activates nanog	Mouse, chick	No	Yes	(Dai and Cserjesi 2002; Hashimoto, Myojin et al. 2009)
Miscellaneous proteins					
Neurofilament	Cytoskeleton component of neurons	Chick, mouse, rat	No	Yes	
N-cadherin	Calcium-dependent adhesion molecule	Mouse	Yes	Yes	(Gammill and Roffers-Agarwal 2010; Kulesa and Gammill 2010)
Nestin	Intermediate filament protein	Rat, mouse	Yes	Yes	(Kawaguchi, Miyata et al. 2001; Wiese, Rolletschek et al. 2004)
4E9R	NC-specific intermediate filament, related to vimentin	Mouse	Yes	Yes	
E/C8	Antibody to Avian-specific, neurofilament-associated protein	Chick, quail	Yes	Yes	
HNK-1 and NC-1	Monoclonal antibodies that recognise the carbohydrate epitope of a family of glycoproteins	Chick, quail, rat, dog, pig, human	Yes	Yes	

Chapter 2

Materials and methods

2.1 Animals

Wild-type CD-1® mice were purchased from Charles River Laboratories International, Inc. Time-mated females were killed in accordance to Schedule 1 of the Animals (Scientific Procedures) Act 1986. Embryos were obtained following Home office regulations and decapitation was performed on any embryos from half way through gestation onwards.

2.2 Detection of protein using immunostaining techniques

Preparation for immunofluorescence and generation of frozen sections

Mouse embryos at embryonic stages (E) between E7.5 and E16.5 were dissected from maternal and extra-embryonic tissues. The embryos were incubated at 4°C in 4% paraformaldehyde (PFA) for fixation (Table 2.1). The fixed embryos were washed 3 times for 5 minutes in phosphate buffered saline (PBS) to ensure no PFA was remaining. They were then incubated overnight at 4°C in 20% sucrose solution. This was done to protect the integrity of tissues during the freezing process. Individual embryos were then embedded in Shandon cryomatrix embedding compound (Thermo Scientific) and frozen using solid carbon dioxide (CO_2) and 2-propanol. The frozen embryos were wrapped in foil and were stored at -80°C until ready for sectioning. Embryos were sectioned using a cryostat at -20°C using Superfrost plus slides (Thermo Scientific), placing between 4 and 12 sections per slide depending on the embryonic stage.

Immunohistochemistry on frozen sections

Frozen sections were removed from -80°C and allowed to thaw at room temperature for 5-10 minutes. Slides were kept in humidified conditions to prevent the tissue from dying out. Once thawed, they were washed 3 times in PBS to bring them back into a physiological state. The tissue was then permeabilized with 0.25% Triton solution (v/v) (Fluka) for 10 minutes at room temperature before three more 5 minute washes in PBS. Blocking was performed for 1 hour at room temperature using 2% bovine serum albumin (BSA). During this blocking step primary antibodies were diluted to their working concentration in 2% BSA (w/v) (Table 2.1). The sections were incubated in primary antibody overnight at 4°C. Negative controls were incubated in 2% BSA without primary antibody. The next day the primary antibody was washed off using three 5 minute PBS wash steps. During this time secondary antibodies plus DAPI were diluted (Table 2.1). Sections were incubated with secondary antibody in the dark at room temperature for 1 hour. This was followed by another three 5 minute PBS washes to ensure that no antibody was left over. Slides were then mounted with anti-fade mounting media (Electron Microscopy Sciences) and glass cover-slips. They were left to dry for 10 minutes and sealed using clear nail polish. For prolonged storage the slides were kept at 4°C.

Neural tube explants were cultured at 37°C in DMEM (Sigma) plus 5% NCS and 5% horse serum (Sigma). They were plated onto cover-slips which had been coated with a 0.5% gelatine solution and placed into 24 well plates. They were fixed for 10 minutes at room temperature in 4% PFA and stained with antibodies as described above.

Kidney stem cells (KSC) were seeded on 8-well chamber slides in high glucose DMEM (Invitrogen) supplemented with 2mM glutamine and 10% FCS. The cells were fixed for 10 minutes at room temperature in 4% PFA and were stained with antibodies as described above.

Immuno-staining on whole-mount mouse embryos

E8.5 mouse embryos were fixed in 4% PFA (w/v) at 4°C for 45 minutes. They were washed three times in PBS for 5 minutes and dehydrated through a series of methanol concentrations (25%-75% (v/v) each for 30 minutes) into 100% methanol. They were then stored at -20°C until ready for use. Embryos were bleached in 6% hydrogen peroxide (H_2O_2) diluted in methanol for 1 hour at room temperature. They were then rehydrated through the methanol series (75%-25% for 30 minutes) into PBS-0.25% Triton (PBST) at room temperature, rocking. Embryos were permeabilized with three 20 minute washes in PBS-1% Triton (PBST) at room temperature, rocking. Blocking was followed by incubating embryos in PBSMT (PBST + 2% skimmed milk) for 1 hour at room temperature, rocking. They were then incubated with primary antibody diluted in PBSMT (Table 2.1) overnight at 4°C, rocking. On day 2 three brief washes in PBSMT were followed by five 1 hour washes with PBSMT at 4°C, rocking. They were then blocked once again in PBSMT for 1 hour at 4°C. Secondary antibody coupled to horse radish peroxidise (HRP) was diluted in PBSMT and the embryos were incubated overnight at 4°C, rocking (Table 2.1). The third day started with three brief washes in PBSMT. They were then washed at 4°C for 1 hour in PBSMT, rocking. Samples were then washed with PBST for 20 minutes. After this the colour reaction was carried out as follows: the embryos were washed for 20-30

minutes in PBS (no triton) containing 0.5% nickel chloride ($NiCl_2$), 0.3mg/ml DAB (Sigma). H_2O_2 was added to reach a final concentration of 0.01% and they were incubated for 5-10 minutes whilst colour developed. After this they were washed with PBST and fixed overnight in 4% PFA at 4°C.

2.3 Molecular biology

Wt1 full-length cDNA probe was obtained from the Kreidberg lab, Children's Hospital Boston. In order to recover the plasmid after transportation the sample was added to 10mM Tris at pH7.6. This was followed by brief vortexing and was allowed to hydrate for 10 minutes. The solution was centrifuged briefly and the supernatant was then prepared for the transformation of competent bacteria.

Heat shock transformation of bacteria with plasmid DNA

5µl of plasmid DNA was added to 200µl aliquots of competent bacteria and mixed gently. This was left on ice for 30 minutes. During this time the water bath was set to 42°C. Following incubation on ice the cells were placed into the water bath for 90 seconds. After heat shock treatment the cells were returned to ice and then transferred into 800µl Luria broth (LB) trans and placed into the bacterial shaker at 37°C for 1 hour. LB broth plates were incubated at 37°C whilst cells were in the shaker in order to warm. 50µl of the transformed bacteria was plated onto LB agar plates containing ampicillin using a pipette and Bunsen burner. The plates were then incubated at 37°C overnight.

Plasmid selection and mini-culture set up

LB broth plates were removed from the incubator the next morning. A 5ml LB plus ampicillin (1:1000) solution was set up for each transformation. 1 colony per transformation was chosen and cells from this colony were transferred into the LB/ampicillin culture. This was then placed into the shaker at 37°C over night.

Generation of glycerol stocks

Glycerol stocks were produced from mini-cultures for future use. 1.5ml of bacterial transformation was added to 0.5ml 60% glycerol. The solution was mixed completely by vortexing and the solution was stored at -80°C.

Preparation of plasmid DNA

In order to confirm the insert within the plasmid a mini plasmid preparation was carried out using the TENS method. 1.5ml from the mini-culture was placed into a microfuge tube and span in the centrifuge for 1 minute at full speed. The supernatant was discarded leaving only a small volume (around 50µl) with the pellet. The pellet was resuspended in the remaining LB broth by vortexing. 300µl of TENS buffer was added in order to lyse the cells. The samples were placed on ice for 5 minutes and inverted occasionally to ensure they remained mixed. Once the sample had incubated on ice and became milky 150µl 3M NaAc (pH5.0) was added followed immediately by inverting. The high salt content and acidic pH neutralised the sample and they became clear with a white precipitate. The white precipitate contained the DNA and protein and the plasmids, which re-annealed remained in the solution. The samples were then centrifuged for 5 minutes at maximum speed. The supernatant was collected and transferred to a separate tube

containing 900µl of ethanol. This was mixed and incubated at -20°C for 30 minutes in order to gain maximal plasmid precipitation. The samples were then centrifuged for 5 minutes at full speed, the supernatant was decanted and 700µl of 70% ethanol was added twice to wash out any remaining salt. This was centrifuged briefly leaving behind an opaque pellet. The supernatant was removed immediately. The pellet was allowed to dry by evaporation and once it was completely dry 30µl TE buffer was added. The pellet was resuspended by vortexing. The preparation was stored at 4°C ready for restriction enzyme digestion.

Restriction enzyme digestion of plasmid DNA

*Not*I (Biolabs, Inc.) and *Eco*RI (Fermentas) restriction enzymes were used on DNA from mini plasmid preparations in order to make sure that the insert was present and the correct size. Restriction digests were set up containing 0.5µl *Not*I restriction enzyme, 0.5µl *Eco*RI restriction enzyme, 1µl 10x buffer, 5.5µl H_20 and 3µl of plasmid DNA. They were incubated for 2 hours at 37°C and analysed on a 1% agarose gel. In order to produce larger quantities for generating sense and antisense probes for use with in situ hybridisation experiments transformed bacteria was grown overnight in 100ml LB/ampicillin (100µg/ml). The plasmid was prepared using Qiagen maxi plasmid preparation kit.

Linearising plasmid for transcription

20µg of plasmid containing the full length cDNA mouse Wt1 insert of 1.4kb was linearised using the *Not*I (antisense probe) and *Eco*RI (sense probe) restriction enzymes. This was achieved by mixing 20µl of DNA, 10µl of 10x buffer, 5µl

restriction enzyme and 35µl H_2O was added to a final volume of 100µl. This mix was incubated at 37°C for 2 hours. At this point 5µl was removed and run on an agarose gel to control for complete linearization. After linearization a further 100µl of H_2O was added to the mixture and Phenol-Chloroform extraction was performed. 200µl Phenol was added and mixed by vortexing. This was then centrifuged for 2 minutes at 1300rpm. The upper phase was collected and transferred to a fresh tube. This was repeated once, and the upper phase was collected and transferred to a fresh tube. To this 200µl of Chloroform-Isoamylalcohol (Sigma) was added, mixed by vortexing and centrifuged for 2 minutes at 1300rpm. The watery phase was aspirated and added to 20µl sodium acetate (NaAc) (1:10 dilution). Three volumes of 100% ethanol were added (600µl). This mix was incubated at -20°C for 30 minutes. After incubation the mixture was centrifuged at 4°C for 20 minutes. The pellet was washed in 70% ethanol and allowed to dry. It was then resuspended in diethylpyrocarbonate (DEPC)-treated H_2O and stored at -20°C until transcription.

In vitro transcription of a Wt1 in situ probe

In order to prepare the Wt1 probe for in situ hybridisation 1µg of linearised template plasmid was added to 20µl total volume with final concentrations of 1x transcription buffer, 1x DIG-RNA labelling mix (Roche), 1x DTT, 1U/µl RNAse inhibitor and 1U/µl RNA-polymerase (T3 antisense, T7 sense – Roche), diluted in RNAse free H_2O. This mixture was incubated at 37°C for 2 hours. The following was then added to make the total volume up to 50 µl: 1x DNAse buffer (RNAse free) (Roche) and 2U DNAse (RNAse free) (Roche), diluted in RNAse free H_2O. This solution was incubated at 37°C for 30 minutes. 1µl of this transcription mix

was removed and added to 20µl of 50% Formamide, TE and loading buffer for gel estimation. The probe was then purified using Sephadex Columns (GE Healthcare). A further 1µl was taken out and added to the Formamide buffer. This was loaded along with the pre-purification mix onto a 1.5% agarose gel. 2µl of RNAse inhibitor was added to the labelled probe for prolonged storage.

2.4 Detection of mRNA using in situ hybridisation

Whole mount in situ hybridisation

All solutions for RNA work were treated with DEPC or derived from DEPC-treated stock solutions. All glass ware was baked at 180°C for 2 hours prior to use. Only filter pipette tips and pipettes were used. A 4% PFA solution was made up using DEPC-treated H_20 and PBS. This was mixed in a glass beaker for RNA work that had been baked for 2 hours at 180°C. This was sterile filtered and stored at 4°C for up to 2 weeks. Mouse embryos between E7.5 and E10.5 were dissected from maternal and extra-embryonic tissues. Embryos were placed in 4% PFA at 4°C, rocking gently for fixation (Table 2.2). After fixation the embryos were washed three times in PBT (PBS + 0.1% Tween-20) for 10 minutes each. They were then dehydrated through a methanol series (25%-100% meOH/PBT) for 30 minutes each at 4°C with two washes in 100%. They can be stored in this way at -20°C. To continue the procedure a 4:1 solution of methanol and 37% H_2O_2 was prepared and the embryos were bleached at room temperature for 1 hour, rocking. They were then rehydrated back through the methanol series (75%-25%) for 30 minutes each, into PBT at room temperature, rocking. The rehydrated embryos were then washed three times for 10 minutes in PBT at room temperature, rocking.

At this point the hybridisation oven was set to 70°C. A proteinase K/PBT digest was set up at a concentration of 10µg/ml, and to stop the proteinase K reaction a 2mg/ml glycine (Sigma) and PBT solution was also prepared. The timing of digestion was incredibly critical, to ensure the embryos were not completely/under digested. The optimal digestion times for each embryonic stage are detailed in table 2.3. To perform the proteinase K reaction the PBT was removed and the embryos were incubated in proteinase K/PBT at room temperature for their allotted digestion time. Following incubation the proteinase K/PBT solution was removed promptly and the glycine/PBT solution was added in order to stop the reaction. The digested embryos were then incubated at room temperature, rocking; twice for 5 minutes in glycine/PBT in order to make sure all proteinase K had been removed. They were then washed twice for 5 minutes in PBT, rocking. A post-fixative solution was prepared consisting of 4% PFA and 0.2% glutaraldehyde. The embryos were fixed again for 20 minutes at room temperature, rocking. They were then washed twice for 5 minutes in PBT. At this point the pre-hybridisation solution was prepared (2ml). This consisted of 50% Formamide (Fisher scientific), 5x SSC (pH 4.5-5.0), 1% SDS, heparin (50µg/ml), yeast tRNA (5µg/ml) final concentrations. The embryos were transferred into small glass vials, which had been coated in Sigma Coat to prevent tissue sticking to them, and as much PBT as possible was removed. 300µl of pre-hybridization solution was added. This was mixed briefly and removed. It was replaced by the remaining 700µl of pre-hybridisation solution and the cap was fastened tightly. The embryos were incubated at 70°C in the hybridisation oven for at least 1 hour. During this time the hybridization solution was prepared (1ml). This consisted of 50% Formamide, 5x SSC (pH 4.5-5.0), 1% SDS, heparin (100µg/ml), yeast tRNA (10µg/ml) (Roche)

and 0.5µg of *Wt1* probe final concentrations diluted in DEPC- H_2O. Once the embryos have incubated remove as much pre-hybridisation solution as possible. I had to be very cautious here as the embryos tend to be transparent at this stage so it was easy to discard them with the solution if you were not careful! 300µl of hybridisation solution was added and mixed briefly. This was then removed and replaced by the remaining 700µl of hybridisation solution. The cap was again fastened tightly and the embryos were returned to the oven and incubated overnight at 70°C. The second day of this procedure began by preparing the wash solutions the use DEPC-treated solutions was no longer necessary. Solution 1 was made up to final concentrations of 50% Formamide, 5x SSC, 1% SDS diluted in H_2O. This was pre-heated to 70°C. Solution 2 was made up to final concentrations of 0.5M NaCl, 10mM Tris-HCl, 0.1% Tween-20 diluted in H_2O at room temperature. Solution 1/2 consisted of equal volumes of solution 1 and 2. This was pre-heated to 70°C. Solution 3 was made up of final concentrations of 50% Formamide, 2x SSC diluted in H_2O. This was pre-heated to 65°C. After preparation of the solutions the procedure continued. Hybridisation solution was discarded as much as possible, ensuring the embryos remained in the glass vial. They were washed for 5 minutes in a small amount of pre-heated solution 1. This was removed and the embryos were washed twice for 10 minutes in solution 1 at 70°C, rocking. They were washed in solution 1/2 for 10 minutes at 70°C. The embryos were then washed twice in solution 2 for 10 minutes at room temperature, rocking. At this point the hybridisation oven temperature was changed to 65°C and the RNAse/solution 2 mix was prepared. This was done by diluting RNAse A (10mg/ml) to a final concentration of 100µg/ml in solution 2 and pre-warming to 37°C. The embryos were incubated in the RNAse A solution twice for 30 minutes

at 37°C, rocking. They were then washed twice for 30 minutes in pre-heated solution 3 at 65°C, rocking. At this point embryo acetone powder was heat inactivated. A pinch of embryo acetone powder was suspended in 1ml TBST/Levamisole (Sigma) (1:500) and heated to 65°C for 30 minutes. The Levamisole was added in order to block endogenous alkaline phosphatase. The solution was centrifuged and TBST/Levamisole was discarded. After this 80% TBST/Levamisole, 20% BM blocking reagent, 0.01% heat inactivated sheep serum (HISS) (Sigma), and 0.5µl anti-DIG antibody (1:2000 dilution) was added to the embryo acetone powder. This was then incubated for 1 hour at 4°C, rocking. Once incubated the supernatant was collected. This contained the pre-absorbed antibody. After the embryos had been incubated in solution 3 they were washed in TBST/Levamisole three times for 10 minutes at room temperature, rocking. At this time the blocking solution was prepared (2ml). The final concentrations of the blocking solution were 70% TBST/Levamisole, 10% HISS and 20% BM blocking solution. The embryos were transferred into the blocking solution and incubated at room temperature for at least 1 hour, rocking. The blocking solution was then discarded and the embryos were incubated in the pre-absorbed antibody solution (1ml per vial) overnight at 4°C, rocking. The third day started with 3 brief rinses in TBST/Levamisole. This was followed by four 1 hour long washes with TBST/Levamisole at room temperature, rocking. Whilst the embryos were washing the NTMT (alkaline phosphatase buffer) was prepared (10ml). This was made to final concentrations of 100mM NaCl, 100mM Tris-HCl pH9.5, 50mM $MgCl_2$, 0.1% Tween-20 diluted in H_2O. After the last TBST/Levamisole wash the embryos were incubated in NTMT/Levamisole twice for 20 minutes at room temperature, rocking. They were then transferred to a 4-well dish, as much NTMT was removed

as possible and 1ml/well of BM purple alkaline phosphatase substrate (Roche) was added. They were mixed gently. The embryos were placed in a dark place and they were watched carefully for the colour development. To stop the reaction they were washed twice for 10 minutes in NTMT at room temperature and then washed in PBT pH 5.5. This treatment was to reduce any purple background staining. The embryos were then post-fixed in 4% PFA/0.2% glutaraldehyde for 20 minutes at room temperature and then washed twice in PBT for 10 minutes.

In situ hybridisation on frozen sections

Sections were generated as previously described. Slides were transferred from the freezer (-80°C) to a slide box in cold conditions to avoid too much condensation developing on the sections. The slides were dried at 50°C for 15 minutes. Using glass trough, which held 200ml, the sections were post-fixed in 4% PFA for 20 minutes. They were then washed twice in PBS. Following PBS washes they were carbethoxylated in active 0.1% DEPC-PBS twice for 15 minutes. This was done to decrease any background later on in the procedure. The sections were then equilibrated in DEPC-treated 5x SSC for 10 minutes. The slides were transferred to slide mailer boxes, which were sealed with parafilm, and they were pre-hybridised for 2 hours at 58°C in pre-hybridisation buffer. This consisted of final concentrations of 50% Formamide, 1x SSC and 40µg/ml salmon sperm DNA (Sigma) which had been heat denatured for 10 minutes. This solution was diluted in RNAse free H_2O. The sections were then hybridised in the hybridisation buffer, which contained the same ingredients as the pre-hybridisation buffer, listed above, with a final concentration of 0.4µg/ml DIG labelled probe added to it also. This was incubated overnight at 58°C. 300µl per slide of hybridisation buffer was used

and the slides were covered in parafilm. The slides were placed in trays containing paper towels soaked in 50% Formamide and 5x SSC. The trays were then sealed. This was done to maintain a humidified environment in order to prevent the slides from drying out. From day 2 DEPC-treated solutions were no longer needed. Post-hybridisation wash solutions were prepared and allowed to pre-warm before the procedure was continued. Antisense and sense probes were kept separate during at least the first wash step, to prevent contamination between the two. To continue the protocol the parafilm was removed from the slides and they were washed twice for 30 minutes in 2x SSC at room temperature. They were then washed in 2x SSC for 1 hour at 65°C. After which they were washed in 0.2x SSC for 1 hour at 65°C. The slides were then washed in PBS/0.05% Tween-20 for 10 minutes at 65°C. Finally they were washed in PBS/Tween-20 for 10 minutes at room temperature. During this time the blocking solution was prepared. This contained final concentrations of 1x PBS, 0.05% Tween-20, 5-20% sheep serum, 0.5-5% milk powder and was diluted in autoclaved H_2O. The sections were incubated in the blocking solution for 2 hours at room temperature in humidified conditions. After this the sections were incubated overnight at 4°C in the same blocking solution as listed above, but also contained anti-DIG-AP (Roche) diluted to 1:5000. The third day began with three 30 minute post-antibody washes in PBS/0.05% Tween-20 at room temperature. The slides were then equilibrated for 5 minutes in alkaline phosphatase buffer, which consisted of final concentrations of 100mM Tris/HCl, 100mM NaCl, 50mM $MgCl_2$ diluted in autoclaved H_2O at pH9.5. The sections were then incubated in developing solution. This was made by adding 45µl NBT and 35µl BCIP per 10ml alkaline phosphatase buffer. The slides were then incubated at room temperature in the dark for a few hours to overnight for developing to occur, keeping watch over

their progress, making sure they were not over-developed. This reaction was stopped by washing in PBS. The sections were then post-fixed in 4% PFA for 20 minutes. They were washed in DEPC-H_2O and dehydrated by submerging once in 70%, 90%, twice in 100% ethanol and twice in Histoclear (National diagnostics) for two minutes each step. The slides were then mounted with Eukitt (Fluka) for imaging and prolonged storage.

2.5 Preparation of neural tube explants

The abdominal cavities of time-mated female mice were opened by making two incisions through the abdominal wall and underlying peritoneum, one horizontally and one vertically in the midline. The bicornuate uterus was dissected away from both ovaries and transected at the cervix. The embryos and uterus were placed in DMEM with 4500mg glucose/L, L-glutamine, $NaHCO_3$ and pyridoxine.HCl (Sigma D5796) plus 10% neonatal calf serum (v/v) (NCS, Gibco) at 37°C. Glass cover-slips were coated in 0.5% gelatine. They were incubated at 37°C for one hour. The gelatine was then removed and replaced by DMEM plus 5% NCS (v/v) and 5% horse serum for immediate use. All maternal and extra-embryonic tissues were removed from each embryo using forceps (Fine Science Tools, size 55). The vagal neural crest was excised by removing all tissues rostral to somite one, and caudal to somite seven using tungsten needles. The embryonic pieces were then typsinised in 0.05% trypsin (in PBS, v/v) (Gibco) at 4°C for 30 minutes to dissociate all unwanted tissues i.e. somites, heart, underlying mesenchyme. After incubation in trypsin the samples were drenched in media plus serum and freed by micro-dissection from remaining surrounding tissues. The neural tubes were then

transferred into 24 well plates with gelatine-coated coverslips containing pre-warmed (37°C) DMEM (Sigma) plus 5% NCS and 5% horse serum (Sigma) (Jaenisch 1985) for overnight incubation.

Neural tube explants were photographed at specific time-points over a 7 day period. Cells were measured from the outer margin of the explant to the migration front (μm). This was calibrated against the scale bar. Each image was taken with a 10x objective and was scaled to 10cm by 7cm so they could be placed on to A4 paper. The scale bar for each image was 200μm, which measured 15mm on the page, meaning each 1mm measured approximately 13μm of migration. For example if a sample measured 10mm on the page then the calculation performed to convert this number to microns would be 200/15 x 10 = 133μm.

Neural tube explants were fixed for 10 minutes at room temperature in 4% PFA. Immunofluorescence was carried out at varying time-points following the protocol for immunofluorescence on frozen sections, described on page 50 of this thesis.

Sharpening tungsten needles

Tungsten wires were placed into metal holders. Protective gloves were worn throughout. A glass beaker was filled with sodium hydroxide (NaOH) and a large paper clip was hung over the side so that it was partially sub-merged. This acted as one electrode. Two wires were attached via crocodile clips to the positive and negative parts of a 9V battery. One wire was attached to the paperclip and the other wire was connected to the metal holder containing the tungsten wire, acting as the second electrode (Figure 2.1) (Brady 1965). The tungsten wires were sharpened to a fine point by quickly dipping the tip up and down in the NaOH. Tiny bubbles

appeared when the tungsten wire was sub-merged indicating that the circuit was complete. The tungsten wire was examined under a dissecting microscope to gauge sharpness.

2.6 Culture of kidney-derived stem cells

Kidney-derived stem cells (KSC) were obtained from Dr Patricia Murray's lab, University of Liverpool (Fuente Mora, Ranghini et al. 2011). KSC were seeded on 8-well chamber slides in high glucose DMEM (Invitrogen) supplemented with 2mM glutamine and 10% FCS. KSC were cultured until approximately 70% confluent.

SiRNA silencing of *Wt1* gene expression

This protocol was adapted from the original obtained from Dr. Michael Cross, University of Liverpool. Two sterile tubes each containing 50µl of Optimem media (Gibco/Invitrogen) were set up. To one of these tubes 0.5µl Lipofectamine 2000 (Invitrogen) was added to give a final concentration of 0.1% v/v, to the other tube 15µl siRNA duplex (10µM stock solution) was added. The solutions were incubated at room temperature for 5 minutes. After incubation, the Lipofectamine mixture was slowly added to the tube containing the SiRNA (Qiagen). The solutions were mixed by gently pipetting up and down. This was then incubated for 30 minutes at room temperature in order to allow the siRNA to form a complex with the Lipofectamine. Just prior to the end of this incubation, the chamber slides containing the KSC we prepared for transfection. This was achieved by aspirating the media and adding 0.4ml Optimem per chamber. 115µl of transfection mix was

added slowly to each chamber to give a final volume of 515µl. The chamber slide was then gently swirled to ensure the solutions were mixed sufficiently. The slides were then incubated for 4 hours at 37°C. After the incubation step the transfection mix was aspirated from the slides and the cells were washed twice with PBS containing Mg^{2+} /Ca^{2+}, whilst gently swirling the slides to ensure a thorough wash. The PBS Mg^{2+} /Ca^{2+} wash step was repeated. After the cells had been thoroughly washed the PBS was aspirated and 0.4ml of KSC media was added to the cells and they were returned to the incubator at 37 °C. After 48 hours in culture the cells were prepared for immunofluorescence as described on page 50 of this thesis.

2.7 Microscopy and image capture

Fluorescent microscopy was carried out on an upright Leitz DMRB (Leica microscope). Dissection of neural tube explants was conducted using a Leica M165FC dissection microscope. The migration of NCCs from neural tube explants was imaged using the inverted Leica DMIRB microscope. All images taken during these experiments were captured using Leica Application Suite V3 software. Confocal microscopy was carried out using the Leica DMIRE2 microscope and images were captured using Metamorph® software. Images were viewed and compiled using Adobe Photoshop and Illustrator CS2.

2.8 General reagents and solutions

10x Phosphate buffered saline (PBS), 1L

80g NaCl (Sigma), 2g KCl (Sigma), 14.4g Na_2HPO_4, and 2.4g KH_2PO_4 was added to 800ml H_2O, pH adjusted to 7.4, filled to a final volume of 1L with H_2O and autoclaved.

4% (w/v) paraformaldehyde (PFA), 100ml

4g PFA (Fisher scientific) was dissolved in 10ml 100ml 1x PBS. This was sterile filtered and kept at 4°C for up to two weeks.

25% (v/v) Triton solution, 100ml

25ml Triton (Fluka) was added to 75ml 1x PBS. This was further diluted in PBS to 0.25% as a working solution.

2% (w/v) Bovine serum albumin (BSA) solution, 100ml

2g BSA (Fluka) was diluted in 100ml 1x PBS at 37°C and then stored at 4°C.

DEPC-H_2O, 1L

100µl (0.01% v/v) DEPC was added to 1L H_2O. This was stirred over night at room temperature, then autoclaved

TE

10mM Tris-HCl and 1M EDTA adjusted to pH 8.0

Luria broth (LB), 100ml

2g LB dissolved in 100ml H_2O

LB trans media

LB supplemented 10mM $MgSO_4$, 10mM $MgCl_2$ and 20mM glucose. The high glucose content allows for bacterial recovery.

TENS buffer

TE, 0.1M NaOH and 0.5% (w/v) sodium dodecyl sulphate (SDS).

20x Sodium chloride, sodium citrate (SSC)

175.3g NaCl and 88.2g sodium citrate were dissolved in 800ml H_2O, the pH was adjusted to 7.0, and the final volume was adjusted to 1L. Final concentrations were 3.0M NaCl and 0.3M sodium citrate.

Sodium hydroxide (NaOH)

400g NaOH pellets (Fisher scientific) were slowly added to 800ml H_2O, stirring continuously. The beaker was kept on ice and once the pellets had completely dissolved the volume was adjusted to 1L with H_2O.

NB This is an exothermic reaction resulting in a large amount of heat energy which can break glass beakers. It is therefore prepared in a plastic beaker.

3M Sodium Acetate (NaAc)

246.09g NaAc (Sigma) was dissolved in 800ml H_2O. The pH was adjusted to 5.2 with glacial acetic acid and H_2O was added to a final volume of 1L.

10x Tris-buffered saline (TBS), 100ml

8g NaCl, 0.2g KCl and 25ml 1M Tris in H_2O were adjusted to pH7.5 and H_2O was added to make a final volume of 100ml.

Table 2.1 Information on antibodies used throughout immunofluorescence experiments in this thesis

Primary antibodies				
Name of Antibody	**Polyclonal/ Monoclonal**	**Raised in**	**Company**	**Dilution**
Wt1	M	Mouse	Upstate	1µg/ml or 1:500
Wt1	P	Rabbit	Santa Cruz	1:200 – 1:500
Sox10	P	Goat	Santa Cruz	1:100
Hu	M	Mouse	Invitrogen	200ng/ml or 1:50
P75	P	Rabbit	Abcam	1:500
Foxd3	P	Rabbit	Patricia Labosky	1:1000
B-Gal	P	Rabbit	Cappel/ICN	1:5000
Tuj1	M	Mouse	Abcam	1:500

Secondary antibodies				
Raised in	**Reacts against**	**Company**	**Spectral data**	**Dilution**
Donkey	Rabbit	Invitrogen	Alexa fluor® 488	1:1000
Donkey	Mouse	Invitrogen	Alexa fluor® 488	1:1000
Donkey	Goat	Invitrogen	Alexa fluor® 568	1:1000
Goat	Rabbit	Invitrogen	Alexa fluor® 488	1:1000
Goat	Mouse	Invitrogen	Alexa fluor® 568	1:1000
Goat	Rabbit	Jackson ImmunoResearch	Horse radish peroxidise (HRP)	1:500
Chicken	Rabbit	Invitrogen	Alexa fluor® 488	1:1000
Chicken	Goat	Invitrogen	Alexa fluor® 594	1:1000

4',6-Diamidino-2-phenylindole (DAPI)	Sigma	1:1000

Table 2.2 Fixation times using 4% PFA for different mouse embryonic stages. Fixation times varied according to the size/stage of the embryo and the subsequent technique these are shown in the table below

Embryonic stages	Immunohistochemistry	In situ hybridisation
E7.5	30 minutes	30 minutes
E8.5	45 minutes	45 minutes
E9.5	1 hour	1 hour
E10.5	1 hour	1 hour 15 minutes
E11.5 – E14.5	1 hour 30 minutes	-
E15.5 – E16.5	2 hours	-

Table 2.3 Optimal Proteinase-K digestion times for mouse embryos. Digestion times varied according to the size and stage of the embryo and are shown in the table below

Embryonic stage	Digestion times
E7.5	30 seconds
E8.5	45 seconds
E9.5	60 seconds
E10.5	90 seconds

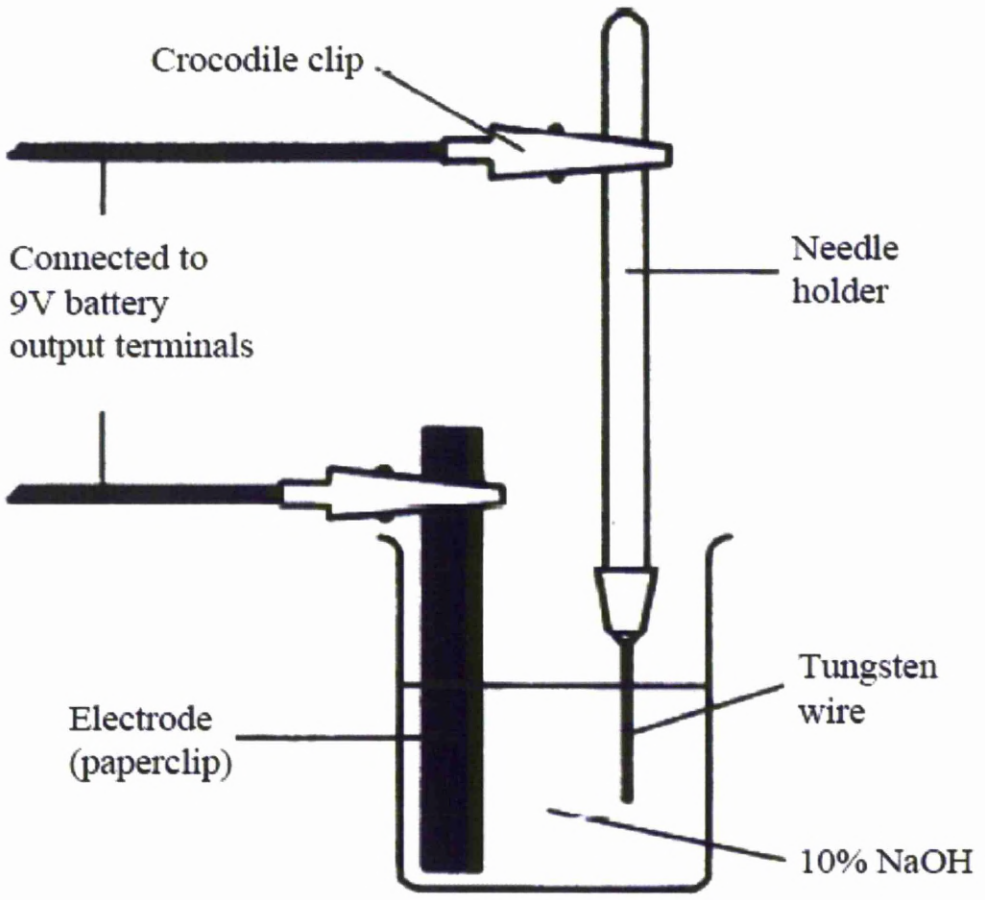

Figure 2.1 Schematic diagram representing the apparatus needed to electrolytically sharpen tungsten wires for dissection techniques.

Figure adapted from Brady, 1965

Chapter 3

Results

3.1 The expression of Wt1 in the developing enteric nervous system

Previous findings using the Wt1-Cre Rosa-26-R mouse line revealed that Wt1 is expressed in the enteric nervous system (ENS) of the adult mouse (Figure 1.8). This result indicates that Wt1 had to have been expressed in the ENS during its development from the neural crest. The aim of this chapter is to produce a time-course, which will show where Wt1 is expressed and elucidate the time at which Wt1 was expressed in NCCs during embryonic development and in particular the formation of the ENS. This was achieved by using immunofluorescence on tissue sections and whole mount immunohistochemistry to look at protein expression. Specific antibodies were used to locate NCCs within the mouse embryo, paying particular attention to the developing ENS when conducting co-staining experiments with Wt1 antibodies. To study mRNA expression of Wt1, in situ hybridisation was employed. These experiments were carried out on frozen sections and whole-mount preparations generated from wild-type mouse embryos between embryonic stages E7.5 and E16.5 the pattern of expression od Wt1 was then documented.

3.2 Wt1 expression in the developing mouse ENS at E16.5

According to the immunofluorescence data provided by B. Wilm (unpublished), β-galactosidase, which marks Wt1-derived cells in the Wt1-Cre mouse, was found to co-localise with neuronal marker Hu in the intestinal plexuses of the newborn mouse gut (Figure 1.11). Wt1 must have been expressed in the precursors of the ENS (NCCs) at a particular time-point in mouse embryonic development. To test this hypothesis I began by preparing sections of E16.5 mouse embryos for immunofluorescence and in situ hybridisation. Firstly, using antibodies against

Wt1 and the pan neuronal marker Hu to show the location of neuronal cells within the developing ENS, the immunofluorescence experiments confirmed that at E16.5 in mouse there is no expression of Wt1 in the developing ENS (Figure 3.1). Wt1 was found to be expressed in the nuclei of the mesothelial cells on the outer most margin of the intestine (Figure 3.1, A and C). Hu was expressed in the enteric neurons of the developing ENS. There was no co-localisation between Wt1 and Hu at this time-point.

A similar result was found when analysing Wt1 and the neural crest/glial marker, Sox10 using immunofluorescence (Figure 3.2). Sox10 was expressed in the ENS (Figure 3.2, A and B). Wt1 was expressed in the mesothelial lining of the gut and in the mesentery, which is a double layered sheet of mesothelial cells anchoring the intestinal tract to the posterior abdominal wall. The co-staining revealed that Sox10 and Wt1 are mutually exclusive at this time-point.

In order to confirm that my Wt1 probe generated for RNA in situ hybridisation was functional, I conducted experiments on frozen sections of E16.5 mouse. In the kidney region Wt1 was found to be expressed in the glomeruli of the developing metanephric kidney (Figure 3.3, A). This finding corresponds to that described in the literature (Armstrong, Pritchard-Jones et al. 1993). This indicated, therefore, that the antisense RNA probe was suitable for studying Wt1 expression and investigating if Wt1 is expressed in the ENS of the developing mouse.

As the Cre system had marked cells that were derived from cells that had to have at some time expressed Wt1, these results suggest that the expression of Wt1 in the

developing ENS must have occurred at an earlier time-point in development than E16.5.

3.3 Wt1 expression in the developing ENS at E13.5

Following the results at E16.5, whereby Wt1 was not found to be expressed in NCCs of the developing ENS, I decided to investigate the earlier embryonic stage of E13.5: Could this be the time-point at which Wt1 was expressed within the developing ENS?

Using the Wt1 probe I carried out RNA in situ hybridisation on frozen sections taken from E13.5 wild-type mouse embryos. The results from these experiments showed Wt1 was expressed in the mesothelia surrounding the abdominal cavity and the intestine (Figure 3.4, A and B), in the gonad, the urogenital mesentery and developing metanephric kidney.

Looking at the protein expression of Wt1 at this stage using immunofluorescence (Figure 3.5, A-C), Wt1 protein matched the RNA in situ hybridisation data. Wt1 expression was expressed in the mesothelia (Figure 3.5, A and C). Co-staining revealed the expression of the neural crest cell marker Sox10, to be detected solely in the ENS region of the intestine (Figure 3.5, B and C). There was no co-localisation between Wt1 and Sox10 at this time-point within the ENS (Figure 3.5, C). I continued to use Sox10 as the marker for the ENS from this point onwards as it marks ENS precursors unlike Hu, which only marks cells with a neuronal fate.

The findings were similar to those seen using immunofluorescence at E16.5. The results indicate that the expression of Wt1 in the developing ENS must have occurred at an earlier embryonic stage to account for the co-expression of β-Galactosidase and the neuronal marker Hu in the ENS of the newborn Wt1-Cre mouse (Figure 1.11).

3.4 Wt1 expression in the ENS at E12.5

As I was unable to detect Wt1 within the ENS of the E13.5 mouse embryo, I prepared E12.5 mouse sections for Wt1 and Sox10 immunofluorescence co-staining. Wt1 was detected in the same expression pattern as previously described in that it was expressed in the mesothelia surrounding the intraembryonic coelom and abdominal viscera (Figure 3.6, A-F). It was also expressed in the developing kidney and gonad (Figure 3.6, A and C). However, as was the case at E13.5 and E16.5 Wt1 did not co-localise with Sox10 and was therefore not expressed in the ENS at this stage of development (Figure 3.6, A-F). These results indicate that an even earlier time-point must be considered to find expression of Wt1 within the developing ENS.

3.5 Wt1 expression in the developing ENS at E11.5

Examining an earlier time-point still, I prepared E11.5 mouse embryo sections for immunofluorescence. This was done in order to explore Wt1 expression at this stage of development with the view to detecting Wt1 within the ENS. Co-staining of Wt1 and Sox10 revealed an extremely similar picture to that described at E12.5. Wt1 was expressed in the mesothelium surrounding the abdominal cavity and its contents (Figure 3.7, A-F). There was no co-localisation between Sox10 and Wt1

in the ENS of the midgut at this time-point (Figure 3.7, D-F). Wt1 was also detected in the pleura enveloping the lungs and the mesothelium surrounding the oesophageal region of the foregut (Figure 3.8, A-C). However, co-localisation between Wt1 and Sox10 in the ENS of the foregut was not found (Figure 3.8, C). Putative expression of Wt1 was also seen in the mesonephros, which is the developing urogenital system, and the gonadal ridge. The mesonephric tubules were negative for Wt1 (Figure 3.8, D) as would be expected according to previous findings in the literature (Armstrong, Pritchard-Jones et al. 1993). Wt1 was also detected in the epicardium of the heart (Figure 3.8, E). It is worth noting that Sox10 was found to be expressed in the midgut. However, there was no Sox10 expression found in the hindgut (Figure 3.7, B and C). This corresponds to the literature, whereby NCCs have migrated through the entire foregut and have migrated through the caecum but have not yet reached the hindgut at this stage (Kapur, Yost et al. 1992; Young, Hearn et al. 1998).

These findings signify that in order to disclose expression of Wt1 within the developing ENS investigation was required into the earlier embryonic stages of mouse development, starting with the examination of E10.5 embryos.

3.6 Wt1 expression in the developing ENS at E10.5

I conducted immunofluorescence experiments on frozen sections of E10.5 mouse embryos, as my previous results had failed to show Wt1 expression within the ENS. This suggested that Wt1 must have been expressed earlier in development based on the β-galactosidase expression in the ENS of the Wt1-Cre newborn mouse. My findings from experiments on E10.5 embryos revealed Wt1 expression

in the intermediate mesoderm, the mesothelium surrounding the foregut and body cavity, and in the epicardium lining the developing heart (Figure 3.9, A and C). Sox10 positive NCCs migrating towards the foregut from the neural crest passed very closely to the Wt1-expressing intermediate mesodermal cells. However, they remained mutually exclusive (Figure 3.9, C and Figure 3.10, A-C). There was no co-localisation of Wt1 and Sox10 within the ENS of the foregut at this stage (Figure 3.9, C). Wt1 was found to be expressed in the mesonephric mesenchyme, the dorsal mesentery anchoring the gut tube to the posterior abdominal wall, and in the mesothelium lining the coelomic cavity and the intestinal tract (Figure 3.10, D-F). There was no expression of Wt1 found within the ENS distal to the heart region (Figure 3.10, F). These findings correspond to whole-mount RNA in situ hybridisation data (Figure 3.11, B). From the lateral aspect Wt1 activity could be seen in the intermediate mesoderm along the length of the trunk, in the epicardium of the heart, in the septum transversum and intraembryonic coelom. However, all these findings suggest that Wt1 expression in the developing ENS must have occurred even earlier in development.

3.7 Wt1 expression in the developing mouse ENS at E9.5

My previous findings showed no expression of Wt1 in the developing ENS between E16.5 and E10.5. This indicates that Wt1 must have been expressed at an earlier time-point in ENS development. It has been reported by the use of immunohistochemistry, carried out by Anderson in 2006, that Sox10-expressing neural crest cells pass through the region of the intermediate mesoderm during their migration to the foregut at E9.5 in the mouse (Figure 3.12, A). The intermediate mesoderm at this embryonic stage expresses Wt1 (Figure 3.12, B).

Following these findings it was hypothesised that, during the migration of NCCs from the neural crest to the foregut, Wt1 is up-regulated in these cells as they migrate through the already Wt1 expressing intermediate mesoderm (Figure 3.12, C).

Immunofluorescence analysis was carried out on sectioned E9.5 mouse embryos using antibodies for Wt1 and the migrating NCC marker Sox10. Results from these experiments showed that Sox10 positive NCCs do indeed pass through the intermediate mesoderm region (Figure 3.13, A, B, D and E). However, the Wt1 positive and Sox10 positive cells remained mutually exclusive in this area (Figure 3.13, A and D). Thus there was no co-localisation between Wt1 expressing cells and neural crest cells at E9.5 in this area, at this time point. Immunofluorescence also revealed Wt1 expression in the septum transversum (Figure 3.10, A), lining the intraembryonic coelom (Figure 3.14, A and C), in the mesonephros (Figure 3.14, B and D), and in the epicardium enveloping the heart (Figure 3.14, E). However, the distal portion of intestine and coelomic cavity was negative for Wt1 (Figure 3.14, B). This is because this area was found to be initially devoid of mesothelium, but as development progresses mesothelial cells were found to migrate to and surround the gut tube (Wilm, Ipenberg et al. 2005).

This data indicated that an even earlier embryonic time-point must be investigated to find Wt1 expression in the developing ENS. The literature has never reported expression of Wt1 before E9.0 in the mouse (Armstrong, Pritchard-Jones et al. 1993; Moore, Schedl et al. 1998). However, as the time-point at which Wt1 was expressed in the developing ENS has not been determined from my findings so far,

it can be assumed that Wt1 must have been expressed at a time before NCCs had reached the foregut. It was therefore important to consider the E8.5 mouse embryo as a possible candidate for Wt1 expression in NCCs that had just begun their migration to the foregut.

3.8 Wt1 expression in NCCs of the developing E8.5 mouse embryo

Following my previous data collected between the embryonic stages of E16.5 and E9.5, which had revealed there to be no expression of Wt1 in ENS precursors, I carried out whole-mount RNA in situ hybridisation for Wt1 on E8.5 mouse embryos. This was done in order to determine if a signal for Wt1 could be detected and if so to study where expression of Wt1 was found. Wt1 mRNA was expressed in the E8.5 mouse embryo (Figure 3.15, A). Wt1 could be seen in the head and branchial arch region, in the neural folds, the primitive heart and caudal to the heart around the somites. Sections taken from the whole-mount preparations revealed Wt1 in specific cells within the embryo (Figure 3.15, B-D). Wt1 signal was localised to the neural folds and what looked like the neural crest region (Figure 3.15, C and D, figure 3.16, A-C). The negative controls showed no unspecific signal. This suggested that the Wt1 signal detected in these experiments was not an artefact.

In order to confirm these results, whole-mount immunohistochemistry using horse-radish peroxidise/DAB staining instead of a fluorophore was carried out on E8.5 embryos to determine if there was Wt1 protein being expressed. The results from this experiment tended to correspond with the in situ hybridisation data. Wt1 signal was found in the neural folds (Figure 3.17, A). The dorsal surface of the embryo

revealed staining for Wt1 in what look like streams of cells migrating away from the neural tube. This was seen along the length of the closed part of the neural tube, including the region of interest, adjacent to somites 1-7 (Figure 3.17, B): This is the portion of crest that will go on to from the ENS (Yntema and Hammond 1954). The negative control was clear (Figure 3.17, C). This suggested that this result was not an artefact.

Immunofluorescence was carried out on frozen sections taken from E8.5 mouse embryos. These were co-stained for Wt1 and the neural crest cell marker Sox10. Wt1 was expressed in various cells throughout the E8.5 embryo, most importantly in the neural folds (Figure 3.18, A and B). Wt1 was detected in cells in the region of the neural crest. The area contained within the orange box (Figure 3.18, B,D and F) contains 70 cells. Approximately 45% of these cells were Sox10 positive, 30% were Wt1 positive. Approximately 20% of these cells were positive for both Sox10 and Wt1, 15% were sox10 positive and Wt1 negative, and 10% were Wt1 positive and Sox10 negative. This suggested Wt1 was being expressed in some NCCs at this stage (Figure 3.18, E and F).

In order to confirm this result and to determine if there was co-expression of the two proteins in the same cell nuclei, I used confocal microscopy to detect antibodies against Wt1 and Sox10 (Figure 3.19). The results from this experiment revealed that Wt1 and Sox10 were co-localising in the same cell nuclei of neural crest cells (Figure 3.19, A). Out of the 190 cells in the field of view (Figure 3.19) Wt1 was found in the nuclei of approximately 30% of cells (Figure 3.19, A and C). However, there was also some Wt1 staining seen in the cytoplasm of these cells.

Approximately 35% of the cells in the neural crest region were Sox10 positive (Figure 3.19, B) and, therefore, were NCCs. Around 20% of NCCs expressing Sox10 also expressed Wt1 (Figure 3.19, A). Approximately 5% were Sox10 positive and Wt1 negative, and around 10% were Wt1 positive and Sox10 negative (Figure 3.19, A). The negative controls did not reveal any unspecific staining (Figure 3.19, D and E). These results further indicate that Wt1 is expressed in a population of neural crest cells at E8.5.

3.9 Differential expression of Wt1 proteins detected with Wt1 antibodies

The immunofluorescence data described in this chapter were obtained by using both the polyclonal rabbit Wt1 antibody (Santa Cruz) and the monoclonal mouse Wt1 antibody (Upstate). Throughout these studies both the polyclonal and monoclonal antibodies could be used to detect Wt1 protein between E16.5 and E9.5 (Figure 3.20, A and B). However, at E8.5 and E7.5 the monoclonal antibody failed to detect genuine nuclear Wt1 activity (Figure 3.20, C and D). This observation leads to the question: Why this there a difference between the two antibodies at these early embryonic time-points?

The data from E8.5 mouse embryos combined indicate that Wt1 is expressed in NCCs that will go on to form the ENS in mouse. Therefore, LacZ and β-Galactosidase expression found in the ENS of adult and new-born mice (Figure 1.7 and Figure 1.10) appears to originate from this early stage of neural crest formation. The question arises from these results: Is *Wt1* expressed at earlier time-points in neural crest cells?

3.10 Wt1 expression in the E7.5 mouse embryo

In order to investigate if Wt1 was expressed at an earlier time-point than E8.5 I carried out whole-mount in situ hybridisation on E7.5 mouse embryos (Figure 3.21). The results from these experiments revealed Wt1 was expressed in the neural folds and underlying mesenchyme (Figure 3.21, A and B). The negative control was clear, which suggests this result is authentic.

I carried out immunofluorescence experiments for Wt1 and Sox10 at E7.5 (Figure 3.22). The results from these experiments showed that Wt1 is expressed in the E7.5 mouse embryo (Figure 3.22, A). Wt1 expression was found in the nuclei of cells within the primitive streak, neuroepithelium, intraembryonic mesoderm, and in embryonic endoderm (Figure 3.22, A, C and D). There was also cytoplasmic Wt1 staining found in the cells in these regions (Figure 3.22, D arrows). However, co-staining with Sox10 revealed there was no expression of Sox10 at this time point (Figure 3.22, B, C and D). The negative controls from this experiment did not reveal any unspecific staining suggesting the results were genuine.

3.11 Conclusion

The findings presented in this chapter lead me to the conclusion that Wt1 is expressed in the NCCs, some of which will migrate to the gut to form the ENS. Importantly Wt1 expression is transient in these NCCs at E8.5, since at E9.5 there if no longer any Wt1 detected in ENS precursors within the gut tube. This observation leads to an important question: If Wt1 is expressed in NCCs along the neural crest at E8.5, what is its role in these cells?

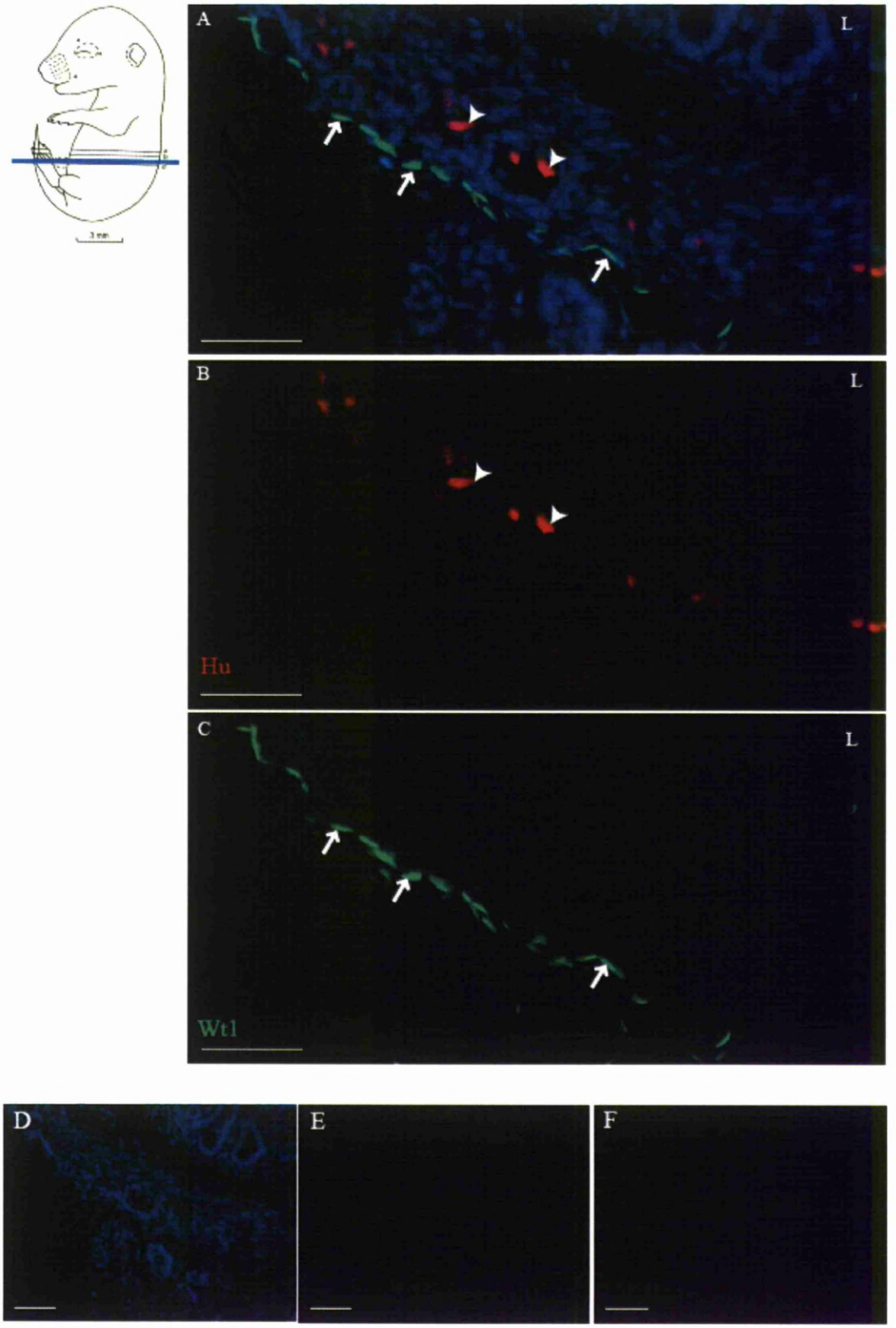
A
L
B
L
Hu
C
L
Wt1
D
E
F

Figure 3.1 Immunofluorescence for Wt1 and Hu in E16.5 mouse intestine

The schematic image of an E16.5 mouse embryo shows the level at which Images A-F were taken, this is represented by a blue line (Kaufmann 1992). Image A is a composite image showing Wt1 (green, arrows) in the mesothelia, the neuronal marker Hu (red, arrowheads) in the ENS, and the nuclear marker DAPI (blue) showing the structure of the gut section. Image B shows Hu (red) in the ENS only. Image C shows Wt1 (green) in the mesothelia surrounding the gut. There is no expression of Wt1 within the ENS. Images D-F show negative controls. Image D is DAPI showing cell nuclei. Image E shows Alexa fluor 488 goat anti rabbit and Image F shows Zenon IgG2b 488. All images were taken with a 40x objective. L, lumen. Scale bars 50μm (A-C) 100μm (D-F).

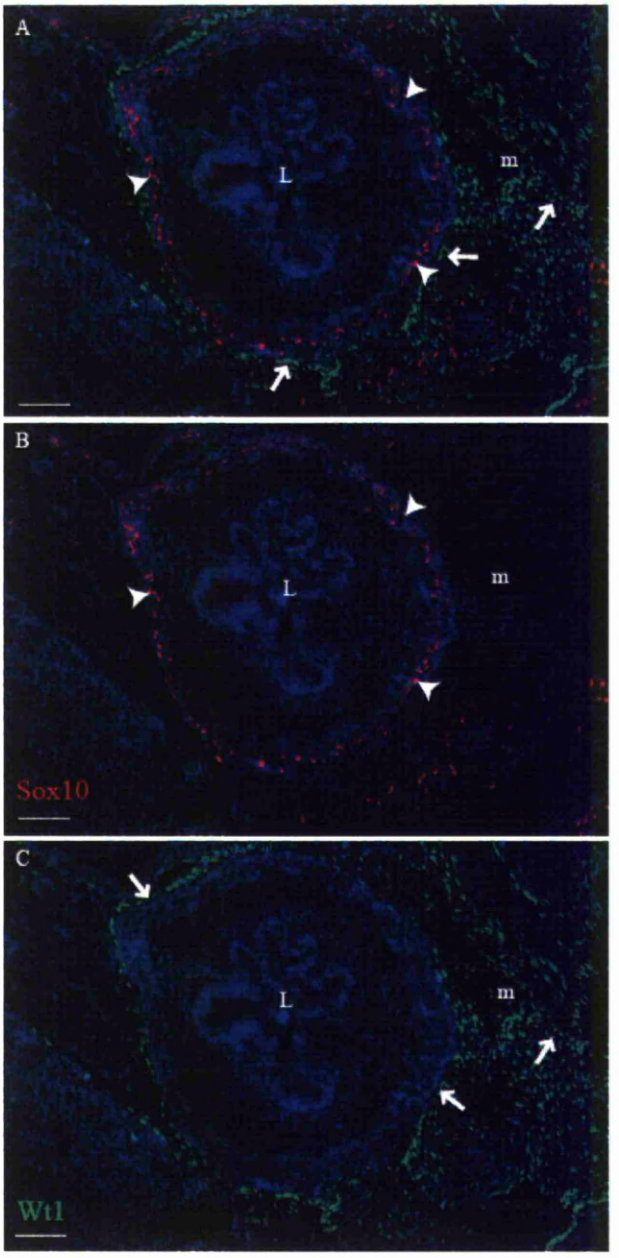
A
L
m
B
L
m
Sox10
C
L
m
Wt1


D
E
F

Figure 3.2 Immunofluorescence for Wt1 and Sox10 in the intestine at E16.5

The sections were taken from a similar level to that shown on the schematic diagram in Figure 3.1. A is a composite image showing expression of Wt1 (green, arrows) in the mesothelia and the ENS precursor marker Sox10 (red, arrowheads) in the ENS. Image B shows Sox10 staining. Image C shows Wt1 staining. DAPI is shown in blue (A-C). There is no Wt1 expression in the ENS. D-F are images of the negative controls. DAPI is shown in D. Alexa 488 donkey anti rabbit is shown in E. Alexa 568 donkey anti goat is shown in F. The negative controls do not show any unspecific staining. All images were taken with a 20x objective. L, lumen. m, mesentery. Scale bars 50μm (A-C) 100μm (D-F)

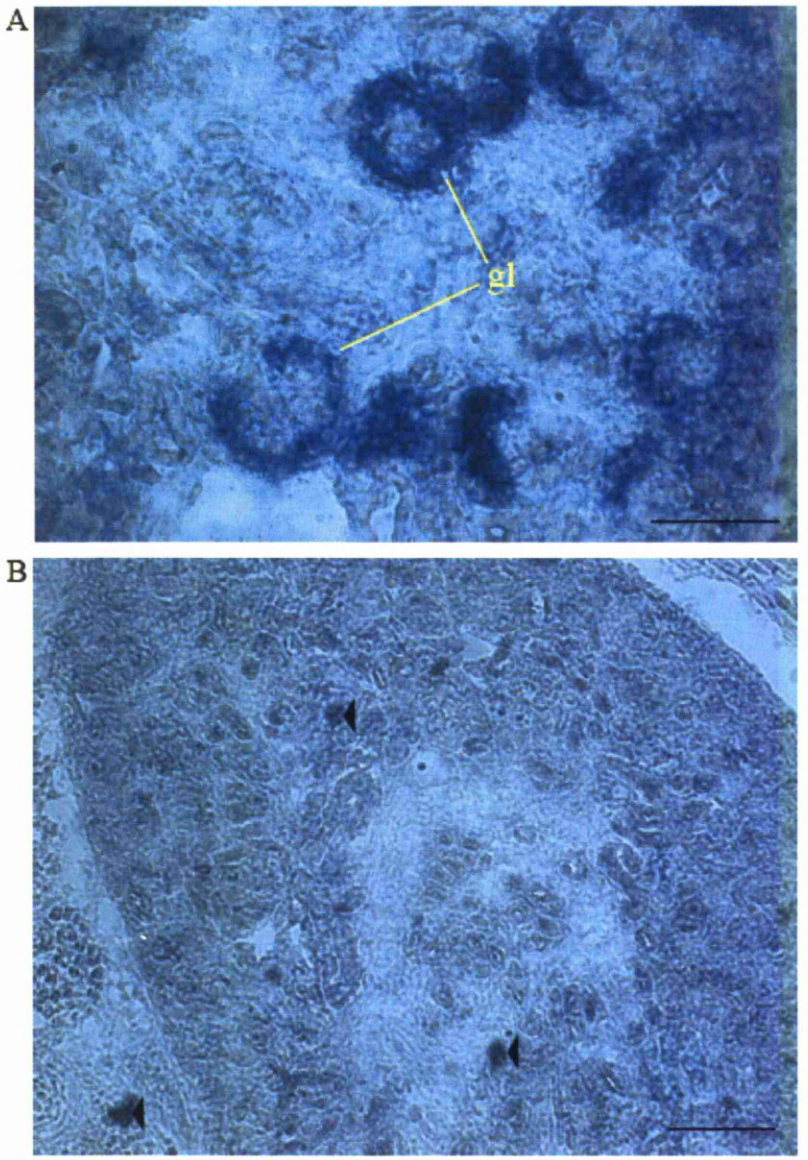

Figure 3.3 Wt1 in the kidney at E16.5

Wt1 RNA in situ hybridisation on transverse sections through E16.5 kidney (A and B) using an antisense probe (A) and sense probe as the negative control (B). A shows Wt1 activity in the developing nephron (gl). B shows some back ground staining but there is not specific Wt1 signal. The arrowheads show dirty patches on the microscope objective. A was taken with a 40x objective and B was taken with a 10x objective. Scale bars 50μm (A) 100μm (B)

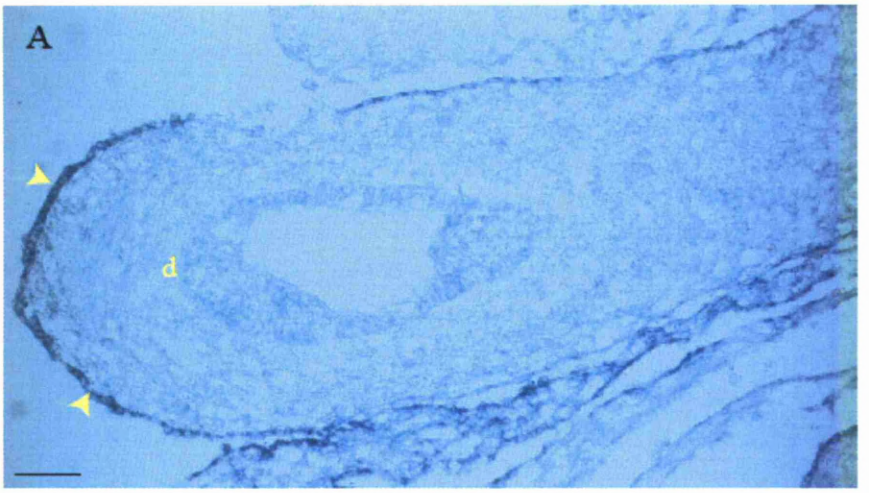
A
d

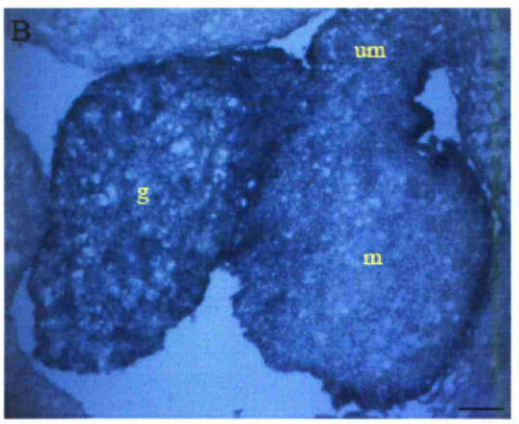
B
um
g
m

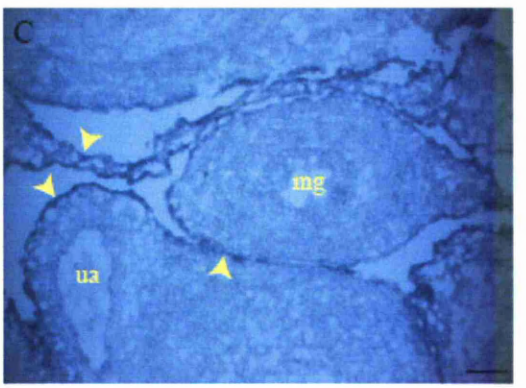
C
mg
ua

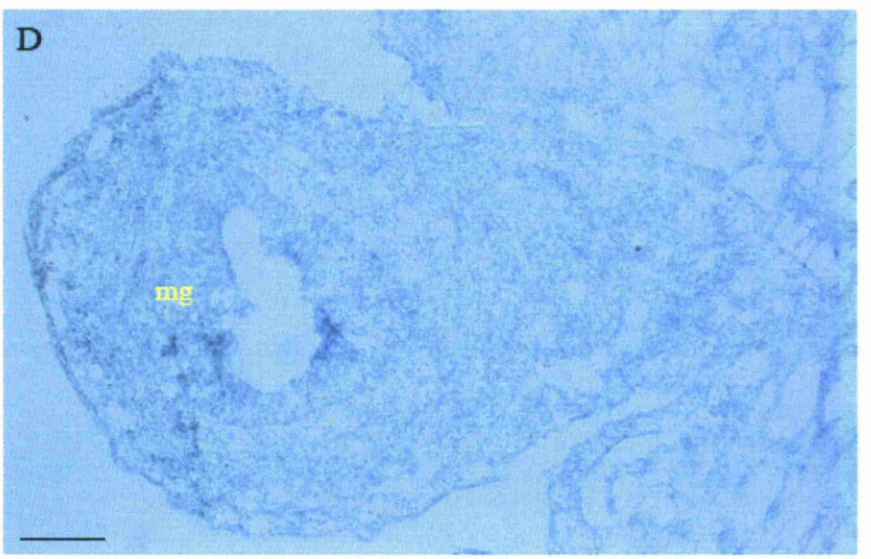
D
mg

Figure 3.4 Wt1 in the E13.5 mouse embryo

Images A-D show Wt1 RNA in situ hybridisation on transverse sections through the gastrointestinal tract of E13.5 mouse embryos. An antisense probe was used in images A-C and the negative control is shown in image D using a sense probe. Wt1 is seen in the mesothelia surrounding the duodenum (d, image A), in the gonad (g), in the developing metanephric kidney (m), the urogenital mesentery (um, image B), and in the mesothelia surrounding the midgut (mg, image C). Wt1 is not found in the region of the ENS. The negative control shows some background staining but no unspecific Wt1 signal (D). Images A-D were taken using a 20x objective. ua, umbilical artery. Scale bars 50μm (A and D) 100μm (B and C).

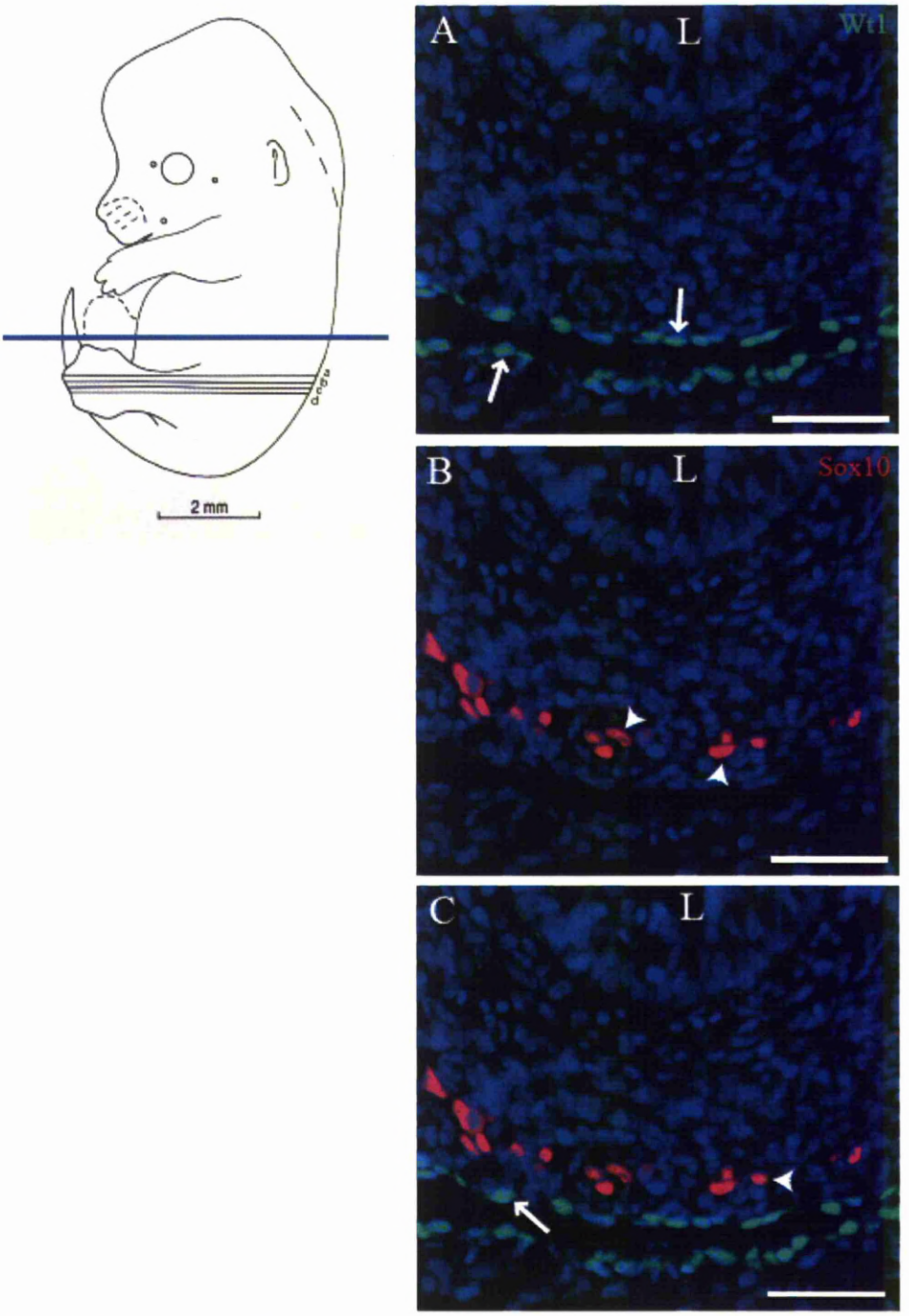
2 mm
A
L
Wt1
B
L
Sox10
C
L
D
E
F

Figure 3.5 Wt1 and Sox10 expression in the E13.5 mouse intestine

The blue line shown on the schematic diagram of E13.5 mouse embryo represents the level at which the sections were taken in images A-F (Kaufmann 1992). A-F were taken with a 40x objective and are immunofluorescence images showing Wt1 (green, white arrows, A), Sox10 (red, white arrowheads, B), and a composite (C). DAPI is shown in blue (A-C). There is no Wt1 staining in the ENS. D-F show images taken of the negative control. DAPI is seen in D. E shows Alexa 488 donkey anti rabbit and F shows Alexa 568 donkey anti goat. No unspecific staining is seen in the controls (E and F). L, lumen. aw, abdominal wall. Scale bars 50μm (A-F).

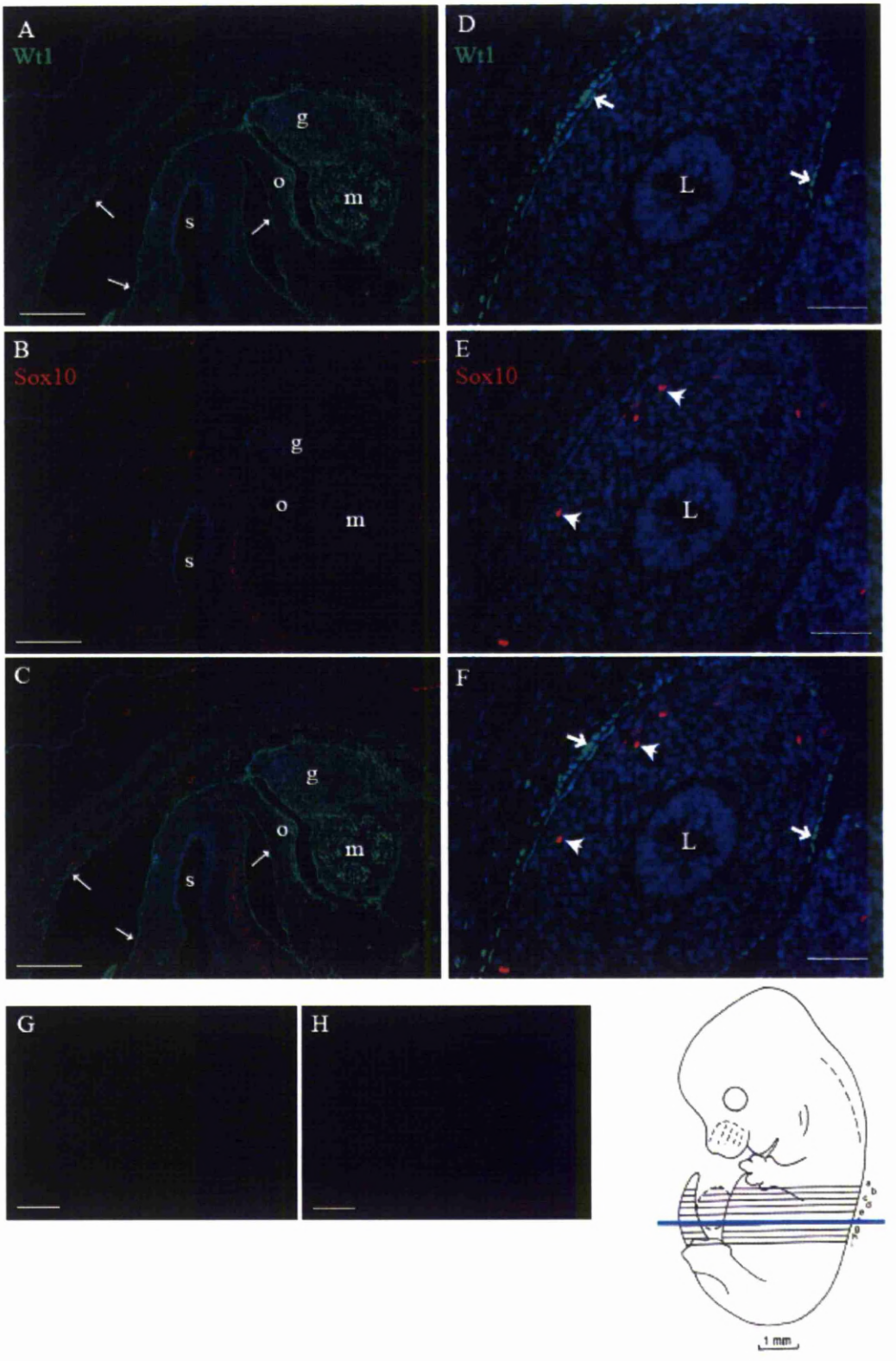
A
Wt1
g
o
m
s
D
Wt1
L
B
Sox10
g
o
m
s
E
Sox10
L
C
g
o
m
s
F
L
G
H
1 mm

Figure 3.6 Wt1 expression and the ENS at E12.5

Images A-F show immunofluorescence on transverse sections through E13.5 embryos co-stained with polyclonal antibodies against Wt1 and Sox10. A-C were taken with a 10x objective and D-F were taken with a 40x objective. A and D show Wt1 expression (green). B and E show Sox10 expression (red, arrowheads). C and F are composite images. Wt1 is expressed in the mesothelia (arrows) surrounding the stomach (s) (A and C), the intestine (D and F), the abdominal cavity and the omentum (o) (A and C). Wt1 is also expressed in the mesonephros (m) and the gonad (g) (A and C). There is no expression of Wt1 in the ENS (C and F). Images G and H were taken with a 10 objective. They are negative controls showing Alexa 488 donkey anti rabbit (G) and Alexa 568 donkey anti goat (H). There is a very small amount of background seen in image G. L, lumen. The blue line on the schematic image of an E12.5 mouse embryo (Kaufmann 1992) represents the level at which the sections were taken from in images A-H. Scale bars 200μm (A-C and G-H) 50μm (D-F)

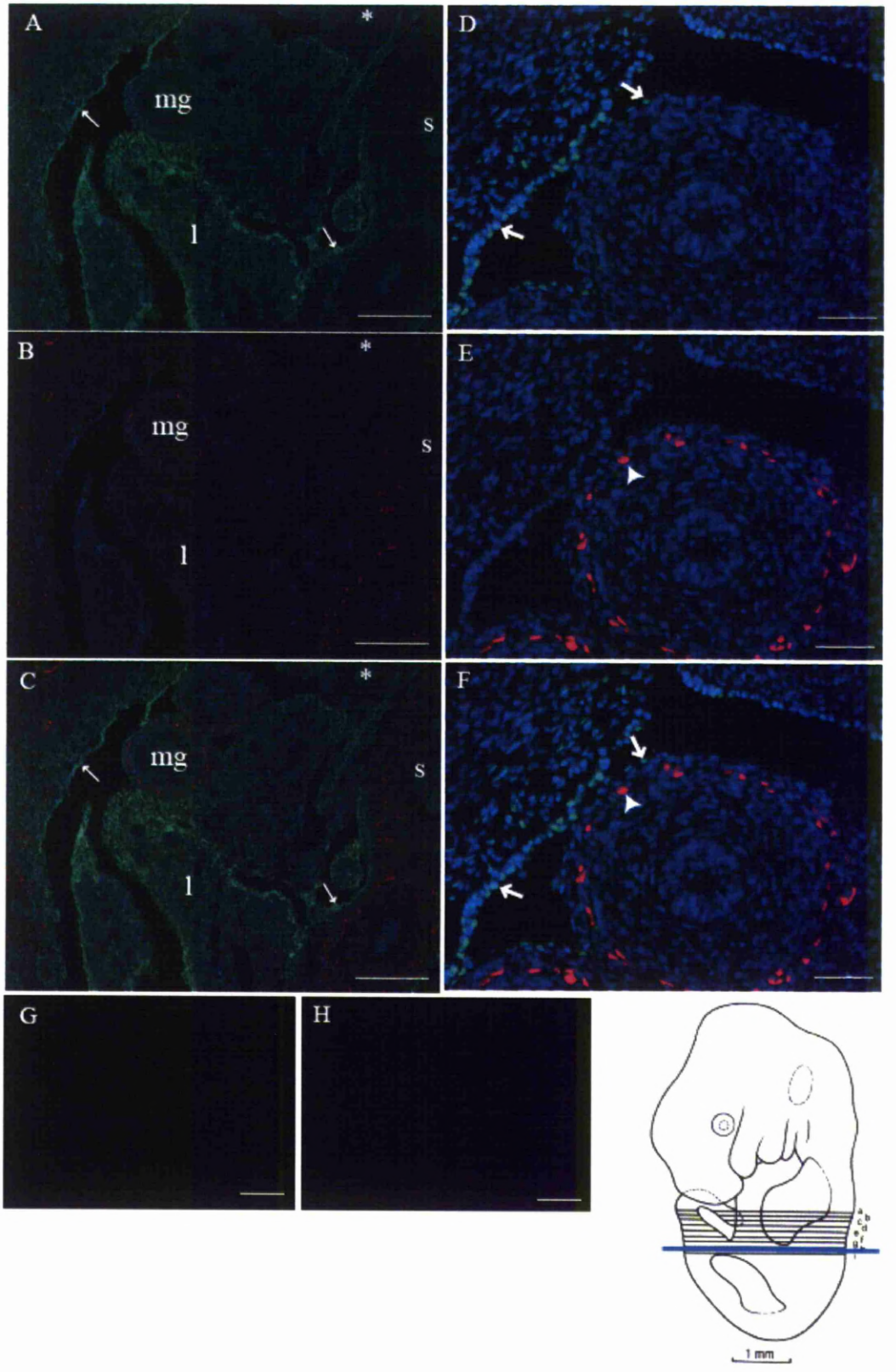
A
mg
s
l
*
D
B
mg
s
l
*
E
C
mg
s
l
*
F
G
H
1 mm

Figure 3.7 Wt1 in the ENS at E11.5

Images A-F show immunofluorescence images co-stained for Wt1 (green) and the ENS precursor marker Sox10 (red) in transverse sections. DAPI is shown in blue. Images A-C were taken with a 10x objective. Images D-F were taken with a 40x objective. A and D show expression of Wt1. B and E show expression of Sox10. C and F are composite images. Wt1 is seen in the mesothelium surrounding the abdominal viscera (arrows). Sox10 is seen in the ENS and plexi in the body wall. Sox10 is not expressed in the hindgut (*). Wt1 is not co-expressed with Sox10 in the ENS (C and F). G and H show the negative control. Alexa 488 donkey anti rabbit (G). Alexa 568 donkey anti goat (G). The blue line on the schematic image of an E11.5 mouse embryo (Kaufmann 1992) represents the level at which the sections were taken from in images A-H. s, stomach. mg, midgut. l, liver. Scale bars 100μm (A-C and G-H) 50μm (D-F)

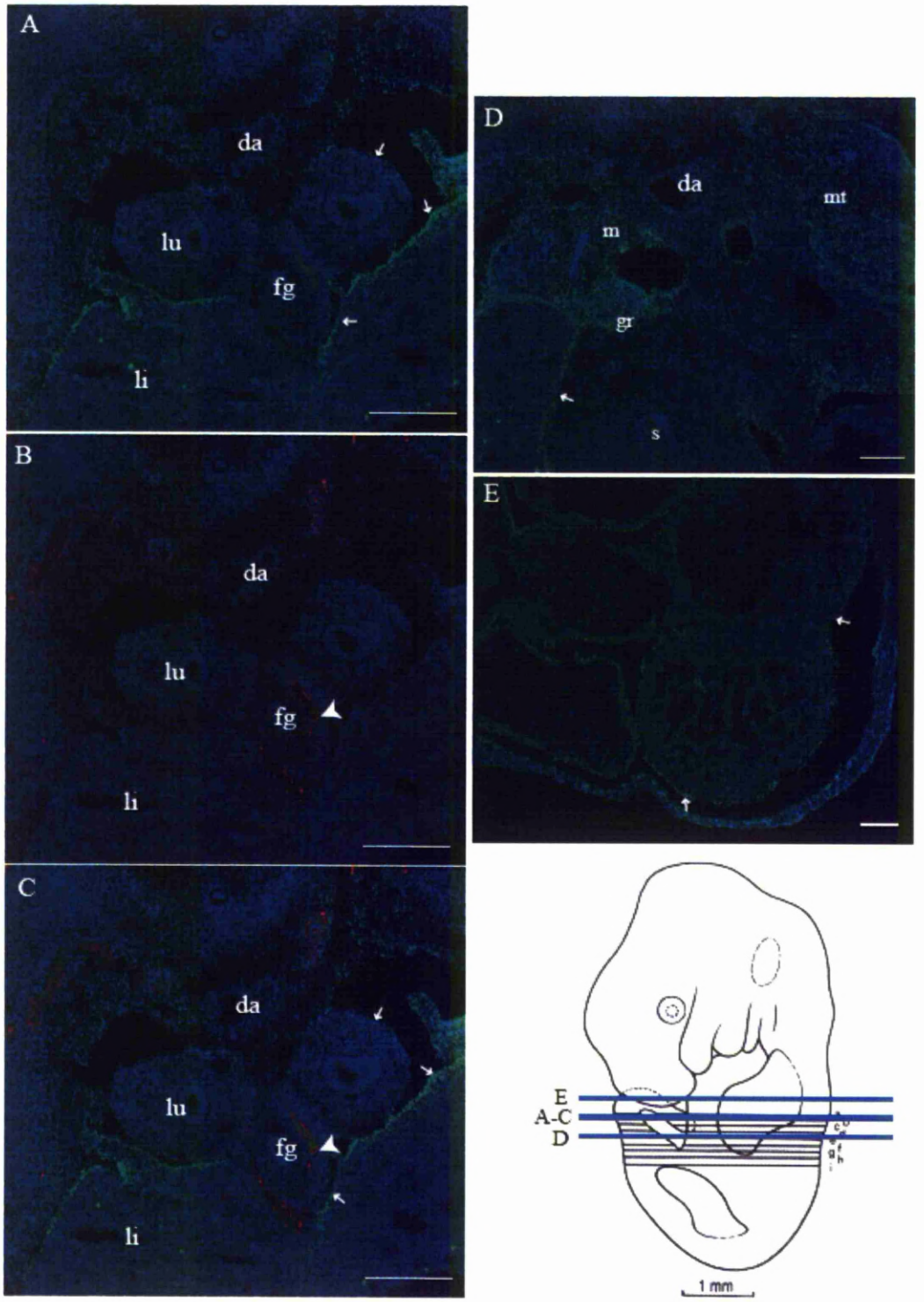
A
da
lu
fg
li
B
da
lu
fg
li
C
da
lu
fg
li
D
da
mt
m
gr
s
E
E
A-C
D
1 mm

Figure 3.8 Wt1 expression at E11.5

Images A-E were generated using immunofluorescence using polyclonal antibodies against Wt1 (green, arrows) and Sox10 (red, arrowheads). A-C are transverse sections at the level of the lungs. A shows Wt1. B shows Sox10. C is a composite image. Wt1 is expressed in the mesothelial cells of the pleura, surrounding the foregut (fg) and liver (li). There is no nuclear Wt1 staining in the ENS. D is a transverse sections at the level of the developing kidneys. Wt1 is expressed in the mesonephros and genital ridge. The mesonephric tubules are negative for Wt1. E is a transverse section through the heart, Wt1 is expressed in the epicardium. The blue lines on the schematic image of an E11.5 mouse embryo (Kaufmann 1992) represents the level at which the sections were taken from in images A-E. Images A-E were taken using a 10x objective. lu, lung. da, dorsal aorta. Scale bars 100μm (A-E).

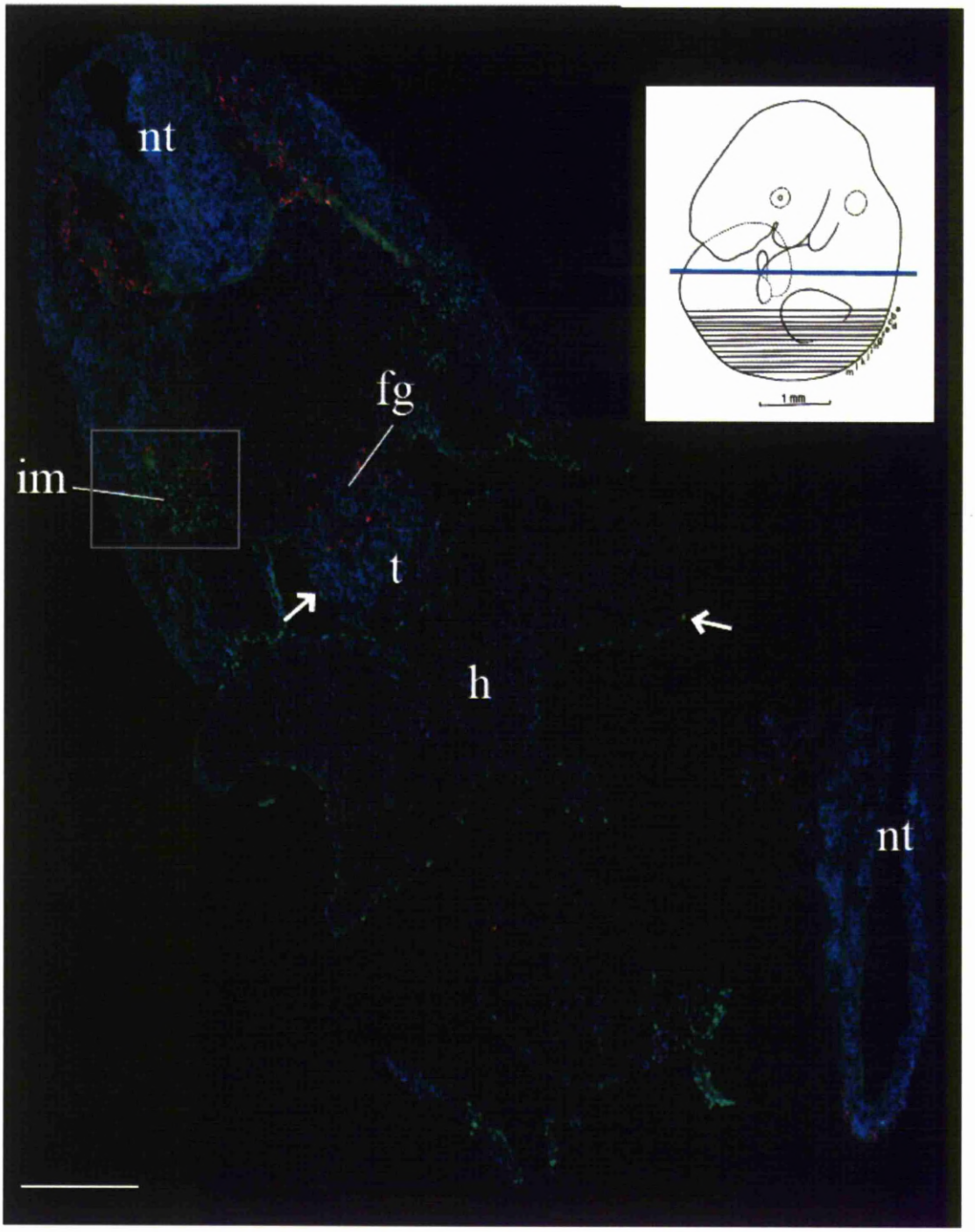
nt
fg
im
t
h
nt
1 mm

Figure 3.9 Wt1 and Sox10 at E10.5

The blue line on the schematic image of an E10.5 mouse embryo (Kaufmann 1992) represents the level at which the section shown in this image was taken. The image shows immunofluorescence on a transverse section at the level of the heart and foregut in an E10.5 mouse embryo co-stained using antibodies against Wt1 (green) and Sox10 (red). DAPI is shown in blue. Wt1 is expressed in the intermediate mesoderm (im) and in mesothelial cells of the epicardium and those surrounding the foregut (arrows). There is no co-localisation between Sox10 and Wt1 in the ENS of the foregut. The boxed area surrounding the intermediate mesoderm is shown at high magnification in Figure 3.10 (A-C). All images were taken using a 10x objective. fg, foregut. t, trachea. h, heart. nt, neural tube. Scale bars 100μm (A-C).

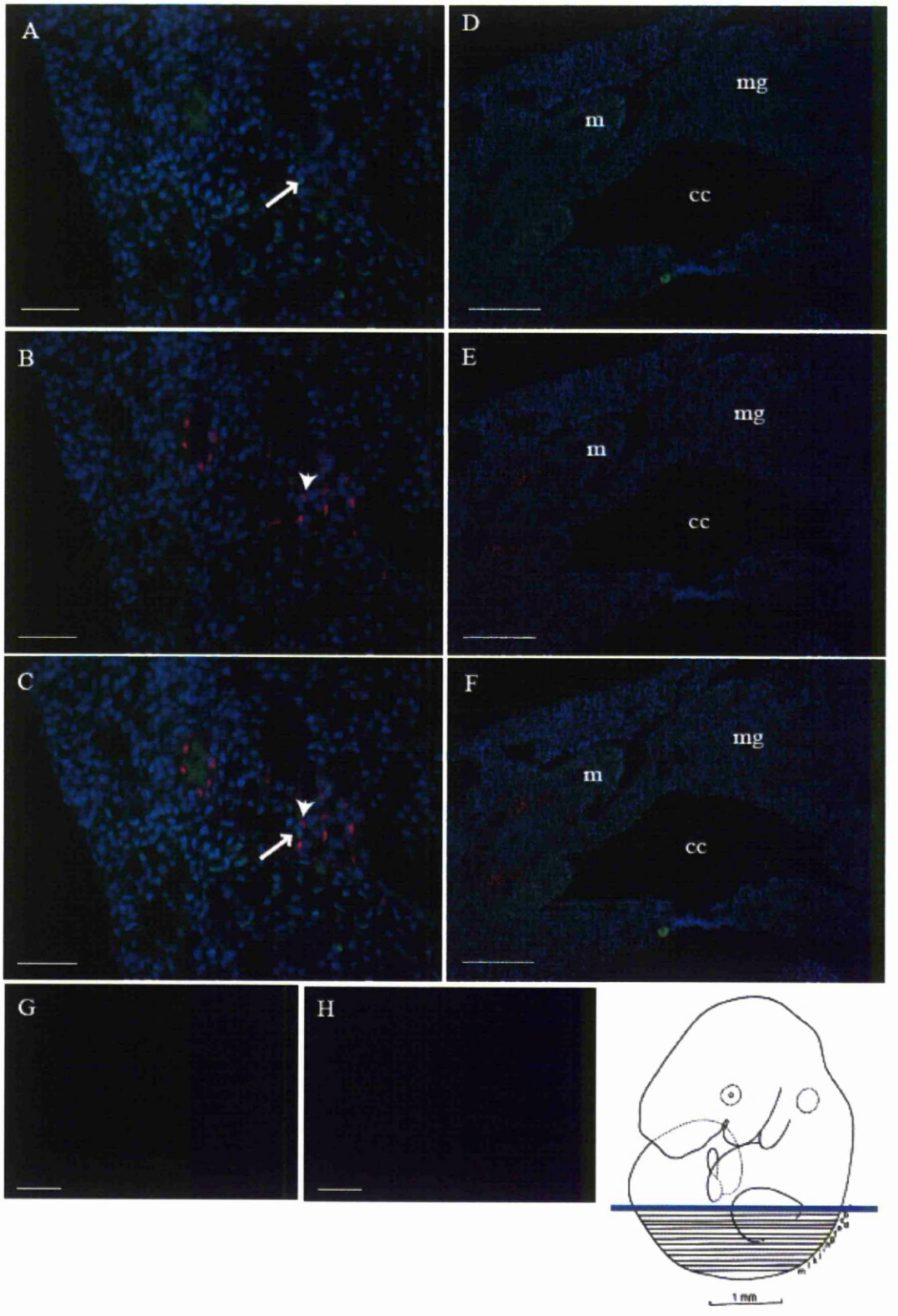
A
D
mg
m
cc
B
E
mg
m
cc
C
F
mg
m
cc
G
H
1 mm

Figure 3.10 Wt1 and Sox10 expression at E10.5

Images A-F are immunofluorescence using polyclonal antibodies for Wt1 (green) and Sox10 (red). A-C were taken in the region of the intermediate mesoderm (im). The level at which these sections were taken from is represented on the schematic diagram on Figure 3.9. There is no co-localisation between Wt1 (arrow) and Sox10 (arrowhead) (C). D-E were taken at the level of the developing kidney. This region is represented by the blue line on the schematic diagram (Kaufmann 1992) Wt1 is expressed in the mesonephric mesenchyme (m), the genital ridge (gr), and the mesothelium surrounding the gut and coelomic cavity (cc). Sox10 is seen in the ENS in the midgut (mg) region and in sacral neural crest cells in the caudal most part of the embryo (E and F). There is no co-localisation between Sox10 and Wt1 in the ENS (F). G and H show the negative controls taken with a 10x objective. G shows Alexa 488 donkey anti rabbit and H shows Alexa 568 donkey anti goat. Images A-C were taken with a 40x objective, images D-E with a 10x objective. Scale bars 50μm (A-C) 200μm (D-F and G-H)

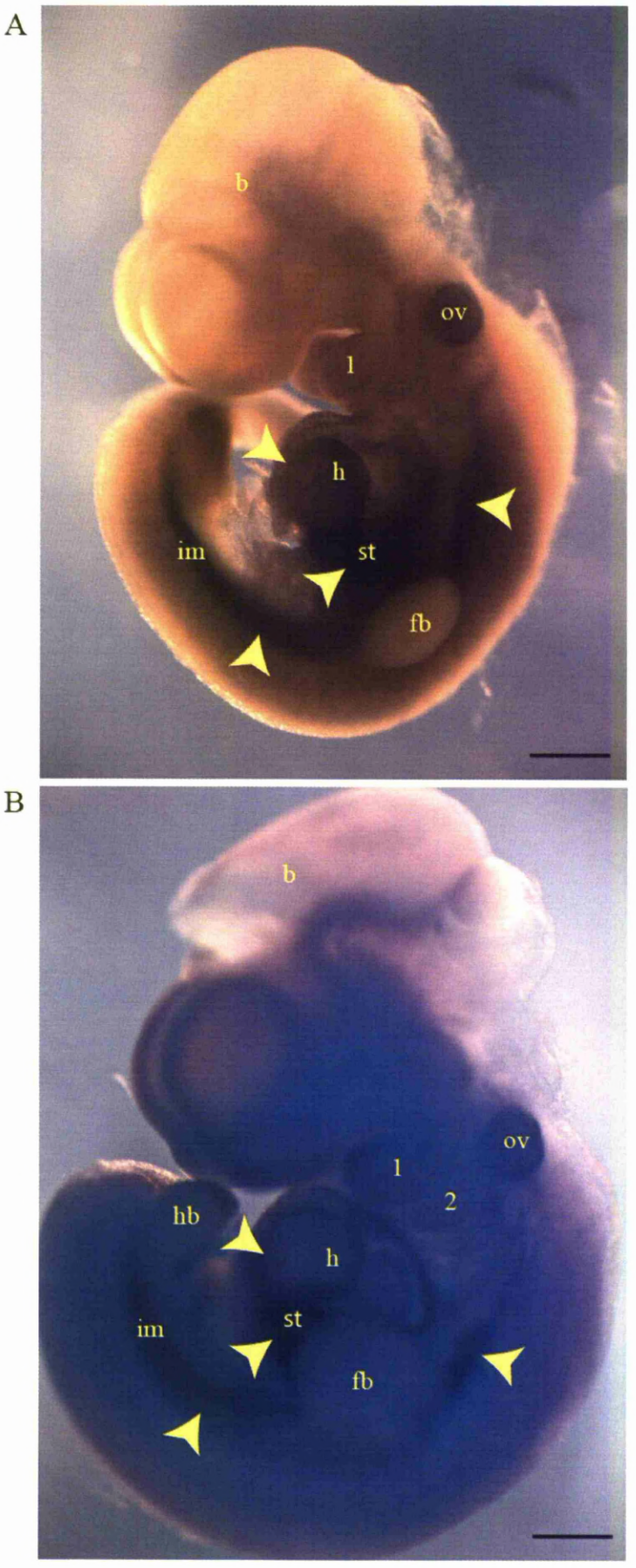
A
b
ov
1
h
im
st
fb
B
b
ov
1
2
hb
h
im
st
fb

Figure 3.11 Whole-mount in situ hybridisation at E9.5 and E10.5.

A and B shows Wt1 mRNA expression (yellow arrows) taken with a 4.0x objective. Wt1 is seen in the intermediate mesoderm (im), the epicardium (h), the septum transversum, and the region of the septum transversum (st) at both E9.5 (A) and E10.5 (B). Trapping is seen in the otic vesicle (ov). This is not positive for Wt1. 1, first branchial arch. 2, second branchial arch. fb, forelimb bud. hb, hind limb bud. b, brain. Scale bars 500μm.

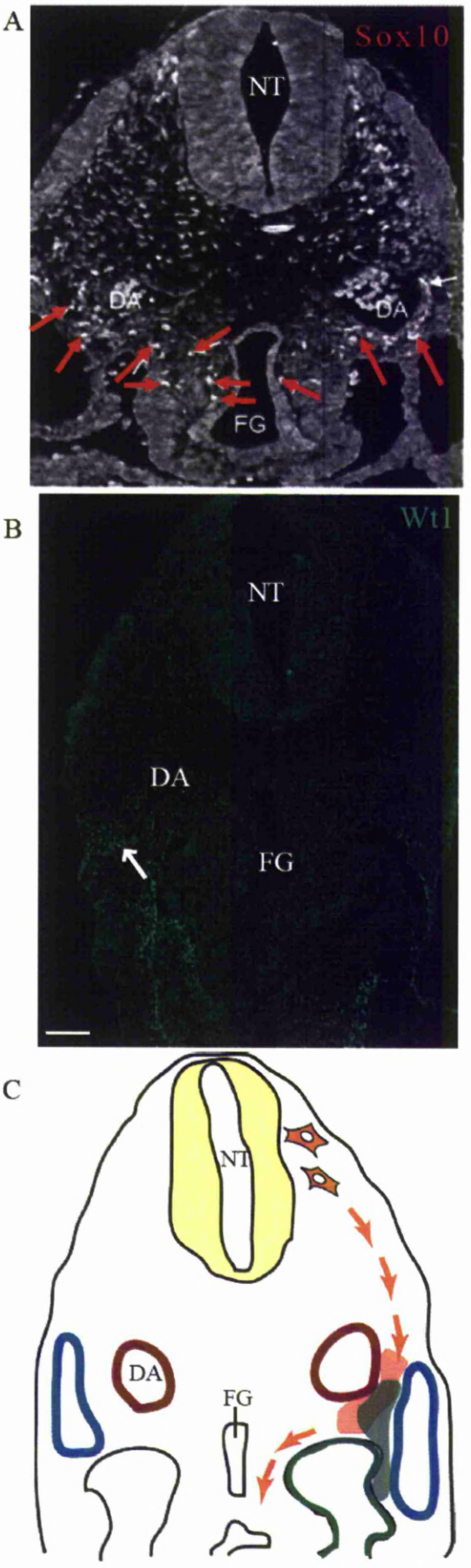
A
Sox10
NT
DA
DA
FG
B
Wt1
NT
DA
FG
C
NT
DA
FG

Figure 3.12 Wt1 and Sox10 in the region of the intermediate mesoderm

A is an image adapted from Anderson 2006 and shows antibody staining of Sox10 positive NCCs migrating to the foregut (red arrows). B is an immunofluorescence image, taken with a 20x objective, showing the expression of Wt1 in an E9.5 mouse embryo. Wt1 (green) is expressed in the intermediate mesoderm (white arrow) and the mesothelial cells of the coelomic cavity. C is a schematic diagram showing Wt1 expression (green) and the migratory pathway of Sox10 expressing NCCs migrating towards the foregut (orange). NT, neural tube. FG, foregut. DA, dorsal aorta. Scale bar 100μm.

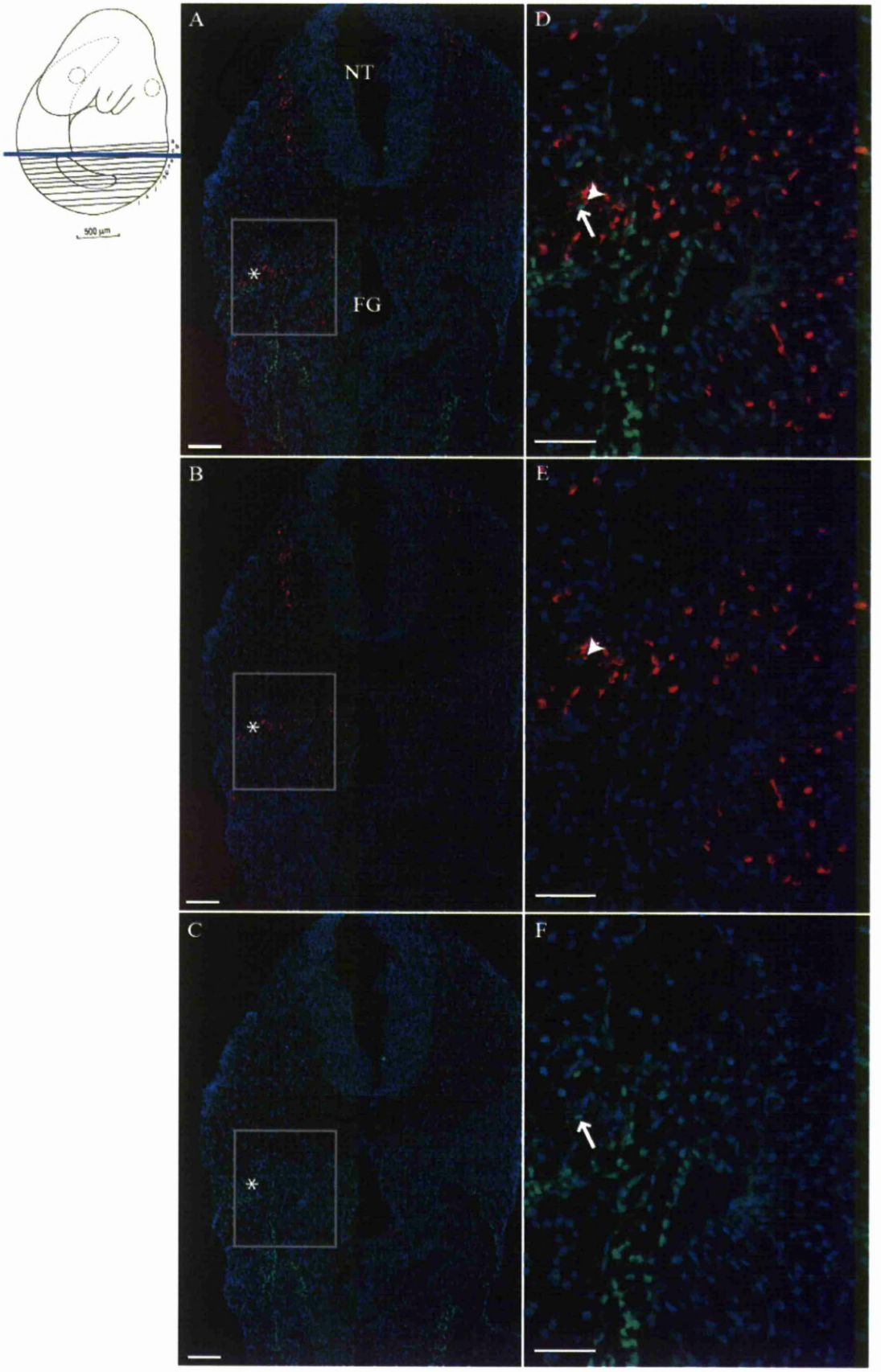
500 µm
A
NT
FG
D
B
E
C
F

Figure 3.13 Wt1 expression and migrating NCCs at E9.5

The schematic diagram of an E9.5 embryo was adapted from Kaufman, 1992. The blue line indicates the level at which the sections were taken from in images A-F. A-C are immunofluorescence images taken with a 10x objective. D-F were taken with a 40x objective of the area marked with the grey boxes in A-C. A and D are composite images showing Wt1 (green, arrows) expression in the intermediate mesoderm (A, star) and lining the coelomic cavity, Sox10 (red, arrowheads) expression in NCCs migrating through the region of the intermediate mesoderm. B and E show Sox10 only. C and F show Wt1 only. DAPI is shown in blue (A-F). There is no co-expression of Wt1 and Sox10 in the region of the intermediate mesoderm at E9.5. NT, neural tube. FG, foregut. Scale bars 100μm (A-C) 50μm (D-F).

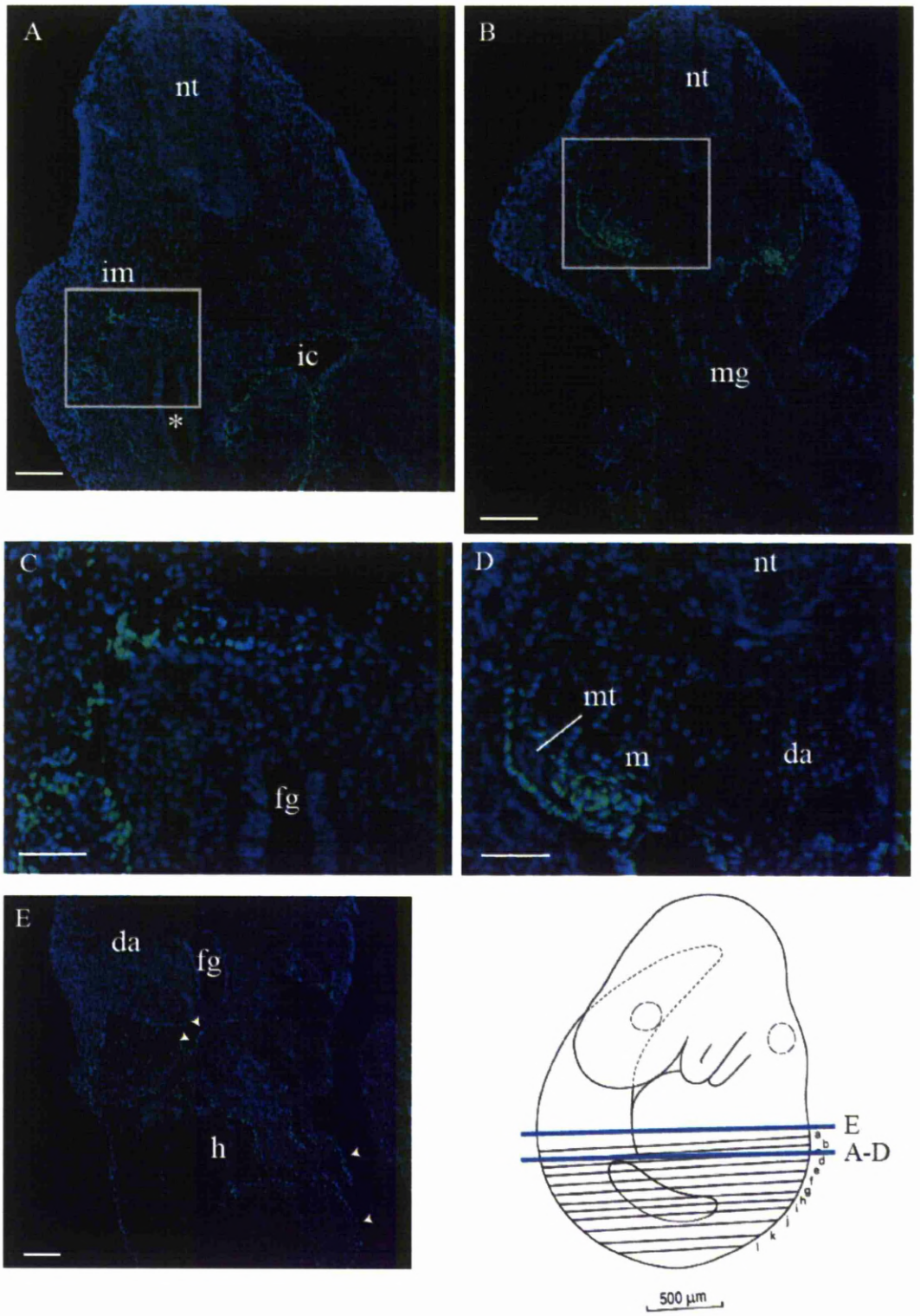
A
nt
im
ic
*
B
nt
mg
C
fg
D
nt
mt
m
da
E
da
fg
h
E
A-D
500 µm

Figure 3.14 Wt1 expression at E9.5

Images A-E are immunofluorescence using the polyclonal Wt1 antibody. A,B and E were taken with a 10x objective. C and D were taken with a 40x objective and are high magnification images of the boxed areas seen in A and B. DAPI is shown in blue. A and C show Wt1 expression in the intermediate mesoderm (im) and surrounding the intraembryonic coelom (ic). B and D show expression of Wt1 in the mesonephric mesenchyme (m). The mesothelium has not migrated over the midgut (mg) region at this stage so is therefore negative for Wt1 (B and D, red arrows). The mesonephric tubules (mt) are also Wt1 negative (D, red arrows). Image E shows Wt1 expression in the mesothelial cells of the epicardium. The schematic diagram of an E9.5 embryo was adapted from Kaufman, 1992. The blue lines indicates the levels at which the sections were taken from in images A-E. nt, neural tube. *, foregut. da, dorsal aorta. h, heart. Scale bars 100μm (A,B and E) 50μm (C and D)

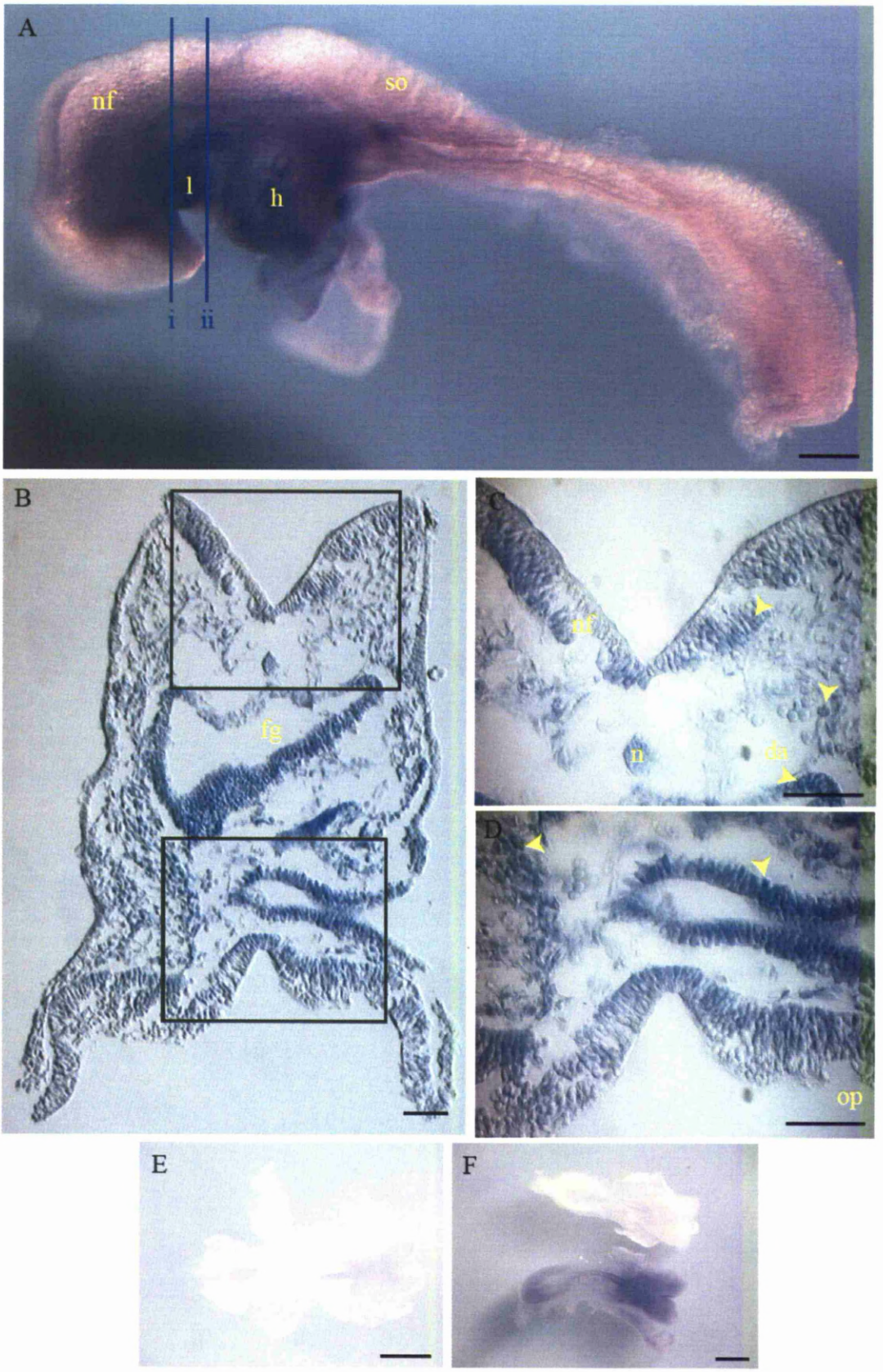
A
nf
so
l
h
i
ii
B
fg
C
nf
n
da
D
op
E
F

Figure 3.15 The expression of Wt1 at E8.5

Wt1 RNA In situ hybridisation on a whole-mount E8.5 embryo is shown in image A from a lateral aspect. Expression is seen in the region of the primitive heart (h) the first branchial arch (1), and in the region of the neural folds. The blue lines represent the level at which the sections seen in figure 3.16 (i) and B-D (ii) were taken. B is a 20μm section taken from the whole-mount. It was taken with a 10x objective. The grey boxes represent the area seen in images C and D, which were taken at a higher magnification using a 40x objective. Wt1 activity (arrowheads) is seen in the neural folds (B-D), around the foregut (fg) (B), and in the region of the neural crest (B-D). Image E shows the sense control from a ventral aspect taken with a 4x objective. Image F shows a comparison between sense control and antisense samples from a dorsal aspect. There appears to be no unspecific staining in the negative controls (E and F). so, somite. n, notochord. op, optic pit. Scale bars 50μm (C and D), 100μm (B) 200μm (A).

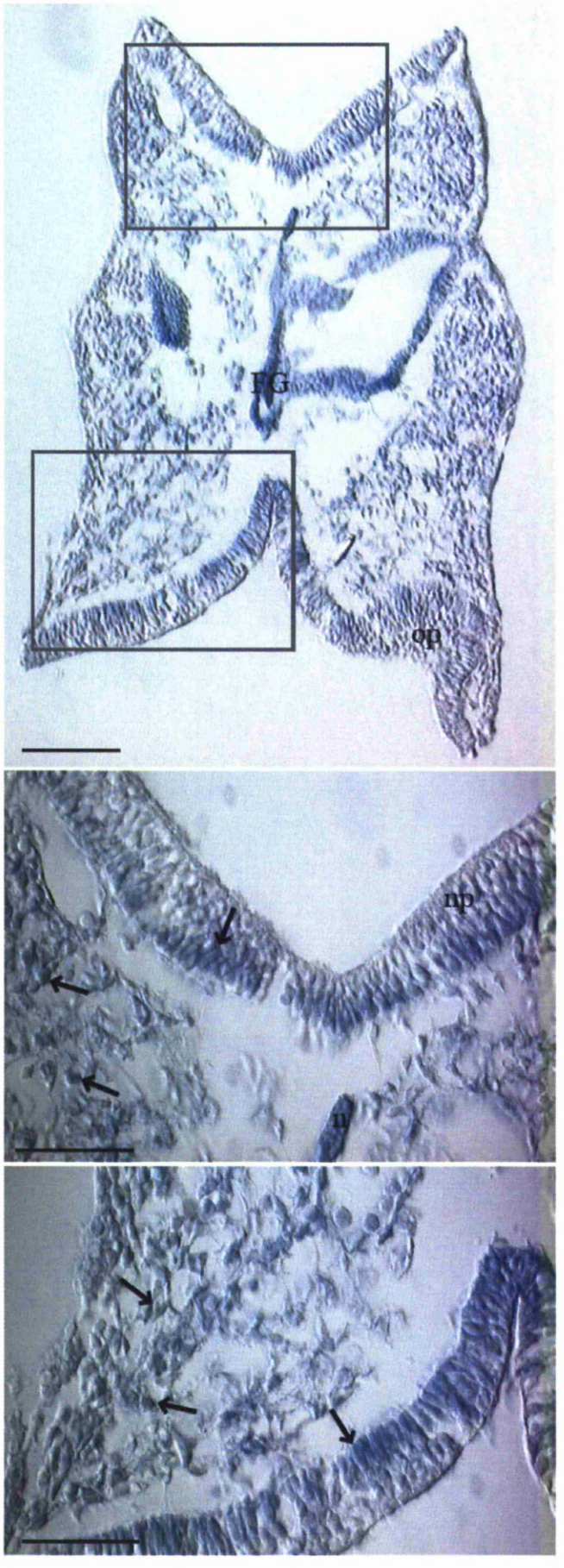
A
FG
op
B
np
n
C

Figure 3.16 Wt1 in the neural crest at E8.5

A-C are images taken from sections the whole-mount preparations of Wt1 RNA in situ hybridisation (Figure 3.15). A was taken with a 20x objective. B and C were taken with a 40x objective, and are high magnification images of the boxed areas seen in image A. Wt1 mRNA was found in the region of the neural crest and in cells in the neural fold (arrows). N, notochord. FG, foregut. np, neural plate. op, optic pit. Scale bars 100μm (A) 50μm (B and C).

A

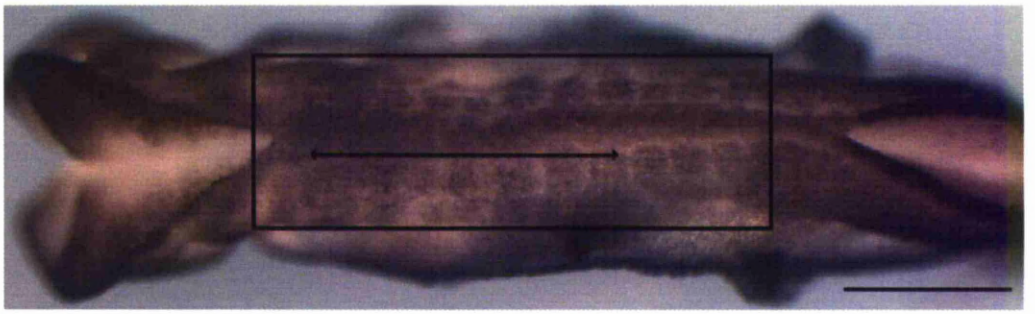

B

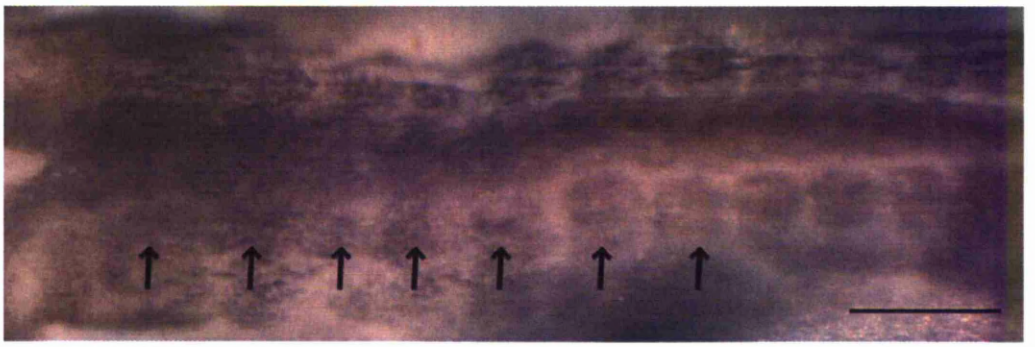

C

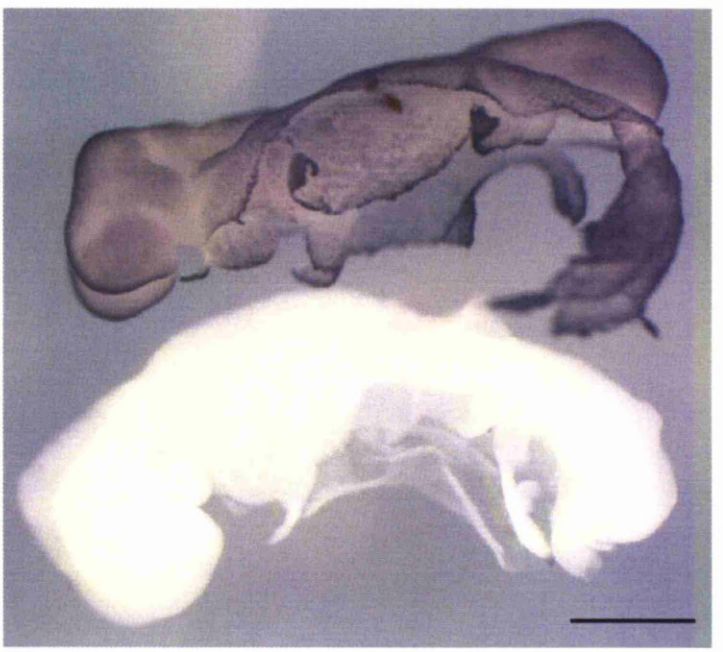

Figure 3.17 Wt1 expression in the neural crest at E8.5

A and B are immunohistochemistry images of E8.5 whole-mount preparations using antibodies against Wt1. A was taken with a 5x objective. B was taken with an 11.5x objective and is a high magnification image of the boxed area seen in A. Somites 1-7 are shown with arrows (A). Wt1 staining can be seen in the region of the neural crest lateral to the neural tube (B, arrows). Image C is a comparison between the negative control (bottom) and Wt1 sample (top) taken from a lateral aspect. The control is clear (C). Scale bars 500μm (A and C) 200μm (B).

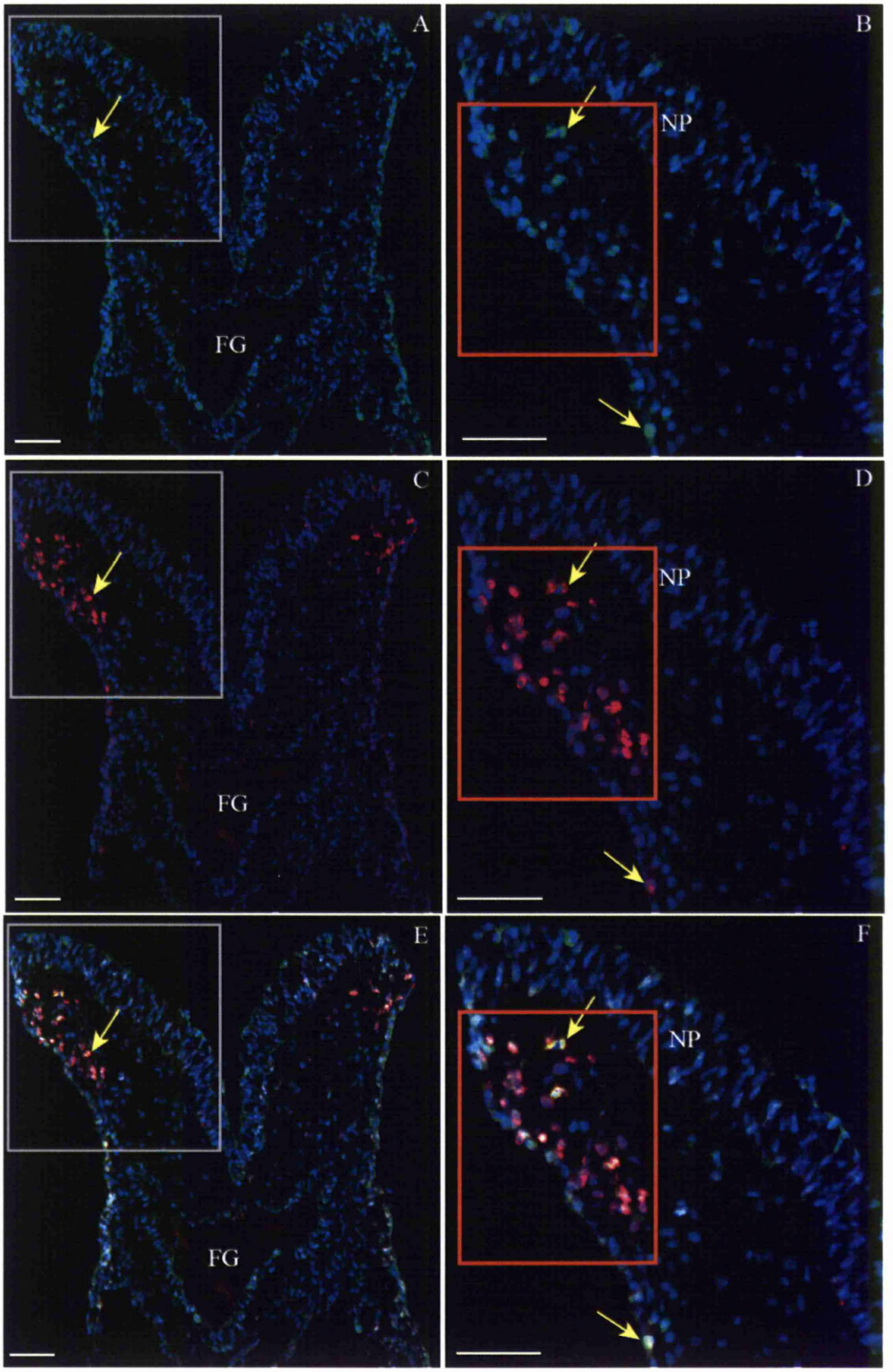
A
FG
B
NP
C
FG
D
NP
E
FG
F
NP

Figure 3.18 Wt1 expression in NCCs at E8.5

Images A-F show immunofluorescence using Wt1 (green) and Sox10 (red) antibodies. A, C, E were taken with a 20x objective. B, D, F were taken using a 40x objective and are high magnification images of the area inside the grey boxes shown in A, C and E. A and B show Wt1 only. C and D show Sox10 only. E and F are composite images showing Wt1 expression in the region of the neural crest and neural folds and co-expression of Wt1 with Sox10. DAPI is shown in blue (A-F). Wt1 and Sox10 co-localise in neural crest cells at E8.5 (yellow arrows). The orange box in images B, D, and F shows the area of neural crest from which cells were counted. NP, neural plate. FG, foregut. Scale bars 50μm. See Figure 3.19 for a diagram to show the levels at which these sections were taken from.

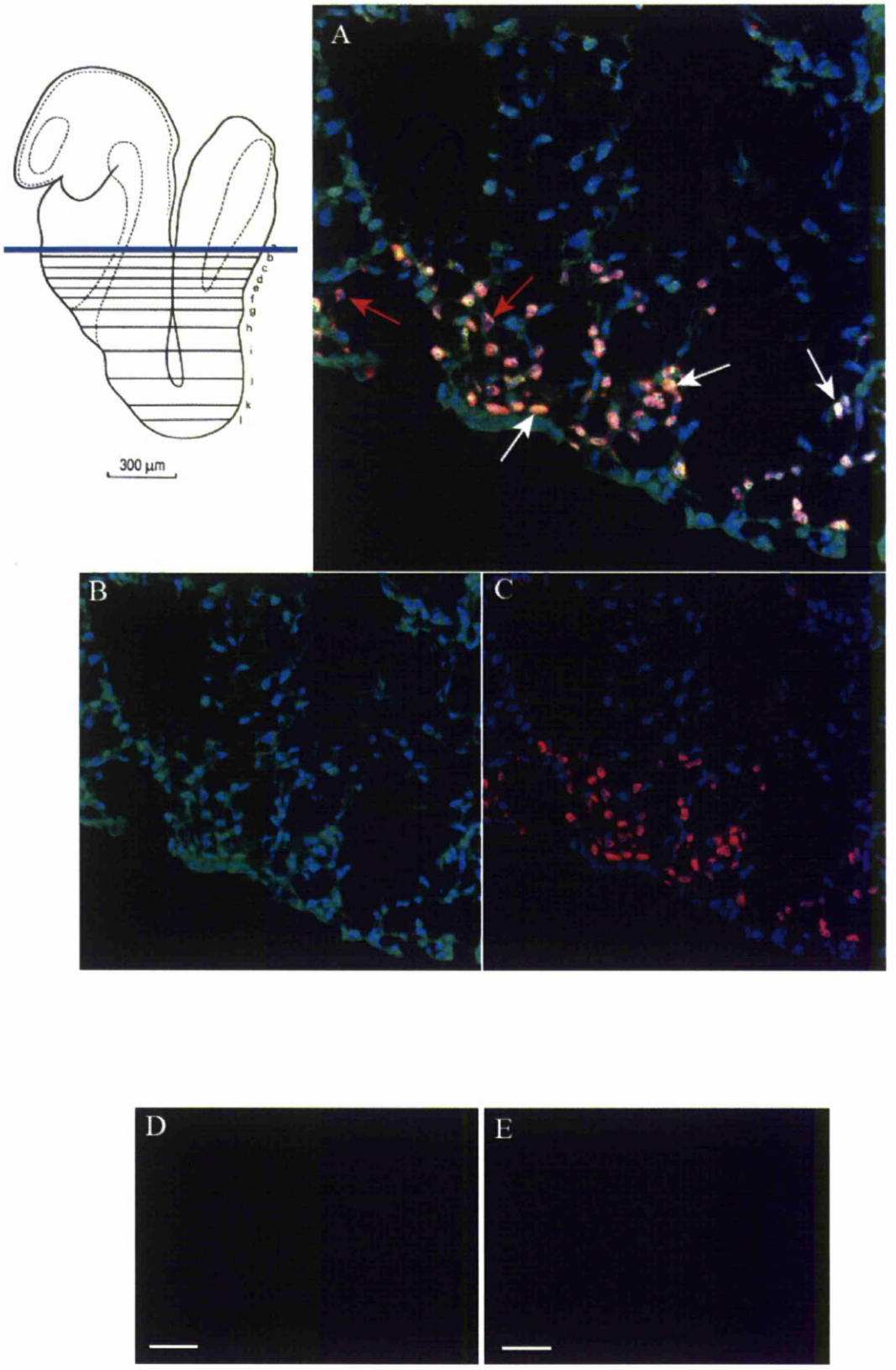
A
B
C
D
E
300 µm

Figure 3.19 Co-localisation between Wt1 and Sox10 in NCCs

The schematic diagram of an E8.5 embryo was adapted from Kaufman, 1992. The blue line indicates the level at which the sections were taken from in images A-E. Images A-C were taken using confocal microscopy using a 63x oil objective. A is a composite image showing immunofluorescence for Wt1 (green) and Sox10 (red). B shows Wt1 only. C shows Sox10 only. DAPI is shown in blue (A-C) Wt1 co-localises with Sox10 at E8.5 in NCCs (white arrows). Red arrows show examples of Sox10 positive cells that are not Wt1 positive. Images E and F show negative controls taken with a 20x objective. Alexa 488 chick anti rabbit (E). Alexa 594 chick anti goat (F). Scale bars 100μm

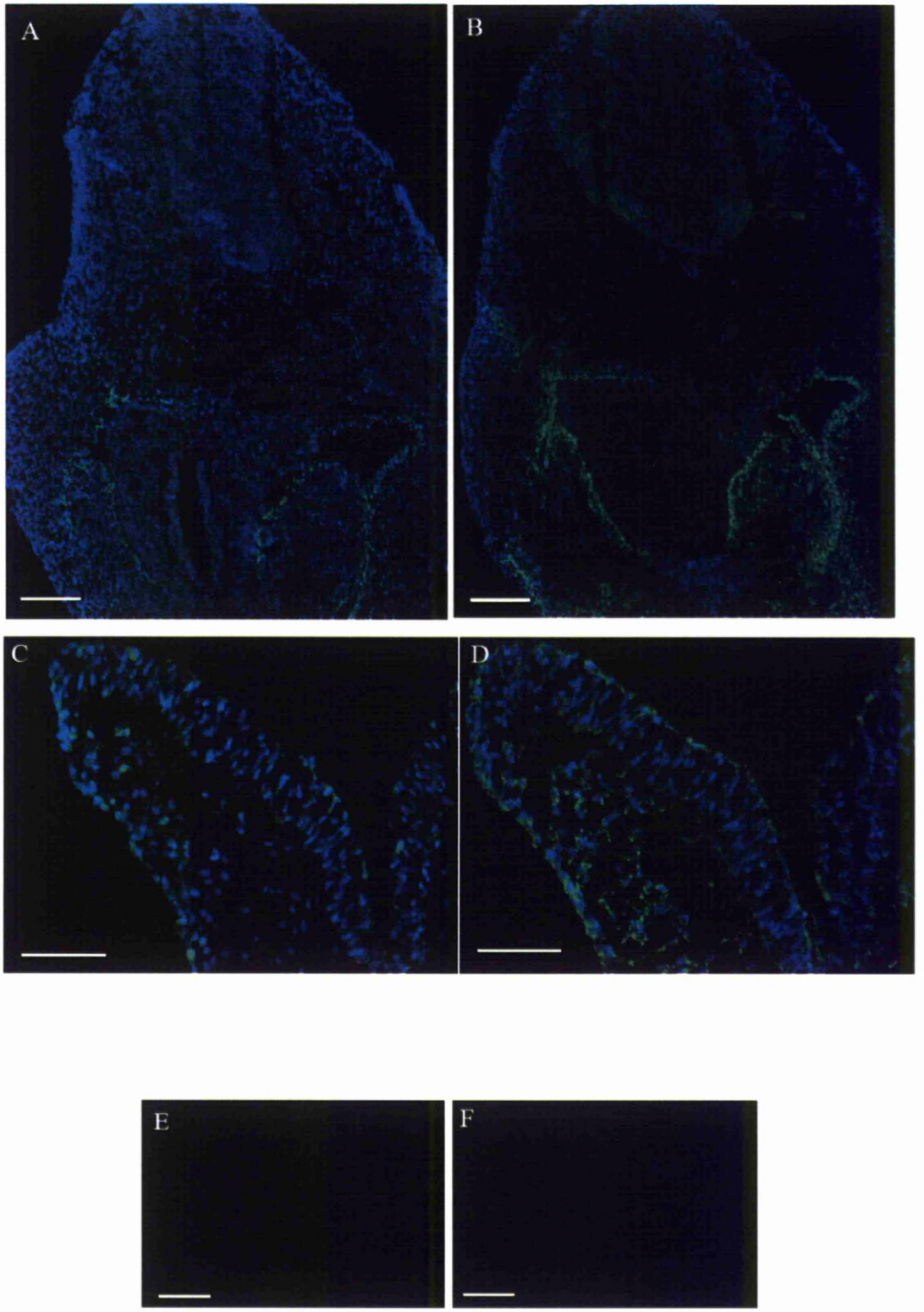
A
B
C
D
E
F

Figure 3.20 Differential staining with Wt1 antibodies at E8.5

Images A and C are immunofluorescence using the polyclonal Wt1 antibody (Santa Cruz). B and D are immunofluorescence using the monoclonal Wt1 antibody (Upstate). A and B were taken with a 10x objective and show very similar expression patterns between Wt1 polyclonal (A) and monoclonal (B) antibodies. The signal is nuclear and matches that previously reported. C and D were taken with a 40x objective. Wt1 staining is nuclear in C using the polyclonal antibody. However, there is no nuclear staining in D using the monoclonal antibody. The negative controls do not show unspecific staining (E and F). Alexa 488 goat anti rabbit (E). Alexa 568 goat anti mouse (F). Scale bars 100μm (A and B) 50μm (C and D) 200μm (E and F)

A

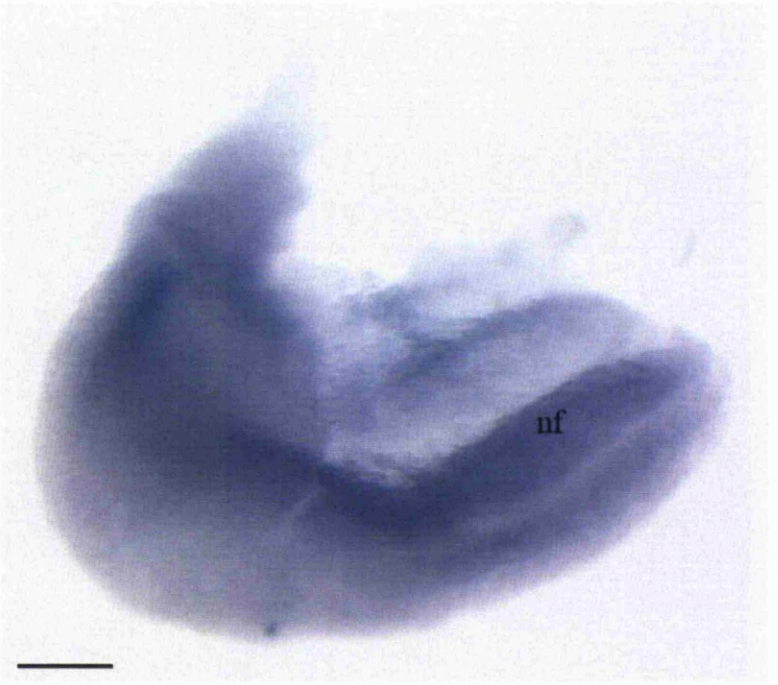

B

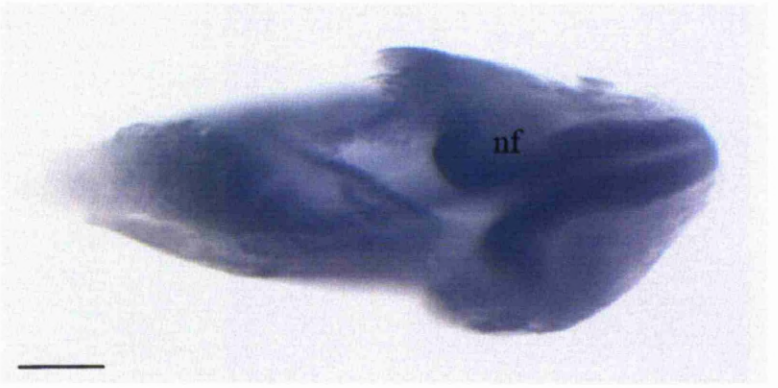

C

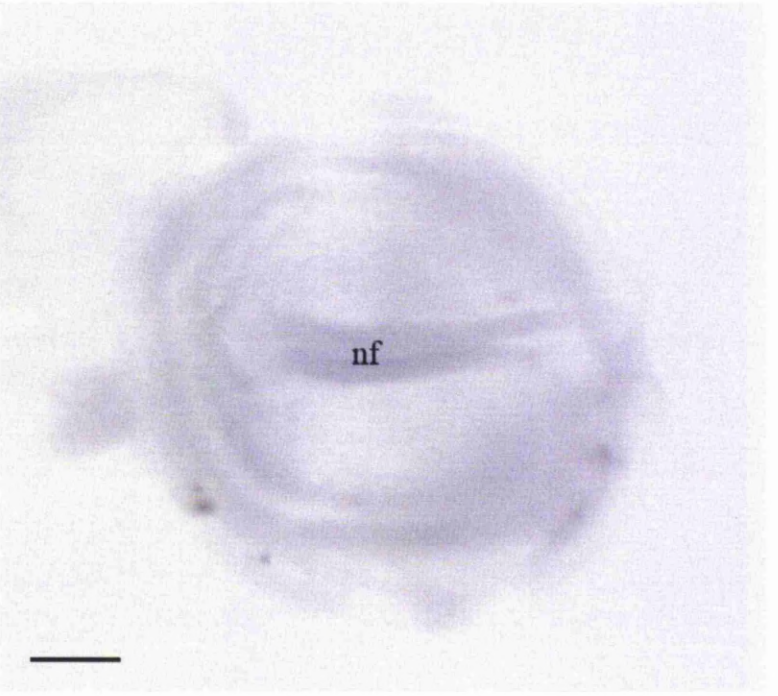

Figure 3.21 Wt1 expression at E7.5

Images A-C are Wt1 RNA in situ hybridisation on whole-mount E7.5 embryos. A and B show hybridisation with the antisense probe. C shows the control, which was hybridised with the sense probe. A is a lateral view and B is a ventral view, both show Wt1 in the neural folds (nf) and underlying mesenchyme. The negative control is a ventral view and is negative for unspecific staining (C). Scale bars 100μm

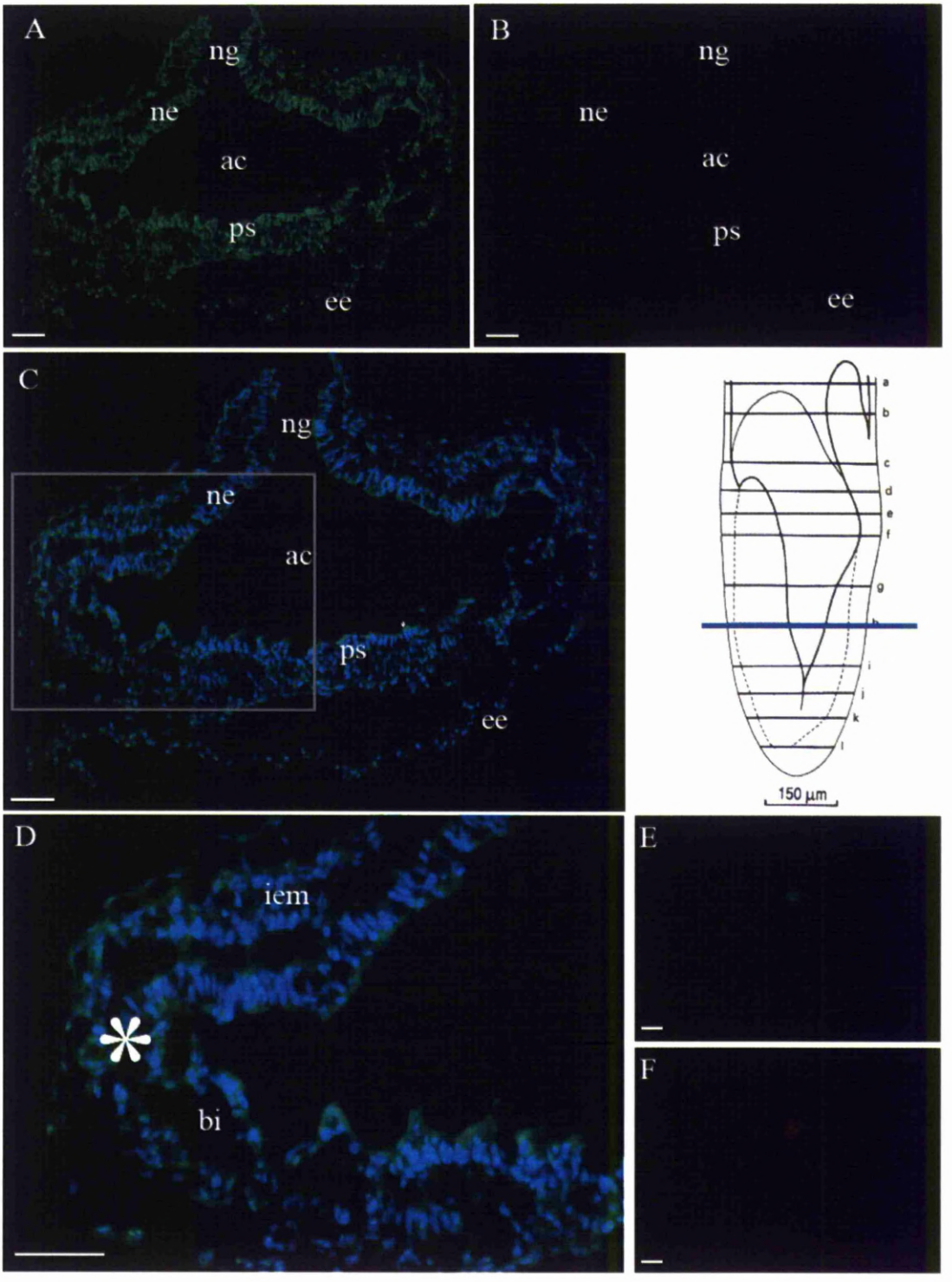
A
ng
ne
ac
ps
ee
B
ng
ne
ac
ps
ee
C
ng
ne
ac
ps
ee
a
b
c
d
e
f
g
h
i
j
k
l
150 µm
D
iem
bi
E
F

Figure 3.22 Wt1 and the neural crest at E7.5

A-C, E and F are immunofluorescence images taken with a 20x objective and image D was taken with a 40x objective. A shows Wt1 only. B shows Sox10 only. C is a composite image of Wt1 (green) and Sox10 (red) DAPI (blue). D is a high magnification image of the boxed area in C. There is no expression of Sox10 at E7.5 (B and C). Wt1 is expressed in many cells at E7.5 (A and C). The schematic diagram of an E7.5 embryo was adapted from Kaufman, 1992. The blue line indicates the approximate level at which the sections were taken from in images A-F. D and E are negative controls. Alexa 488 donkey anti rabbit (D). Alexa 568 donkey anti goat (E). The controls show no unspecific staining except for a dirt particle, which has caused the green (D) and red (E) spots. ng, neural groove. ne, neuroepithelium. ac, amniotic cavity. ps, primitive streak. ee, embryonic endoderm. iem, intraembryonic mesoderm. bi, blood island. *, junction between neural and surface ectoderm. Scale bars 50μm.

Chapter 4

Results

An in vitro system to analyse Wt1 expression in Vagal NCCs

My previous results showed that Wt1 is expressed in neural crest cells (NCCs) at E8.5. Therefore, it raised the question of whether there is a role for Wt1 in these NCCs, particularly the cells destined to migrate to the gut to form the enteric nervous system. In order to investigate this, an in vitro system was to be employed. The intention of this study is to produce a system that could eventually, once optimised, be used to find a role for Wt1 in migrating NCCs by looking at the functional consequences of Wt1 knock down on NCC migration and differentiation using siRNA. It was first necessary to establish in vitro the culture of neural crest explants i.e. a method of dissection of the neural tubes and the necessary culture conditions. It was then important to determine whether the cells that emerged from the neural tube explants were in fact NCCs, if they still expressed Wt1 even under in vitro conditions and to establish a method to measure their migration in addition to assessing their differentiation using marker expression.

4.1 Development and optimisation of a NCC in vitro culture system

There are several methods for preparing neural tubes for NCC culture. The initial method used in these experiments was derived from several protocols described by Bronner-Fraser in 1996, Stemple in 1992, and Barlow in 1998. The vagal level of neural tube (opposite somites 1-7) was dissected from E8.5 mouse embryos using sharpened tungsten wire (Stemple and Anderson 1992; Bronner-Fraser 1996; Barlow, Wallace et al. 2008). Based on these published methods my early experiments failed to show any cells emerging from the explants (Figure 4.1). These explants had been plated onto glass cover-slips, previously coated with either fibronectin at a concentration of 10μg/ml and poly-L-lysine at a

concentration of 10μg/ml (Bronner-Fraser 1996; Barlow, Wallace et al. 2008). The neural tubes were dropped onto the cover-slip in a small amount of culture medium, DMEM supplemented with 10% NCS, in order to allow the neural tubes to attach to the substrate. However, the cells had the appearance of having died and because there had been no expansion of the culture over a period of 7 days it was assumed that this was the case, and therefore the culture conditions needed adjusting (Figure 4.1 A and B).

Following the failure of these initial experiments the literature was searched once again and a method described by Jaenisch in 1985 was found in which glass cover-slips were now coated in a 0.5% gelatine solution (in PBS). The neural tubes were dissociated from surrounding tissues using a 0.05% (w/v) trypsin solution (in PBS) at 4°C for 30 minutes, before dissection with sharpened tungsten needles (Jaenisch 1985). It was also decided, after the failure of the previous method, to place the neural tubes directly into 500μl of culture media. This allowed the explants to sink and attach to the cover-slip without drying out. This proved to be a success and cells began to emerge from the neural tube pieces and over a period of several days the migratory population of cells expanded, which suggested the cells were undergoing proliferation (Figure 4.2).

With a working method of preparation of NCCs in culture, attention was turned to their culture conditions i.e. media. When using DMEM plus 10% NCS (v/v) the morphology of the emerging cells was not optimal. After 48 hours in culture the migrating cells had many vacuoles, the cell population was expanding quite slowly and did not look like migrating cells seen in similar assays in the literature (Ito and

Takeuchi 1984; Jaenisch 1985; Stemple and Anderson 1992; Bronner-Fraser 1996). The explant had also disintegrated (Figure 4.2, A). According to the protocol published by Jaenisch the media was then changed to DMEM supplemented with 5% NCS and 5% horse serum (Jaenisch 1985). The cell morphology appeared considerably healthier in these conditions as there were far fewer vacuoles and after 48 hours under these culture conditions the cell population was still expanding and the central neural tube explant remained intact (Figure 4.2, B).

4.2 Confirmation that migrating cells are NCCs

It was essential to establish if the cells that emerged from the neural tube explants were NCCs. In order to address this question immunofluorescence using antibodies to known markers for migrating NCCs, Sox10, was performed. Sox10 was found to be expressed by a proportion of the migrating cells (Figure 4.3 A-C). This suggested that they were NCCs. However not all of the cells in the culture expressed Sox10, which suggested some of the cells were either not NCC derived, or they had lost their NCC properties during the culturing process.

4.3 Wt1 is expressed in NCCs in culture

To test if these cells expressed Wt1 as shown in vivo immunofluorescence was carried out after 24 hours in culture. This was done using the polyclonal rabbit antibody for Wt1 (Figure 4.4). Wt1 was found to be expressed in around half of the NCCs migrating away from the neural tube explant (Figure 4.4, B, C, E and F). The neural tube explant had detached from the cover-slip during the staining procedure, however a small proportion of the cells remaining on the substrate

where the neural tube had been also expressed Wt1 but there were fewer cells expressing Wt1 here than in the migrating cells.

4.4 Time-course of NCC behaviour and Wt1 expression in culture

In order to determine the most suitable time-point at which attempt to knock-down Wt1, the behaviour of the NCCs was characterised and the expression of Wt1 was documented over a period of 7 days.

Characterisation of NCCs after 24 and 48 hours in culture

Following 24 hours in culture the neural tube explants were photographed and then fixed for immunofluorescence. The neural tube pieces became rounded when in culture and did not maintain their original tube like structure (Figure 4.5, A). The cells that were just emerging from the neural tube had an epithelial-like morphology. In fact, the entire outer border of the neural tube became distorted and was found to form what appeared to be a flattened epithelial expanse (Figure 4.5, A). The first cells to migrate away from the neural tube had multiple processes (Figure 4.5, B-G). These findings correspond to the work of Ito and Takeuchi in 1984. They found similar phenotypes when looking at the migration and differentiation of NCCs in vitro, referring to the migrating cells with multiple processes as "stellate cells" (Ito and Takeuchi 1984).

Using antibodies against Wt1 and neural crest markers p75 and Sox10, immunofluorescence was carried out. The results from this provided further evidence that the migrating cells are neural crest-derived, and there are still undifferentiated NCCs after 24 hours in culture, as both Sox10 and P75 markers

were expressed in these migrating cells (Figure 4.6, A-D) (Young, Ciampoli et al. 1999; Hong and Saint-Jeannet 2005). As described in the previous paragraph, Wt1 was also expressed in around half of the migrating cells after 24 hours in culture (Figure 4.4). Therefore, NCCs have an intrinsic expression of Wt1, which was not induced by their environment in vivo.

The aforementioned results were similar to those seen after 48 hours in culture, (Figure 4.7, A). However, unlike the relatively uniform morphology of the migrating cells after 24 hours, at 48 hours approximately a third of cells had begun to develop long axonal-like processes (Figure 4.7, B-F) suggesting the NCCs were beginning to differentiate into what looked like neuronal cells. Data from immunofluorescence showed that Wt1 was still expressed in around half of cells of the migrating population, a proportion of these cells expressed cytoplasmic Wt1 (Figure 4.8, A-C), and the neural crest marker, Foxd3, was still being expressed in around 30-40% of these cells (Figure 4.3, D-F). However, the neuronal marker, Tuj1, was also being expressed in a number of the cells (Figure 4.8, D-F). Tuj1 was detected exclusively in the processes of the neuronal-like cells observed with bright-field. These results confirmed that after 24 hours and up to 48 hours in culture the in vitro population of NCCs began to differentiate into neuronal cells or due to the whole neural tube being dissected and placed into culture, some of the neuronal cells could be developing motor neurons, projecting from the ventral aspect of the spinal cord. Further investigations would have to be carried out using specific markers to sensory neurons. Table 4.1 shows a comparison between 24 and 48 hours in culture.

Table 4.1 A comparison of data collected from neural crest cell explants at 24 hours and 48 hours of culture.

	24 hours	**48 hours**
Explant appearance	Rounded explant Border of migrating cells	Explant margins: Less defined
Migration (μm)	139	304
Cell shape	Uniform Foot-like processes Stellate cells	More irregular pattern Neurite outgrowth Fewer stellate cells
Expression pattern		
p75	✓	✓
Sox10	✓	✓
Foxd3	✓	✓
Tuj1	X	✓
Wt1	✓	✓

Characterisation of NCCs after 72 and 96 hours in culture

Analysis of cells in the cultured explants at 72 and 96 hours revealed that the cell morphology remained very similar during this time period. There were still a number of stellate-like cells with multiple processes migrating further away from the central piece and this still had the epithelial-like sheet surrounding it. However, at 72 hours the neural tube piece appeared to start to disintegrate (Figure 4.9, A). This result suggested that the neural tube explant could not be maintained in long term culture, under these conditions. The most significant difference between these stages and 48 hours in cell morphology was that the axon-like processes (Figure 4.9, B) projecting from the developing neuronal cells, which were now present on the majority of the cells in the culture, had started to form networks, which had the appearance of plexuses (Figure 4.9, C).

It was found that Wt1 was still expressed in around a quarter of migrating cells (Figure 4.10, A and B). Around a fifth of the total migratory cell population were still NCCs, as they were also expressing Sox10 (Figure 4.10, D and E, Figure 4.3, G-I). The vast majority of Sox10-expressing cells also expressed Wt1. However there was a small proportion of Wt1-expressing cells which did not express Sox10. Approximately half the total number of migrating cells did not express either Wt1 or Sox10 at 96 hours in culture.

The neuronal marker, Tuj1, was still expressed by the developing neuronal cells (Figure 4.11). Tuj1 was still found to be exclusive to the increasing number of processes of the cells with neuronal morphology. The plexus-like formation of the

processes was also apparent with Tuj1 (Figure 4.11, B). However, these cells could also be motor neurons projecting from the spinal cord.

Characterisation of NCCs after 120 and 168 hours in culture

The appearance of the explants at 120 hours resembled that of 72/96 hours (Figure 4.12 and Figure 4.9). There were axon-like processes which had formed complex plexuses. However, following immunofluorescence there was no expression of Wt1 found (Figure 4.13, A and B) and no expression of neural crest marker, Sox10 (4.13, C). This suggests that all NCCs had, by this point, either differentiated, many into neuronal cells as characterised by the expression Tuj1 (Figure 4.11), or had detached from the cover-slip due to cell death or agitation during the staining procedure. At 168 hours many cells had died or had floated away, and the neural tube piece had disintegrated quite significantly in comparison to 120 hour cultures (Figure 4.13, D and E). The remaining cells that were attached to the cover-slip at 168 hours still possessed axonal processes and the general morphology of the cells was similar to that seen at earlier time-points. However there were fewer cells in the migratory population overall (Figure 4.13, F).

4.5 Rate of migration of NCCs in vitro

To determine the rate at which NCCs migrated in vitro, neural tube explants were dissected and plated on cover-slips as previously described. Explants were then photographed at different time-points (24 and 48 hours), the margins of the explants were then demarcated and the distance between the margin and the migration front was measured (Figure 4.14). Seven explants were analysed at each time-point in order to determine the mean rate of migration and to account for the high degree of variability in migration rates between explants.

The results of this migration assay are shown in Table 4.1 and graphically in Figure 4.15. While these results reveal a clear trend in that NCCs do migrate further away from the central neural tube explant over time, there is considerable variability: The mean distance travelled by NCCs after 24 hours in culture was 139 and the mean distance travelled after 48 hours was 304. The data revealed that NCCs have a mean rate of migration of 5.78μm/hour after 24 hours, increasing to 6.34μm/hour after 48 hours (Figure 4.15).

Table 4.2 Distance travelled by NCCs over a period of 48 hours (μm). Measurements were taken at 24 hours and 48 hours. 0 hours refers to the time at which the explants were placed into culture.

Sample	**0 hours**	**24 hours**	**48 hours**
1	0	160	359
2	0	133	266
3	0	133	293
4	0	146	359
5	0	133	293
6	0	146	320
7	0	120	239
Mean (μm)	0	139	304
Standard Deviation	0	12.9	45.1

4.6 Wt1 siRNA knock down of Wt1 in kidney stem cells

This preliminary study was carried in order to test whether it would be possible to knock down Wt1, with the use of siRNA, in kidney stem cells (KSC, Figure 4.16), which are known to endogenously express high levels of Wt1 (Davies, Ladomery et al. 2004; Fuente Mora, Ranghini et al. 2011). The successful application of this method in KSC could eventually be modified for use on neural tube explant cultures in order to elucidate the potential role for Wt1 in early developing NCCs.

In order to confirm that the KSC expressed Wt1, immunofluorescence was carried out as previously described using the polyclonal Wt1 antibody, which has been utilised throughout this thesis. The results of these experiments confirmed that KSC do indeed express Wt1 as Wt1 was shown to be expressed in the cell nucleus every KSC in the field of view (Figure 4.17).

Three samples of KSC were prepared. Each of the three samples was treated with one of the following conditions:

- Transfection with Wt1 siRNA (Qiagen)
- Transfection with control siRNA (Qiagen)
- Transfection solution containing no siRNA

Once the experiment was completed the KSC were fixed and immunofluorescence was performed, the results are shown in Figure 4.18. Wt1 expression did seem to have been repressed to a certain degree in the Wt1 siRNA condition (Figure 4.18, A) compared to the control conditions (Figure 4.18, B and C). However, this is unconfirmed as in the time frame these experiments were carried out in it was not

possible to introduce a system whereby you could determine how much Wt1 expression had been repressed.

4.7 Conclusion

The results presented in this chapter demonstrate that neural tube cultures can be established in vitro and that NCCs do migrate away from the explant. Around half of migrating cells did express Wt1 up to 96 hours in culture but it was then down-regulated at subsequent time-points. This matched the results revealed from in vivo studies as Wt1 was shown to be expressed in around half of the migrating population of NCCs in the E8.5 mouse embryo and was then down-regulated from E9.5. The significant difference in vivo and in vitro studies is that Wt1 was still be detected in NCCs after 4 days in culture, whereas Wt1 ceased to be expressed in NCCs in vivo within 24 hours.

The cultures were not optimised for long term culture and so explants and their migrating cells were unable to be maintained past seven days. This is possibly because a basic medium containing only serum with no growth factors was used throughout these studies. However this is not necessarily important as migration data gathered within the first 48 hours is sufficient for studying migration patterns.

It could be argued that the Wt1 siRNA experiments did repress Wt1 expression to a certain extent, due to the antibody staining looking slightly less vibrant than in the control samples. However, this would need confirming in future projects.

A

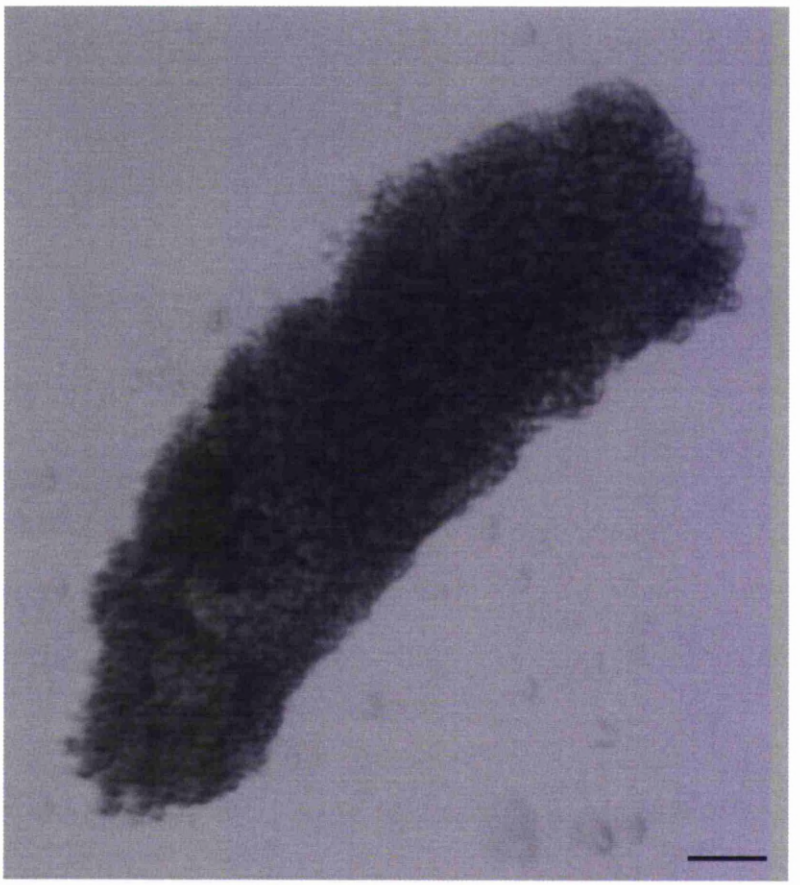

B

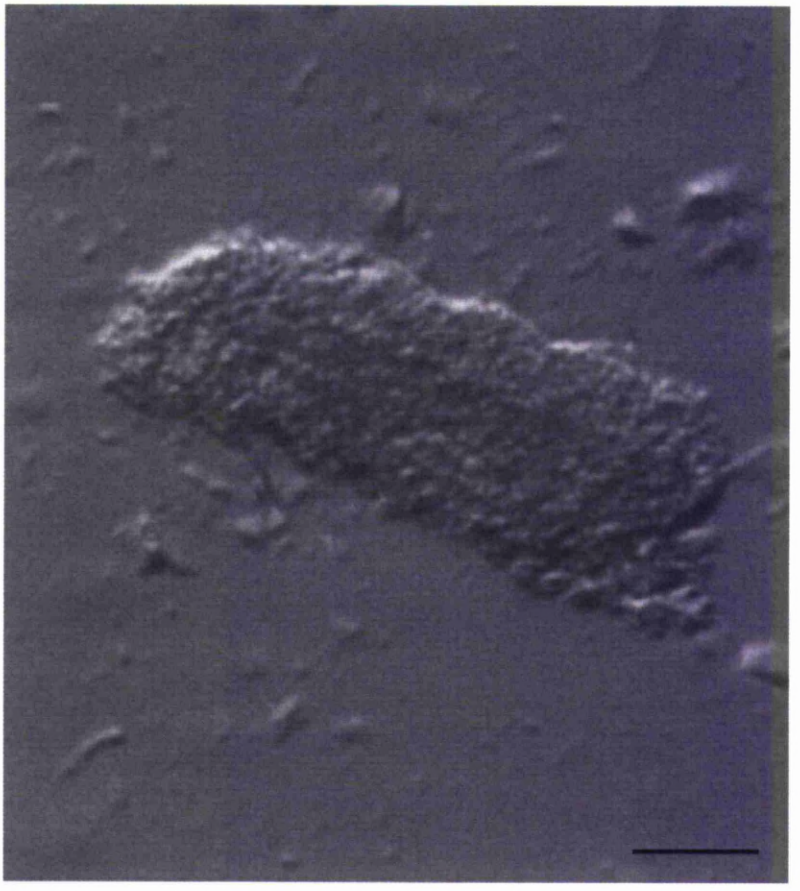

Figure 4.1 Optimising explant preparation

Image A shows a neural tube explant plated on a glass cover-slip, coated in fibronectin. Image B shows a neural tube explant plated on a glass cover-slip, coated in poly-L-lysine. Both images were taken after 24 hours in culture with DMEM + 10% FCS. No cells can be seen emerging from either explant. The cells look dead. Scale bars 50μm.

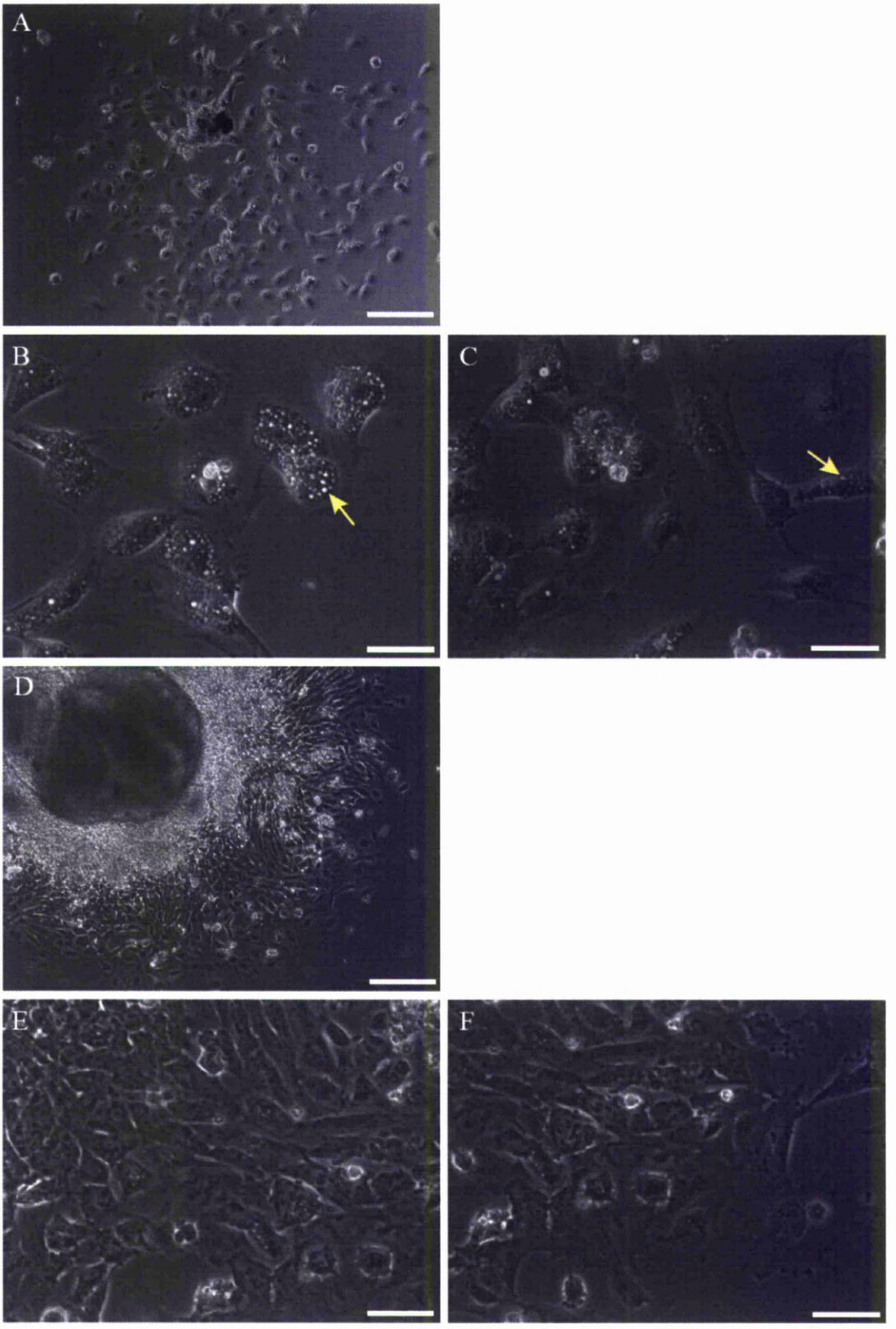
A
B
C
D
E
F

Figure 4.2 Optimising culture conditions of neural tube explants

A-C Neural tube explant after 48 hours in culture with DMEM + 10% FCS. A and D are phase contrast images taken with a 10x objective. Images B, C, E and F are phase contrast images taken with 40x objective. The cells contain a large number of vacuoles (B and C, arrows). D-F show neural tube explants after 48 hours in culture with DMEM + 5% FCS and 5% horse serum. Cells have visibly less vacuoles (E and F). Scale bars 200μm (A and D) 50μm (B, C, E and F).

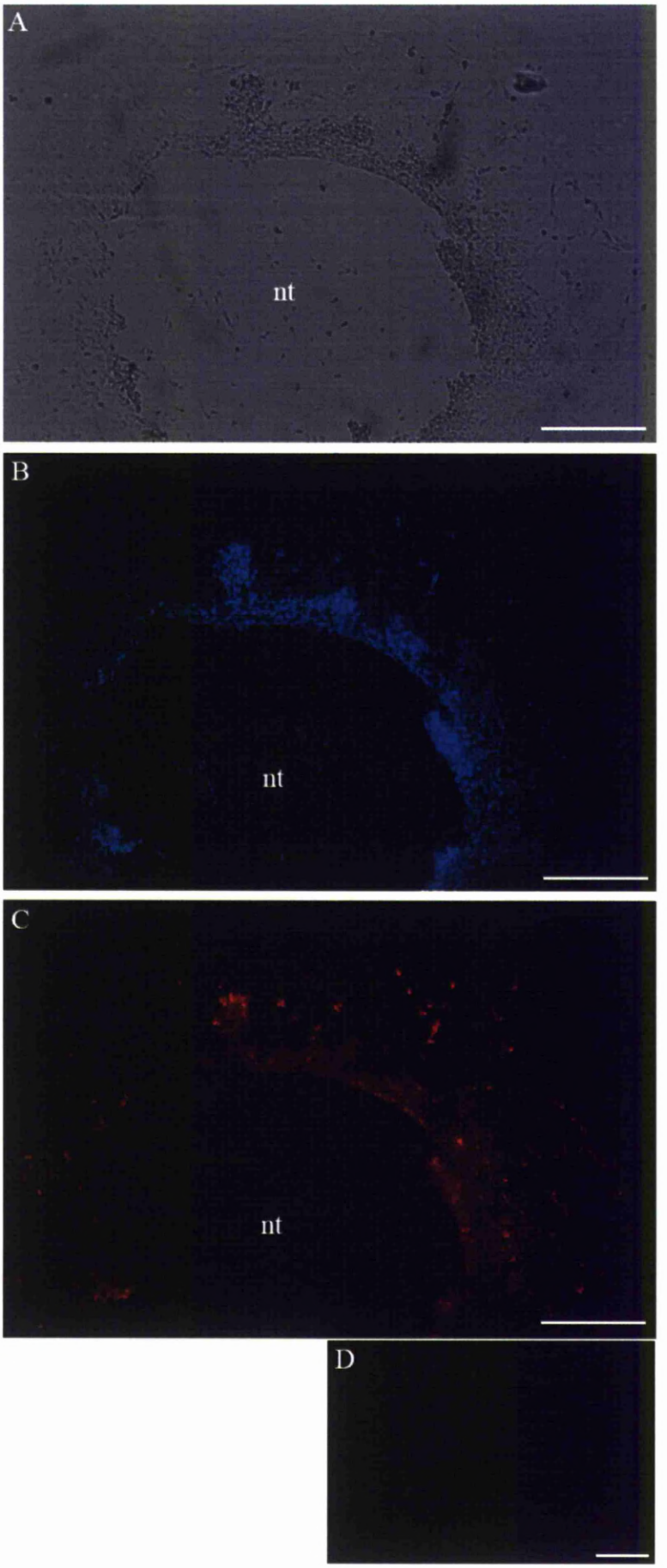
A
nt
B
nt
C
nt
D

Figure 4.3 Confirmation that migrating cells are NCCs

Immunofluorescence was carried out on neural tube explant using antibodies against neural crest markers. A shows a bright-field image of B and C. DAPI is shown in image B. Image C show staining for Sox10 (red). These images were taken with a 10x objective after 96 hours in culture. Image D was taken with a 10x objective. It show the negative control for Alexa 568 donkey anti-goat (D). There was no unspecific staining seen in the control. This was the case throughout these studies, unless otherwise stated. nt – site of neural tube explant. This has detached from the underlying coverslip due to staining procedure. Scale bars 200μm.

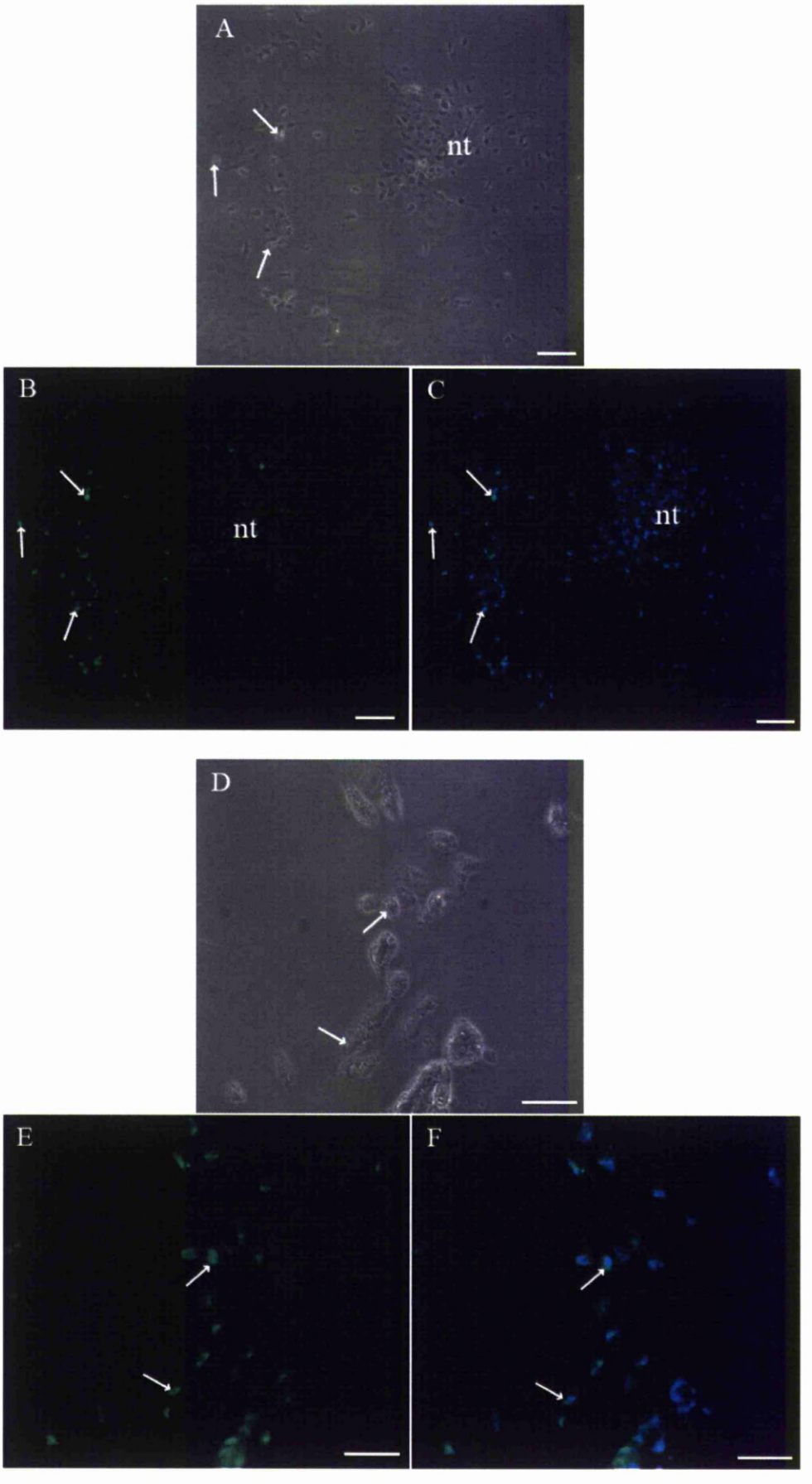
A
nt
B
nt
C
nt
D
E
F

Figure 4.4 Wt1 is expressed in NCCs after 24 hours in culture

Images A-C were taken with a 20x objective. Images D-F were taken with a 40x objective. Image A and D were taken using bright-field. Images B, C, E and F show Wt1 (green) expressed in migrating NCCs from the neural tube explant (arrows). The nuclear stain DAPI (blue) is show in C and F. nt – Site of neural tube explant which is no longer attached to the coverslip after the staining procedure. Scale bars 50μm (A-C) 25μm (D-F).

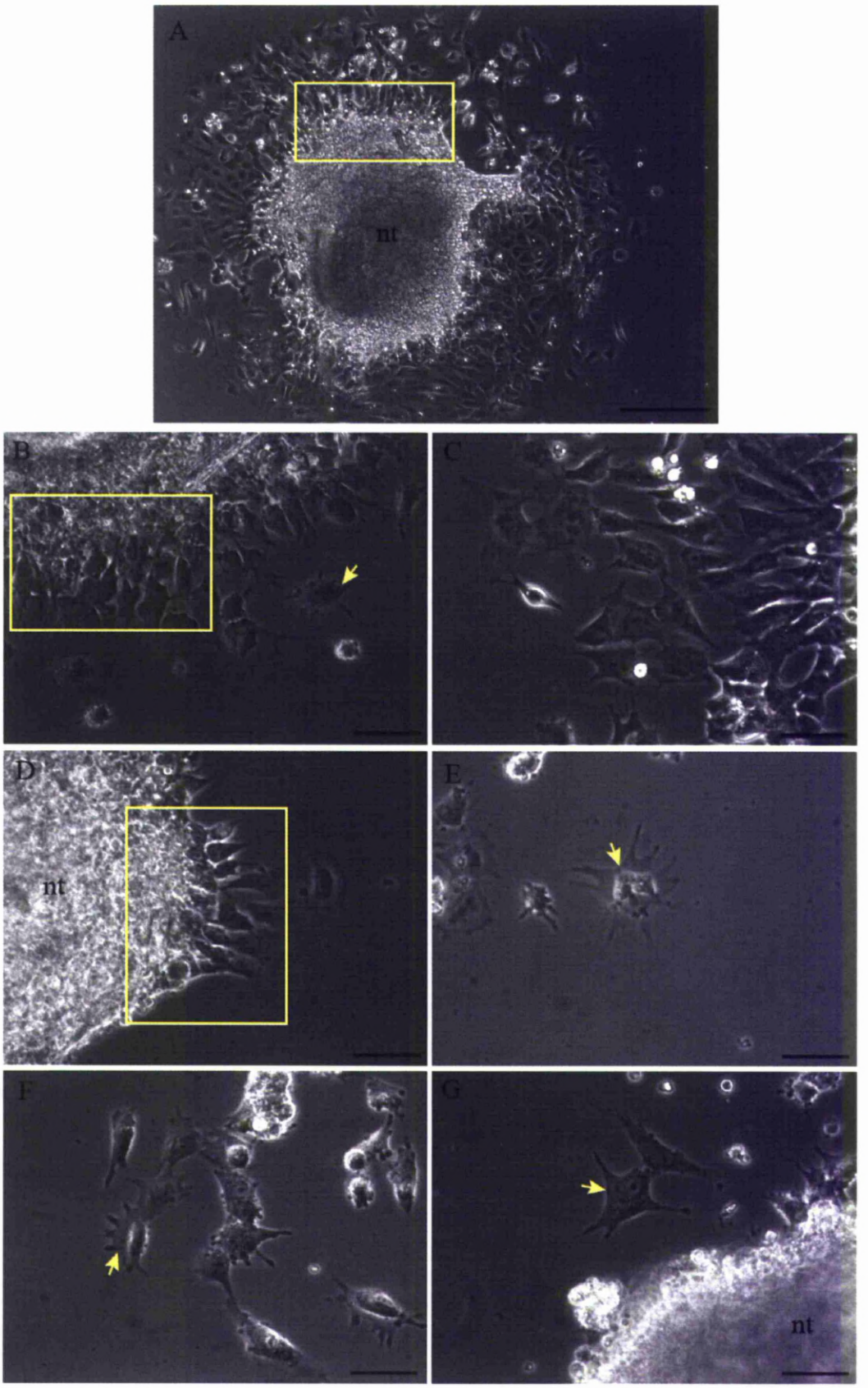
A
nt
B
C
D
nt
E
F
G
nt

Figure 4.5 Characterisation of NCCs after 24 hours in culture

Image A was taken with a 10x objective. The images in B were taken with a 40x objective. All images were taken using phase contrast. The areas inside the yellow boxes show examples of an expanse of flattened epithelial cells (A, B, C and D) emerging from the central neural tube piece. Cells with multiple processes (B, E, F and G, arrows) can be seen migrating away from the neural tube explant. nt – site of neural tube explant Scale bars 200μm (A) 50μm (B).

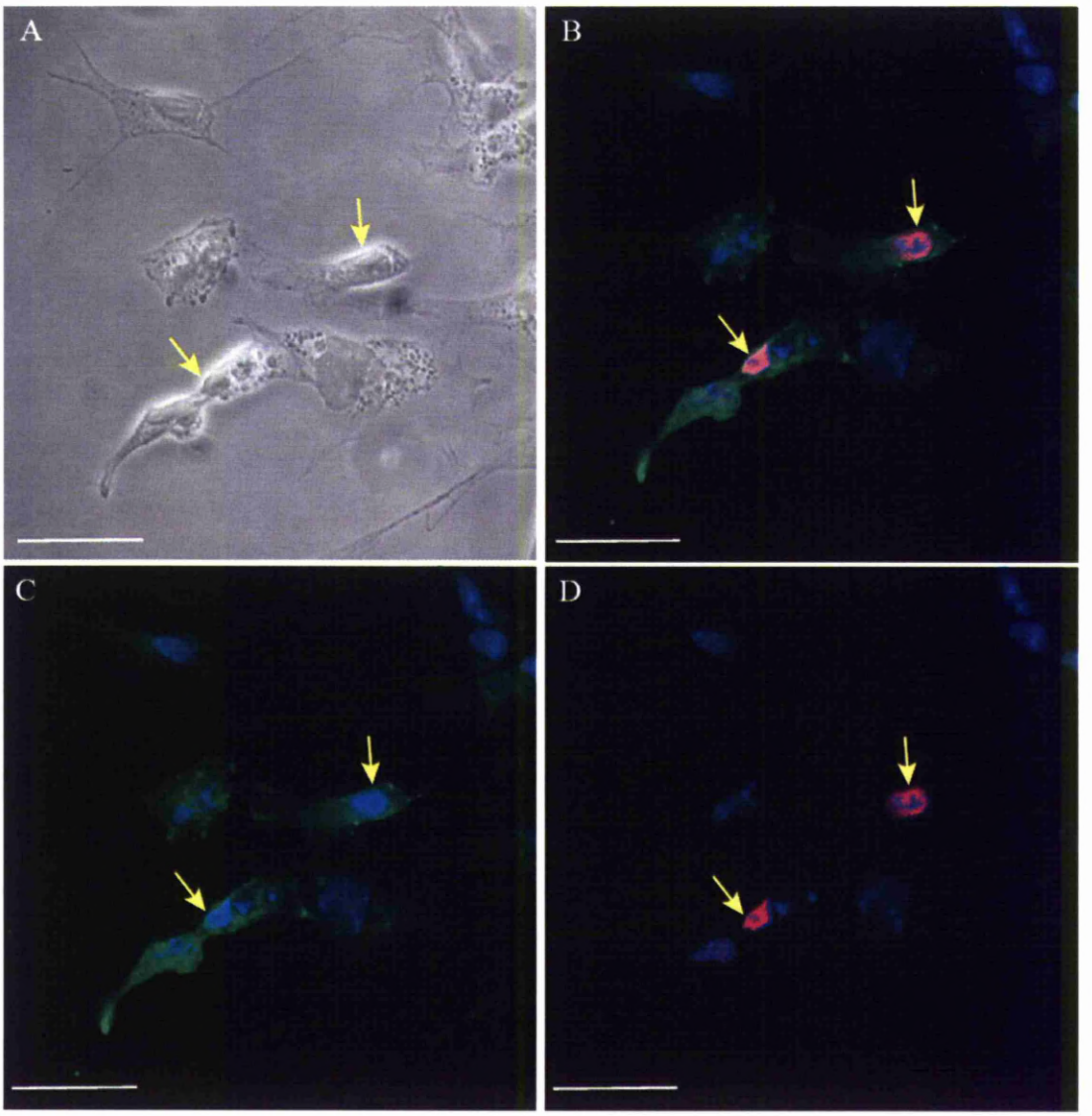

Figure 4.6 Immunofluorescence after 24 hours in culture

Images A-D show antibody staining of neural crest cell markers p75 (green, B and C) and Sox10 (red, B and D) after 24 hours in culture. Image A was taken using brightfield. Image B is a composite image showing expression of P75 (C) and Sox10 (D). The yellow arrows illustrate cells that co-express both P75 and Sox10. DAPI is shown in blue (B-D). All images were taken with a 40x objective. Scale bars 25μm.

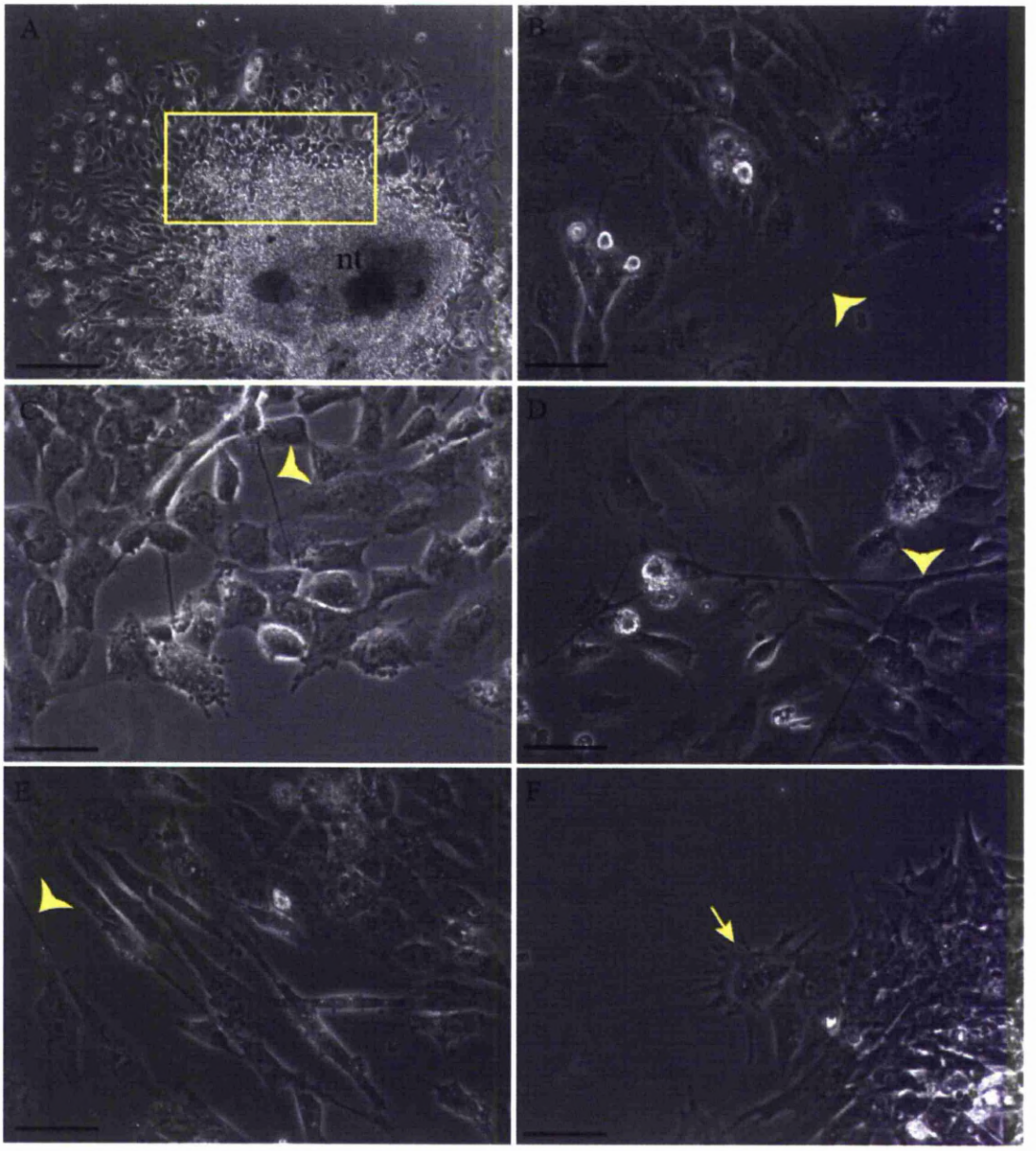

Figure 4.7 NCCs after 48 hours in culture

A-F are brightfield images of neural crest explants taken after 48 hours in culture. A was taken with a 10x objective and B-F were taken with a 40x objective. The area inside the yellow box (A) depicts the epithelial sheet at the outer margin of the neural tube explant. The arrow shows cell with multiple processes migrating away from the central piece (F). The arrowheads indicate axon-like processes arising from the NCCs. nt, site of neural tube explant. Scale bars 200μm (A) 50μm (B-F).

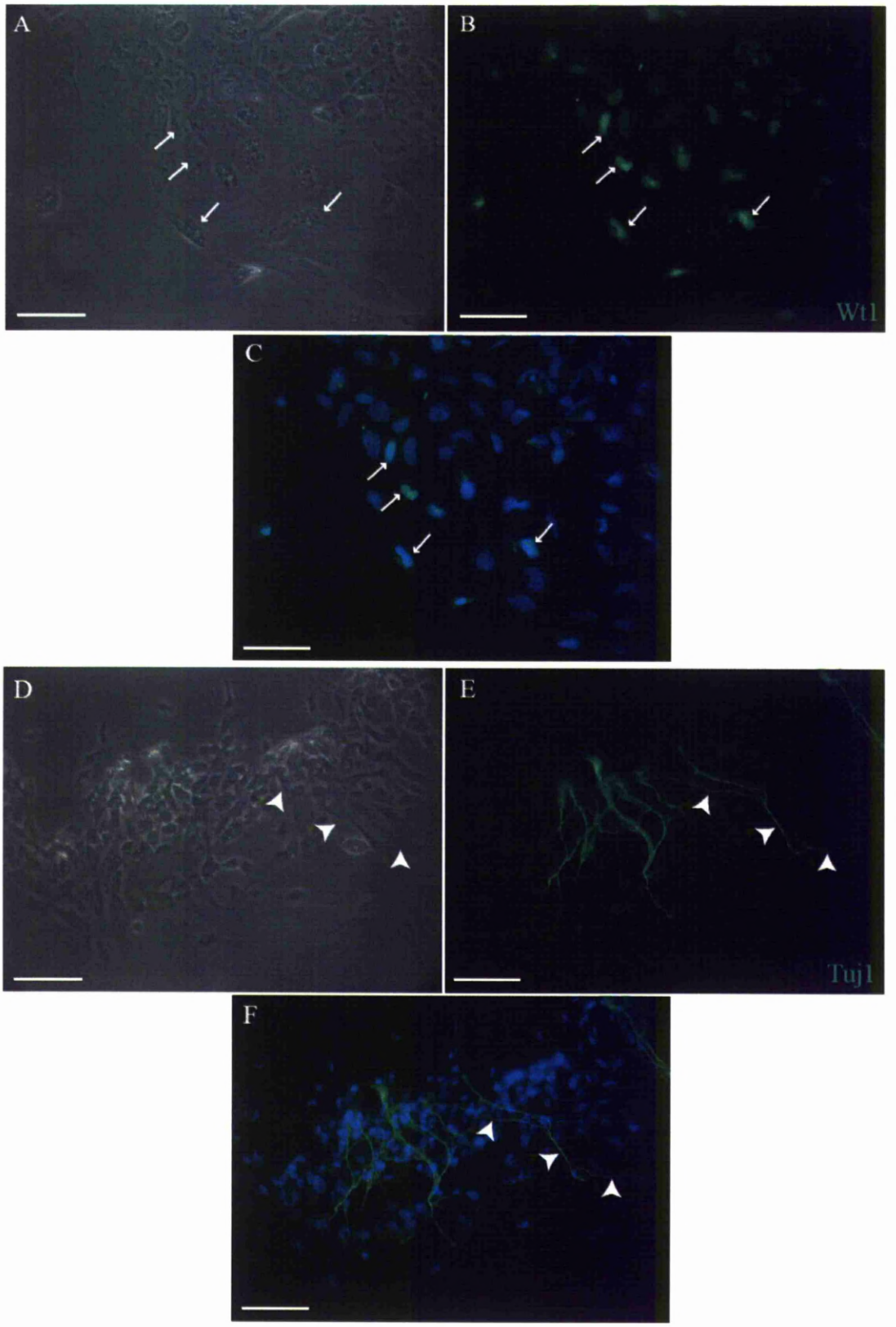
A
B
Wt1
C
D
E
Tuj1
F

Figure 4.8 Neural tube cultures after 48hrs in culture

Immunofluorescence was carried our using the polyclonal antibody for Wt1 (B and C). E and F show immunofluorescence using the monoclonal antibody for Tuj1. All images were taken with a 40x objective. A and D are bright-field images. Arrowheads demarcate axonal-like processes. Wt1 staining is seen in the nuclei (arrows, A-C). Tuj1 staining is seen in differentiating neuronal cells (E and F). DAPI is shown in blue (C and F). Scale bars 50μm.

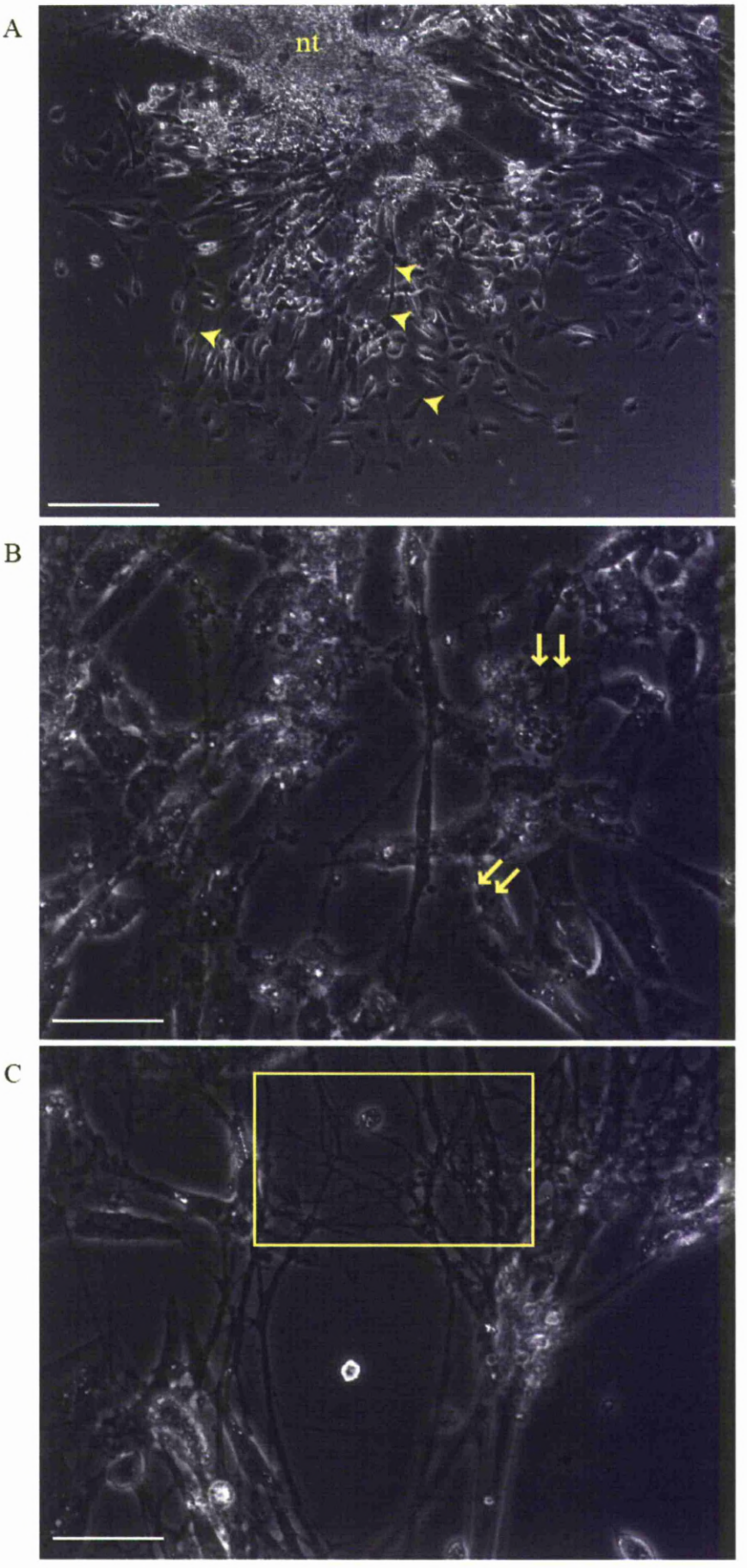
A
nt
B
C

Figure 4.9 NCCs after 72 hours in culture

Image A was taken with a 10x objective. Cells have elongated processes and/or axonal-like projections. The central explant piece has begun to disintegrate. Image B and C were taken with a 40x objective. Image B shows cells that look to have recently divided (arrows). Image C shows axonal-like processes forming complex networks indicative of a neuronal plexus (box). nt, site of neural tube explant. Scale bars 200μm (A) 50μm (B and C).

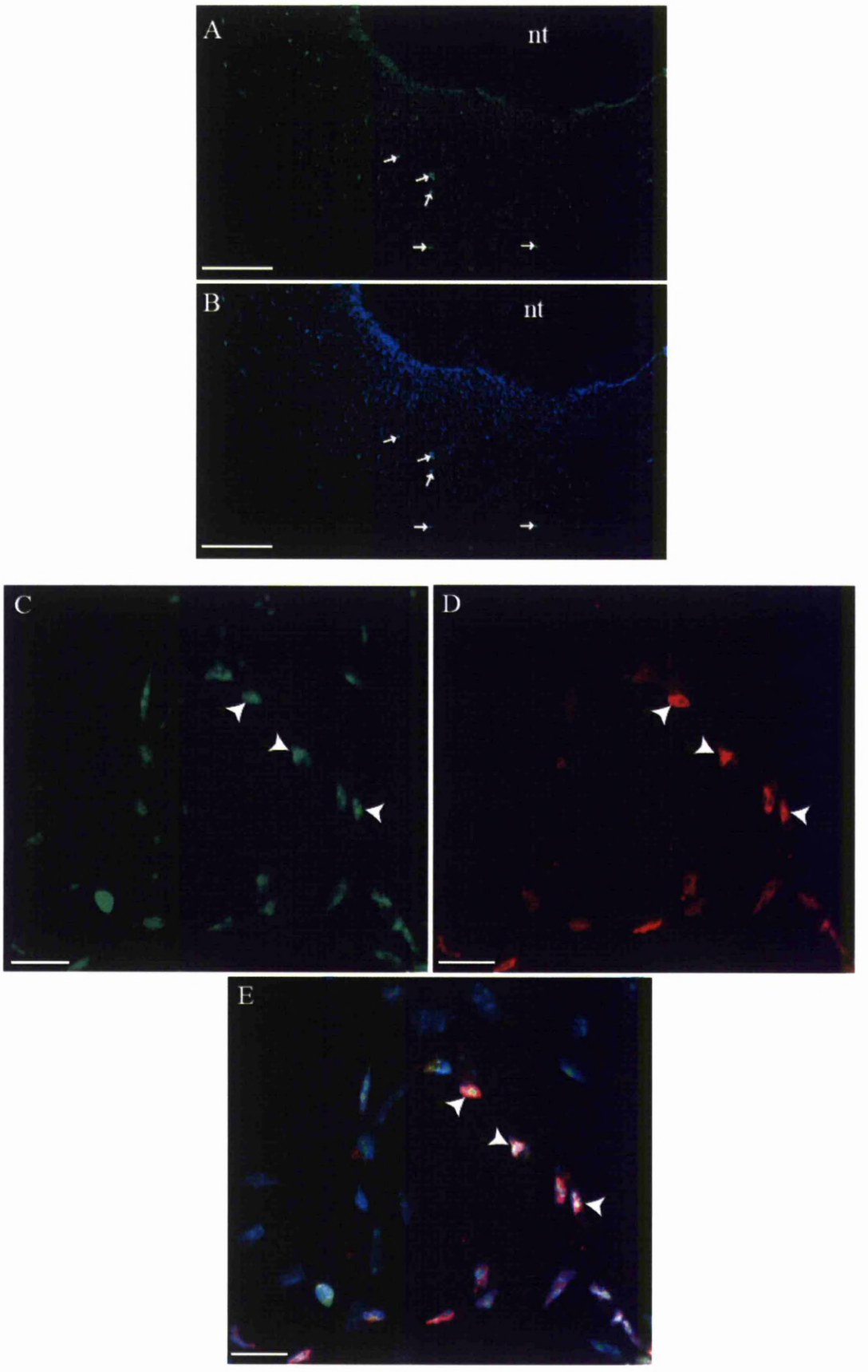
A
nt
B
nt
C
D
E

Figure 4.10 Immunofluorescence after 96 hours in culture

A and B are immunofluorescence images using a Wt1 antibody taken with a 10x objective (green, arrows). A shows Wt1 staining only. B shows Wt1 and DAPI. C-E show immunofluorescence images using antibodies again Wt1 and Sox10 taken with a 40x objective. C shows Wt1 expression only. D shows Sox10 expression only. E is a composite image showing Wt1 and Sox10 with DAPI. Wt1 and Sox10 are expressed together in some cells (arrowheads, C-E). nt, site of neural tube explant. Scale bars 200μm (A and B) 25μm (C-E).

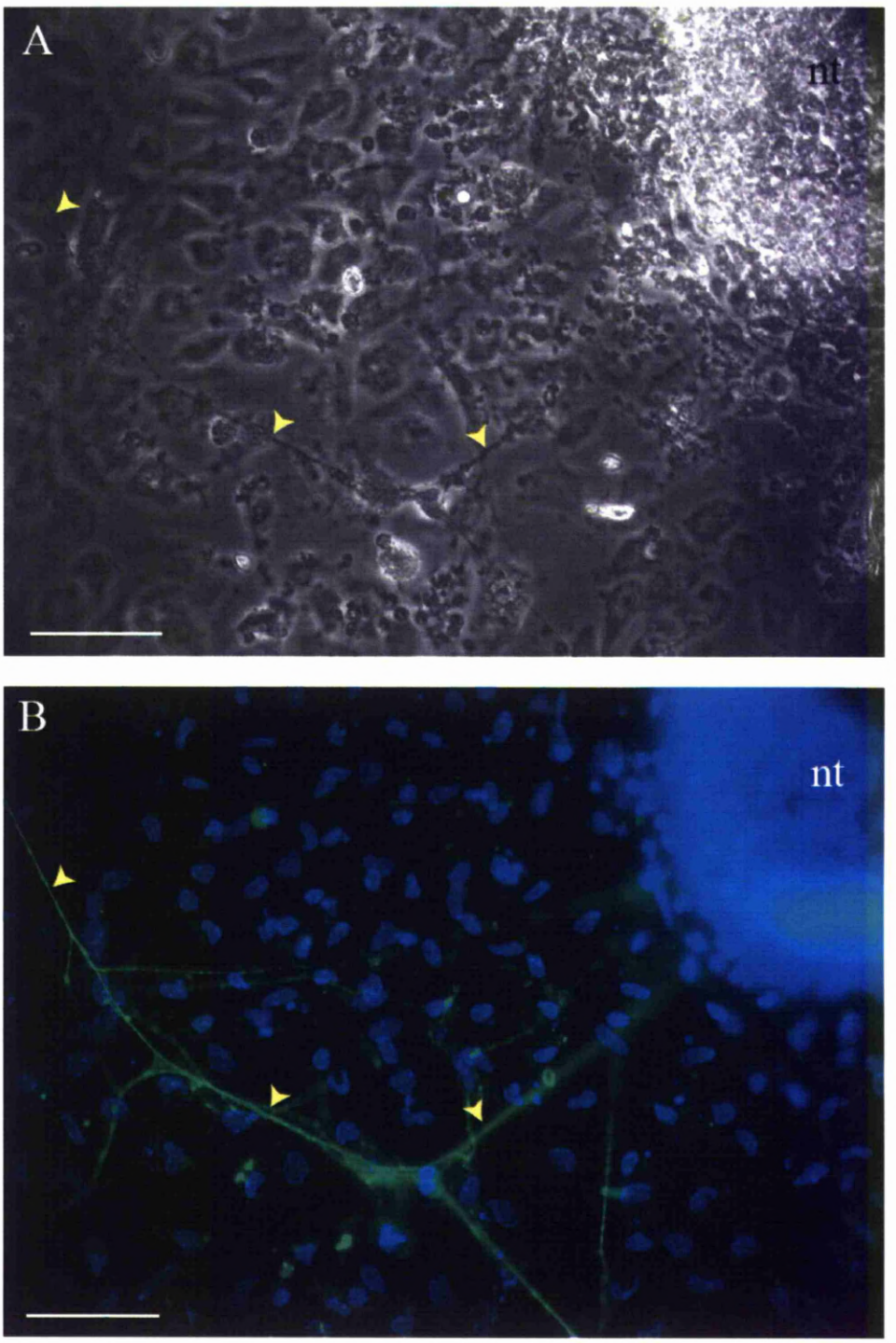

Figure 4.11 Immunofluorescence after 72 hours in culture

A and B were taken with a 40x objective. A is a bright-field image showing axonal-like projections (arrowheads). B shows antibody staining for the neuronal marker Tuj1 in the axonal processes. nt, site of neural tube explant. Scale bars 50μm.

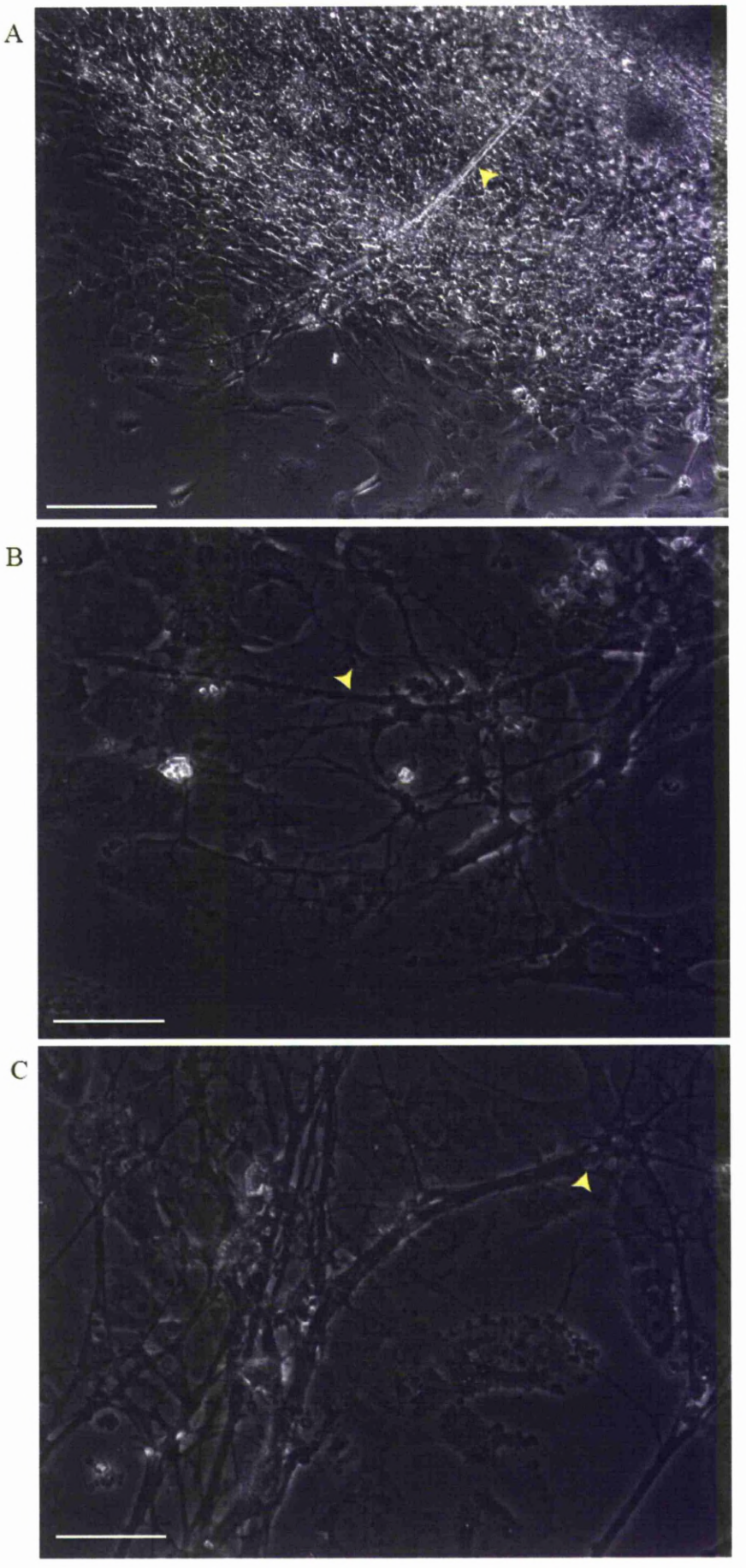
A
B
C

Figure 4.12 NCCs after 120 hours in culture

A is a bright-field image taken with a 10 objective. B and C are bright-field images taken with a 40x objective. Axonal processes in complex networks (A-C, arrowheads). Scale bars 200μm (A) 50μm (B and C).

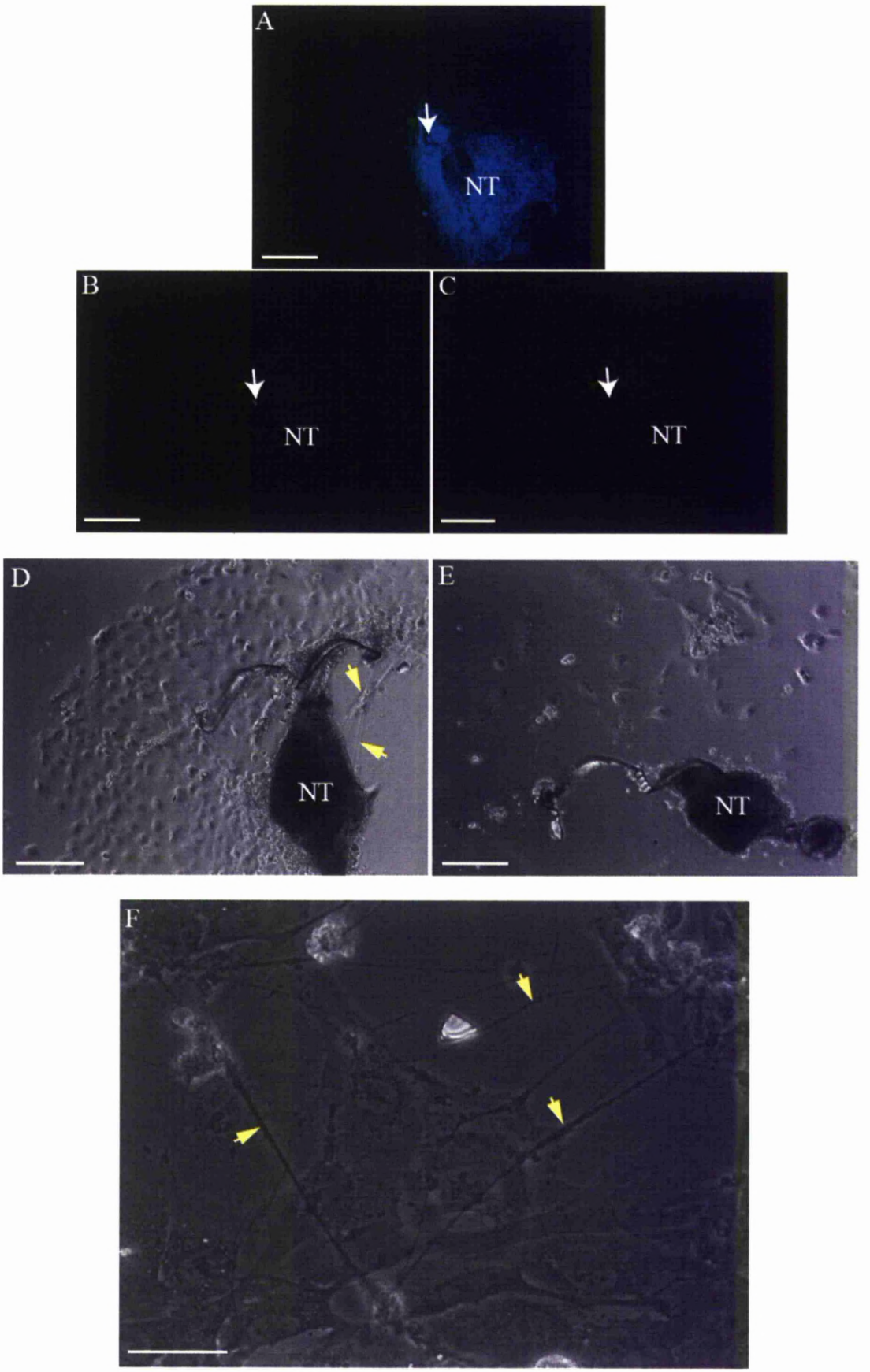
A
NT
B
NT
C
NT
D
NT
E
NT
F

Figure 4.13 Neural tube explants after 120 hours and 168 hours in culture

A-C were captured from immunofluorescence experiments taken with a 10x objective using Wt1 and Sox10 antibodies after 120 hours. Image A shows the cell nuclei stained with DAPI. B shows Wt1 staining only. C shows Sox10 staining only. There is no specific staining of Wt1 and Sox10 (B and C). The arrows indicate a clump of cells which are fluorescent with both the red and green microscope filters. This does not appear to be specific staining (A-C). D and E are bright-field images taken with a 10x objective after 120 hours (D) and 168 hours (E). There are fewer cells after 168 hours and neural tube explant appears to have atrophied (E) in comparison with the neural tube explant at 120 hours (D). F is a bright-field image taken with a 40x objective after 168 hours in culture. Axonal processes are present (arrowheads) but there are fewer cells overall. NT, site of neural tube explant. Scale bars 50μm (A) 200μm (B-F).

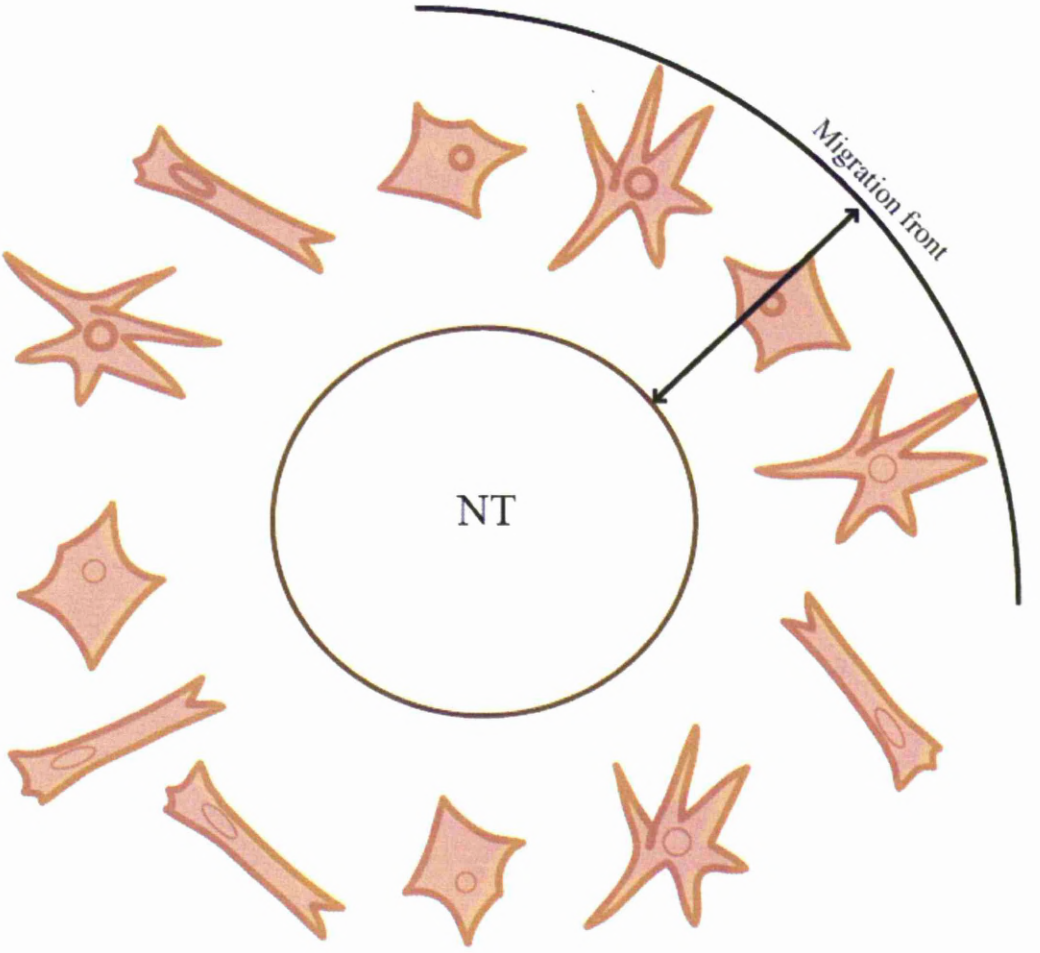

Figure 4.14 Measuring the distance travelled of migrating NCCs

This figure is a schematic diagram representing a typical neural tube explant (NT) in culture. The distance travelled by NCCs in culture was measured from the margin of the explant to the migration front in μm. This was measured at 24 hours and 48 hours after being placed in culture. 7 samples were measured in order to produce an average distance travelled by NCCs over time in culture.

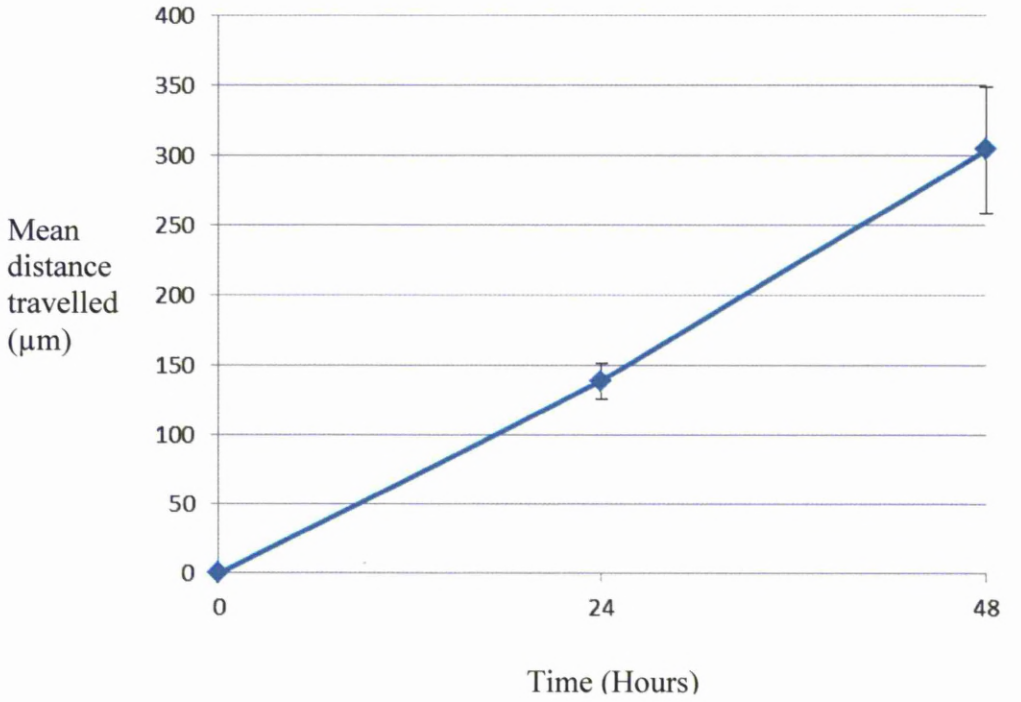

Figure 4.15 Distance travelled by migratory NCCs in culture

The graph shows data collected from the NCC migration assay with an N number of 7. Explants were photographed at 24 and 48 hours after explants were placed in culture (time 0). At 24 hours the NCCs had migrated a mean distance of 138.7143, which gave the cells a rate of migration of 5.78µm/hour. At 48 hours the NCCs had migrated a mean distance of 304.1429 with a rate of migration of 6.34µm/hour. Error bars represent the standard error.

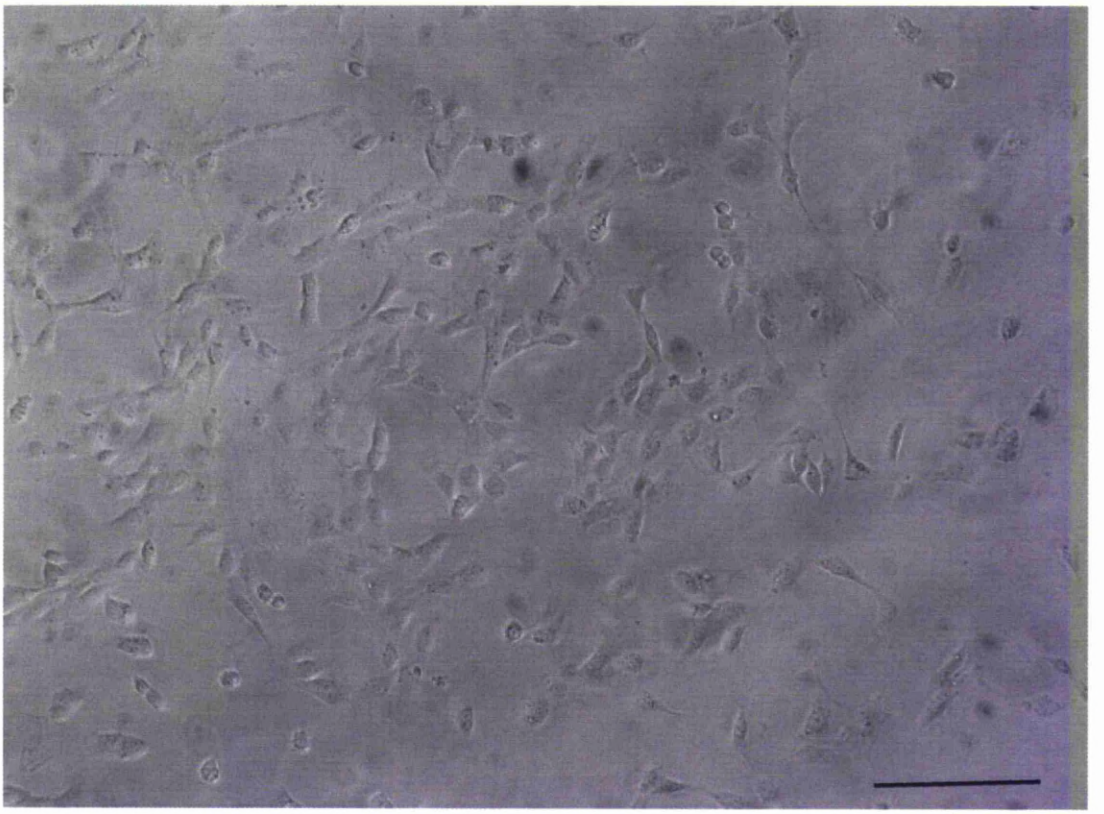

Figure 4.16 Kidney stem cells in culture

The bright field image shows KSC taken with a 10x objective after 24 hours in culture. Once the cells had reached 70% confluence they were ready for transfection with siRNAs. Scale bar 200μm.

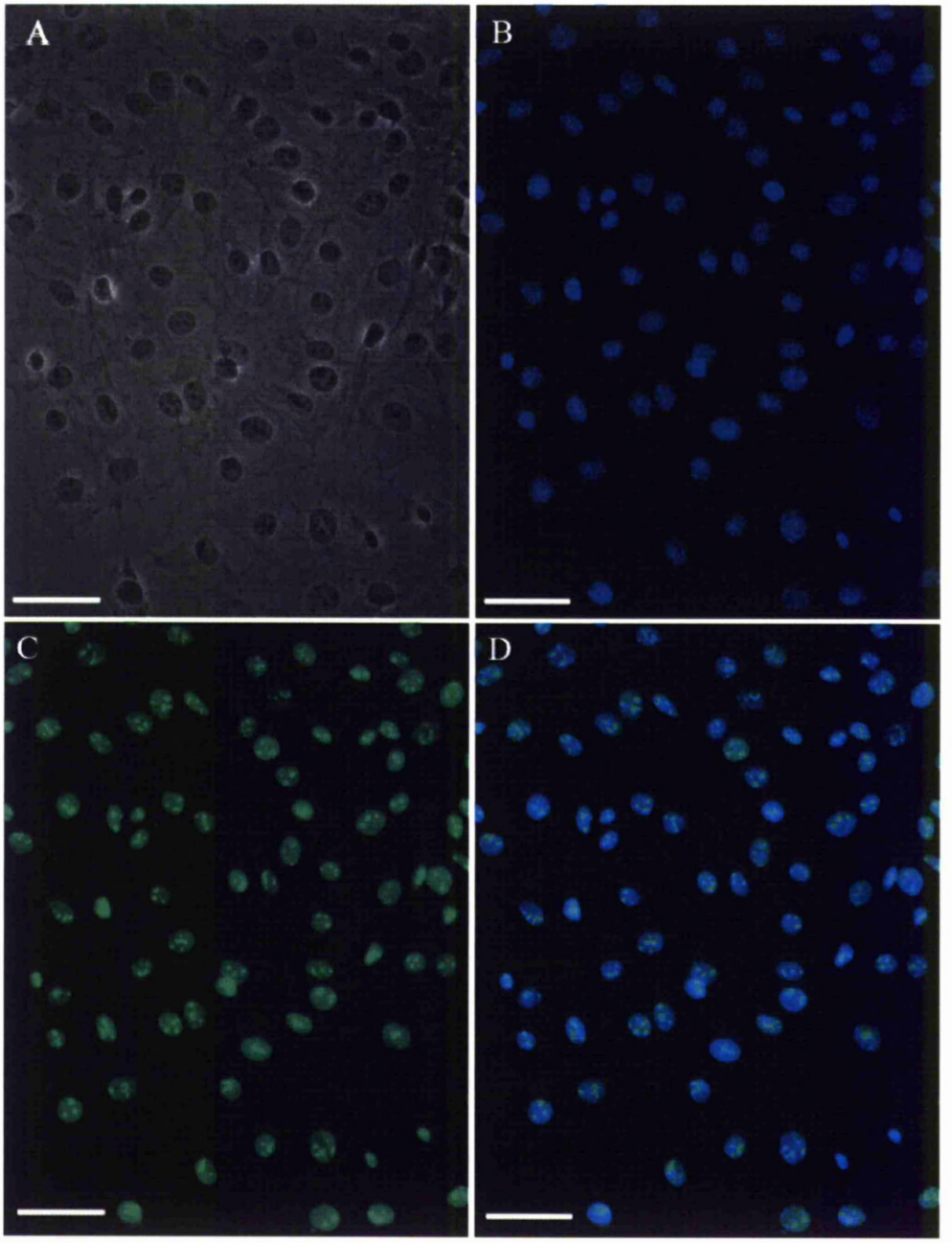

Figure 4.17 KSC express high levels of Wt1

Images A-D show KSC which underwent immunofluorescence using the polyclonal Wt1 antibody in order to confirm that they did express Wt1. Image A is bright field, image B shows DAPI staining, image C show's Wt1 expression within the nuclei of the KSC, and image D show the overlay between DAPI (B) and Wt1 (C). Images were taken with a 40x objective. Scale bar 50μm.

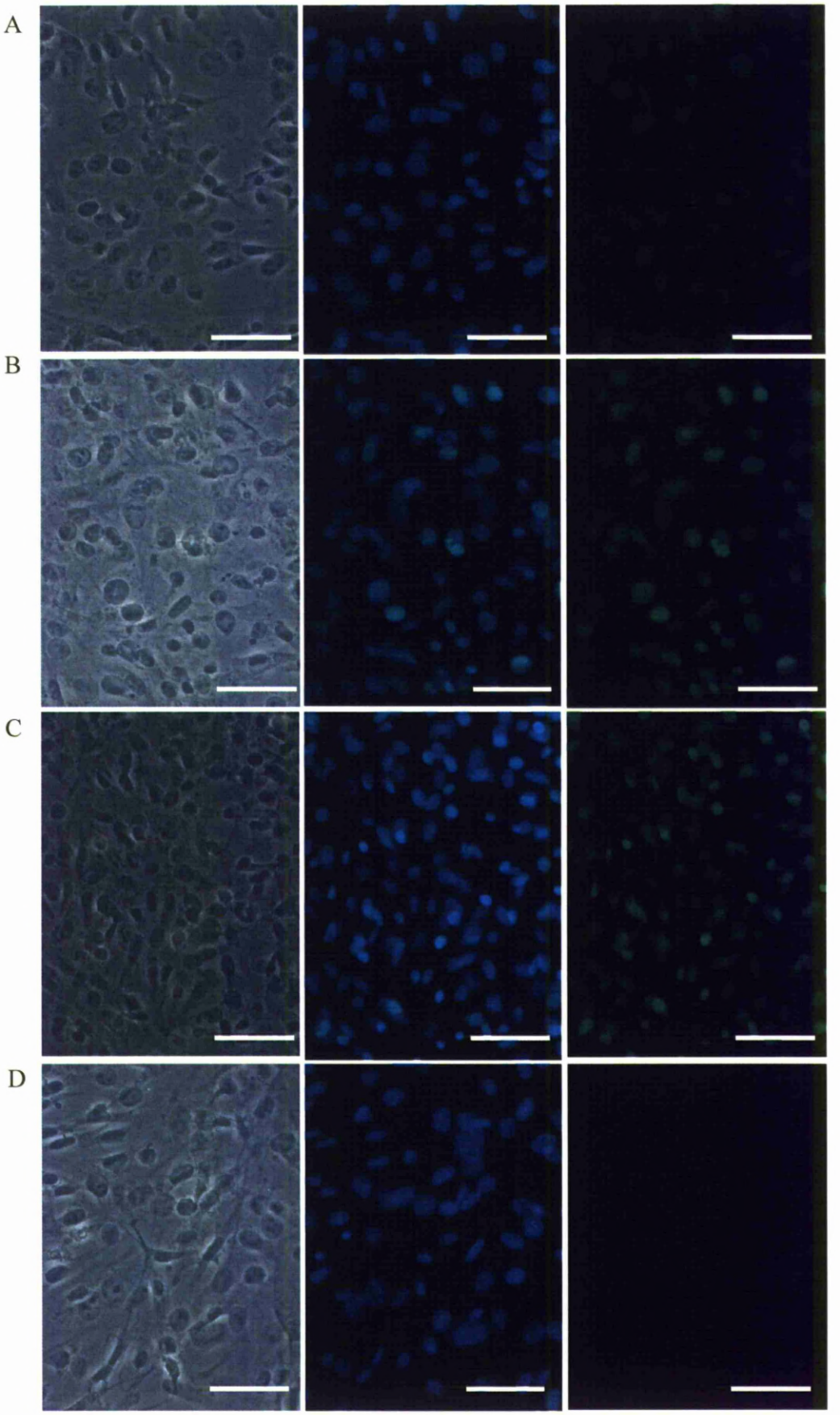
A
B
C
D

Figure 4.18 siRNA repression of Wt1 in KSC

Each set of images (A-C) in this figure show KSC post-transfection with siRNAs or controls which have been fixed and prepared for immunofluorescence to see if Wt1 expression had been repressed. Each set shows bright field image, an overlay of DAPI and Wt1, and Wt1 alone. Image set A shows KSC treated with Wt1 siRNA. Images set B show KSC treated with control SiRNA. Image set C shows KSC treated with the transfection media minus any SiRNA. Image set D is a negative control for the antibody showing KSC treated with siRNA but not incubated with primary antibody during the staining procedure. This was carried out for each of the three conditions and no unspecific staining was found. Scale bar 50μm.

Chapter 5

Discussion

This thesis aimed to establish a time-point at which Wt1 was expressed in developing mouse NCCs, due to results of lineage tracing experiments, by systematically examining mouse embryos with the use of immunohistochemical and in situ hybridisation techniques. I also aimed to characterise the behaviour of vagal level NCCs in vitro and set up SiRNA experiments to knock down Wt1 in cells where Wt1 is known to be highly expressed, kidney stem cells, with the view to eventually using this in vitro/siRNA system on vagal NCCs in an attempt to establish a functional correlation between the *Wt1* gene, and the development of the ENS. Throughout my studies I have shown that Wt1 protein and mRNA can be detected in NCCs of developing mouse embryos with the use of immunohistochemistry and in situ hybridisation both in vivo and in vitro. These aims were achieved and the findings have led me to the following conclusions, which will help direct future projects:

The expression pattern of Wt1 in mouse embryonic development has been described in depth in the literature from E9.0 onwards (Pritchard-Jones, Fleming et al. 1990; Pelletier, Schalling et al. 1991; Armstrong, Pritchard-Jones et al. 1993; Kreidberg, Sariola et al. 1993; Park, Schalling et al. 1993; Moore, Schedl et al. 1998; Moore, McInnes et al. 1999). My results correspond with Wt1 expression patterns described in this literature between the stages of E9.5 and E16.5. Thus, the novelty of my results resides in the expression pattern of Wt1 during earlier periods of embryogenesis. Here I will discuss the expression of Wt1 prior to E9.0 as shown by my data in the previous results chapters, and express ideas for the potential role Wt1 has in NCCs and ENS precursors.

In my analysis I could show that Wt1 and Sox10 are co-expressed in approximately a quarter of the number of NCCs when they begin their migration away from the neural crest at E8.5 in the mouse embryo. This observation suggests that a subpopulation of ENS precursors is derived from Wt1-expressing cells. This novel finding may account for LacZ staining found within the ENS of adult Wt1-Cre mice (Wilm, Ipenberg et al. 2005) and co-staining of Wt1-derived β-Gal and the neuronal marker Hu in newborn Wt1-Cre mouse ENS (Wilm, unpublished). In order to investigate this finding further a conditional, inducible Cre system could be employed, in which a drug-inducible Wt1-driven Cre can be activated at an early embryonic stage. The drug used in this system is Tamoxifen (Danielian, Muccino et al. 1998; Hayashi and McMahon 2002). This mouse could then be mated with the Rosa26 reporter (Soriano 1999) or another reporter mouse line. Only on administration of Tamoxifen would Cre become active and recombination could take place. This could be performed at varying stages during embryogenesis and the resulting staining would reveal information about when the Cre was activated, even once Wt1 was no longer expressed by NCCs.

One of my findings was detection of Wt1 at E7.5 in the mouse embryo. However, co-staining for Wt1 and Sox10, in order to test whether Wt1 could be highlighting emerging NCCs, revealed no expression of Sox10 at this embryonic stage. Sox10 is reported to be expressed from E8.5 onwards, when NCCs delaminate from the neural crest and begin their migration throughout the embryo (Hong and Saint-Jeannet 2005). Therefore, the data collected from these immunofluorescence experiments, which showed no Sox10 expression at E7.5 were to be expected and

correspond to what is already known about Sox10 expression in the developing mouse embryo.

My results revealed that Wt1 expression was confined to a subpopulation of Sox10-expressing NCCs at E8.5 in the mouse. It would be important to determine which particular NCC subset was expressing Wt1 at this time-point. Could it be that Wt1 is only expressed in certain neurons, such as nitric oxide synthase (NOS) neurons or calcitonin gene-related peptide (CGRP) neurons, and is Wt1 expressed in glial cells (Figure 5.1)? Determining the specific neural crest-derived lineage that Wt1 is expressed in would enable us to establish if the migratory potential or phenotype of these cells is disrupted or changed in Wt1 mutant lines.

My finding that Wt1 and Sox10 are co-expressed in NCCs raises an interesting link to another member of the *Sox* gene family, the *Sox9* gene, *Sox9* has been shown to be regulated by *Wt1* during testis development (Gao, Maiti et al. 2006). There is a conserved region 5' of Sox9, which includes a putative binding site for Wt1 (Bagheri-Fam, Ferraz et al. 2001). Importantly, *Sox9* is expressed in NCCs at the same time, E8.5, as Sox10 in the mouse as NCCs begin their migration throughout the embryo into their different lineages (Hong and Saint-Jeannet 2005). It would be interesting to investigate the Sox10 protein and determine if this too has a putative binding site for Wt1. If this was the case it would further support my findings showing co-expression of Wt1 and Sox10 in NCCs. It could also serve as an aid for investigating a role of Wt1 in NCCs and ENS development. A conditional knock-out system could be employed using the Cre-LoxP system where Wt1

would be conditionally knocked-out in Sox10-expressing cells. Analysis of this could determine a role for Wt1 in a subset of cells in the ENS.

The Wt1 monoclonal antibody and the Wt1 polyclonal antibody both were able to delineate the same expression pattern when used on tissue sections generated from mouse embryos between the embryonic ages of E9.5 and E16.5. However, the monoclonal Wt1 antibody was unable to detect a specific signal for Wt1 prior to E9.5. This finding meant I was only able to use the polyclonal Wt1 antibody in immunofluorescence experiments at E8.5 and E7.5. The question that arises from this observation is: Why is there a difference between the two antibodies at early embryonic time-points? One explanation could be that the staining seen at E8.5 and E7.5 is an artefact. However the same expression pattern was observed each time this experiment was performed on both embryos from the same litter and embryos taken from different litters. The expression was nuclear with some cytoplasmic expression, which corresponds to the literature on intracellular localisation of Wt1 within a cell (Rauscher, Morris et al. 1990; Morris, Madden et al. 1991; Pelletier, Schalling et al. 1991; Bickmore, Oghene et al. 1992; Niksic, Slight et al. 2004). Furthermore, RNA in situ hybridisation experiments also detected Wt1 activity in the neural crest region at E8.5 and in some cells of all 3 germ layers at E7.5. Taken together these data suggest that Wt1 staining performed with the Wt1 polyclonal antibody is not artifactual and that there must be an alternative explanation for the differential pattern of Wt1 staining with the two Wt1 antibodies at early embryonic stages.

The answer to this quandary may lie in one of the many Wt1 protein isoforms generated by the numerous alternative splicing events found in the *Wt1* gene. The rabbit polyclonal Wt1 antibody (C-19, Santa Cruz) was raised against peptides at the C-terminus of the Wt1 protein. However, the mouse monoclonal Wt1 antibody (6F-H2, Upstate) was raised against the N-terminus of the Wt1 protein. Alternative splicing has been found to occur in exon one of the *Wt1* gene. As a result a shorter Wt1 protein isoform is produced known as AWT1 (Dallosso, Hancock et al. 2004). It is therefore possible that the monoclonal Wt1 antibody corresponds to peptides which were absent due to alternative splicing in exon 1. Thus it is important to establish if AWT1 is expressed in mouse embryos prior to E9.5. If this is the case it would provide a potential explanation as to why it is not possible to detect a specific signal at E8.5 with the monoclonal Wt1 antibody. In order to establish if AWT1 is expressed, RT-PCR using specific primers for Wt1 exon 1 and AWT1 alternative exon 1 could be employed. I have made some preliminary investigations into this but was unable to optimise the experimental conditions in time and therefore could not make a conclusion. The preliminary data suggested that both Wt1 and AWT1 were being expressed at E8.5 as a band was found for both transcripts. However further work would be needed to confirm if this was in fact the case.

A recent study revealed the –KTS Wt1 isoform has a direct function in regulating EMT during the development of coronary vasculature using a conditional Wt1-knockout mouse generated by mating $Wt1^{GFP/+}$ and Gata5-Cre (Martinez-Estrada, Lettice et al. 2010). The resultant $Wt1^{LoxP/GFP}$ mutant mice knocked-out Wt1 specifically in epicardial cells and embryonic death occurred between E16.5 and

E18.5 due to cardiovascular malformation (Martinez-Estrada, Lettice et al. 2010). It has long been hypothesised that Wt1 has a role in the processes of EMT and MET (Armstrong, Pritchard-Jones et al. 1993; Kreidberg, Sariola et al. 1993; Moore, Schedl et al. 1998; Moore, McInnes et al. 1999). There is now evidence that Wt1 regulates the transcription of key factors in EMT, snail and E-cadherin (Martinez-Estrada, Lettice et al. 2010). EMT is known to be a critical process in the formation of the development of the neural crest from which the ENS is derived (Duband, Monier et al. 1995; Sakai and Wakamatsu 2005). This process is controlled by a balance between E-cadherin and Snail (Cano, Perez-Moreno et al. 2000). Three potential binding sites for Wt1 have been indentified as conserved regions on the Snail (*Snail*) gene. My data presented in this thesis revealed Wt1 is expressed in the neural crest at E8.5. It could be possible that Wt1 plays a role in the process of EMT through the regulation of E-cadherin and Snail in NCC delamination as was shown by Martinez-Estrada in the case of coronary vasculature development. However Wt1 appears not to be expressed in all NCCs and phenotypes related to NCC developmental deficiencies in the mutant mouse have not been described.

As part of Martinez-Estrada's study into the role of Wt1 in EMT a Tamoxifen-inducible Wt1-knockout was generated in immortalised epicardial cells (Martinez-Estrada, Lettice et al. 2010). The in vitro results were similar to the results Martinez-Estrada saw in the conditional Wt1-knockout mouse. Snail was down-regulated and E-cadherin up-regulated after tamoxifen administration in order to induce the Wt1 knockout in a dose-dependent manner (Martinez-Estrada, Lettice et al. 2010). This suggested that the epicardial cells were remaining in an epithelial

state and did not under go EMT to become motile mesenchymal cells. Scratch assays on these mutant cells revealed a decrease in migratory potential of epicardial cells after Wt1 was knocked out when Tamoxifen was administered (Martinez-Estrada, Lettice et al. 2010). Could this be the link to Wt1 within NCCs? Perhaps if Wt1 has a role in EMT at the neural crest then early migratory potential of the subset of Wt1-expressing NCCs is affected and therefore these cells can not migrate in a normal manner within the developing ENS.

Further evidence for a role of Wt1 in cell migration or cell dynamics as a whole comes from Dudnakova and her finding that cytoplasmic Wt1 directly binds with the cytoskeletal molecule actin, which is vital for cell movement (Dudnakova, Spraggon et al. 2010). These studies do provide insight into a role for Wt1 in cell motility and EMT. Therefore further investigation would be needed to confirm if Wt1 is playing a similar role in NCCs, as I was unable to reach the stage where I could acquire a definite measurement for Wt1 knock-down with the use of siRNA on NCCs in neural tube explants in vitro.

The results from my migration assays produced a mean distance travelled of 139μm in 24 hours and 304μm after 48 hours. These results gave a mean rate of migration for NCCs of 5.78μm/hour after 24 hours and 6.34μm/hour after 48 hours. The mean rate of migration could be used as a bench mark for measuring migration in NCCs when Wt1 is knocked-down. There is, however, a discrepancy between my migration data and that of the literature (Barlow, Wallace et al. 2008). The NCCs in my experiments migrated slower than those published by Barlow et al. however, this may be explained by the use of different species. My neural tube

explants were taken from mouse embryos, whereas Barlow et al. worked on avian embryos.

One of my findings showed that NCCs could be maintained in a healthier condition when media composition was switched from DMEM plus 10% NCS to DMEM plus 5% NCS and 5% horse serum (Jaenisch 1985). This finding is supported by investigations made into in vitro culture of plaque-forming cells (PFC) (Levy 1980). A greater number of PFC was shown to be obtained with the use of media supplemented with 5% horse serum and 5% NCS (Levy 1980).

Wt1 was shown to be expressed in approximately half the number of cultured NCCs after 24 hours as part of my in vitro study. This result corresponds to my findings in vivo where around half of Sox10-expressing NCCs in the region of the neural crest, also expressed Wt1. The NCC marker p75 was also expressed by most of the cultured NCCs at this time-point providing evidence that these cells were neural crest-derived. A small population of p75-expressing cells co-expressed with Sox10. Neural crest stem cells (NCSCs) are characterised by the expression of these two markers (Stemple and Anderson 1992; Bixby, Kruger et al. 2002; Kruger, Mosher et al. 2002; Wong, Paratore et al. 2006). NCSCs retain their developmental potential in multi-potent state and can undergo self renewal in adult tissues to replace lost or damaged cells. NCSCs have been isolated in a number of adult tissues including adult mouse gut (Kruger, Mosher et al. 2002). These cells have been shown to have the potential to give rise to enteric neurons and glia both in vivo and in vitro (Kruger, Mosher et al. 2002). It is important to determine if Wt1 is expressed specifically in these NCSCs and would be interesting to

investigate if Wt1 could play a role in these cells, perhaps in self-renewal. Evidence of a role for Wt1 in self-renewal stems from the finding of Wt1 expression in normal human bone marrow (Baird and Simmons 1997). When Wt1 was over-expressed in bone marrow cells an increased number of haematopoietic cells were observed but there was no increase in maturation of these cells (Nishida, Hosen et al. 2006). In the case of leukaemia the constitutive expression of Wt1 in leukemic cell lines was shown to block differentiation and lead to the development of leukaemia (Svedberg, Chylicki et al. 1998). These studies suggest a role for Wt1 in the self-renewal of cells.

I had aimed, in a preliminary study, to knock down Wt1 with siRNA in KSC before eventually adapting this technique for use on vagal NCCs. The initial data gathered from this pilot experiment was not convincing enough with only immunofluorescence as a way of determining how much, if any, Wt1 had been repressed because it was simply showing Wt1 protein expression and could reveal nothing at the mRNA level. siRNA would not necessarily be expected to result in complete loss of Wt1 mRNA, and hence one would need to look at Wt1 levels with/without knock-down with time and to use RT-PCR to see the timing of the effect on the RNA levels. Unfortunately time limitations meant I was unable to optimise this procedure and so this will have to be carried out in future projects.

Wt1 seems to play many different functional roles throughout development. Many of these roles are yet to be determined. It will be interesting to see what function Wt1 has in NCCs and ENS development. It would appear that even after 20 years

of investigation and numerous important developments there is still a lot unknown about the multi-faceted Wt1 protein and its many functions.

E10.5 midgut
E12.5 midgut
E17.5 small intestine
undifferentiated neural crest cell
p75+ Ret+ Phox2b+ (TH)
differentiating glial cell
p75+ Phox2b+
NOS neuron
Ret+ Phox2b+ NOS+
CGRP neuron precursor
?
undifferentiated neural crest cell
p75+ Ret+ Phox2b+
neuronal precursor?
Ret+ Phox2b+
GLIAL CELL
p75+ Phox2b+ GFAP+
NOS NEURON
Ret+ Phox2b+ NOS+
CGRP NEURON
Ret+ Phox2b+ CGRP+
UNKNOWN NEURONS AND GLIAL CELLS
?
p75
Ret
Phox2b
Phox2a

Figure 5.1 Examples of neuronal subtypes in the developing ENS

Image adapted from Young, Ciampoli et al. 1999 showing the differentiation and the changes in gene/protein expression of NCCs. All NCCs are undifferentiated at E10.5 and express p75, Ret, Phox2b. Tyrosine hydroxylase (TH) is expressed in a subset of these cells. At E12.5 NCCs have begun to differentiate based on the differenced in marker expressed, a NOS neuron can be identified as NOS is expressed in this subtype and differentiating glial cells retain expression p75. At E17.5 specific subpopulations of neurons are observed again based on the marker they express, such as NOS and CGRP neurons (Young, Ciampoli et al. 1999).

References

Abzhanov, A., S. J. Rodda, et al. (2007). "Regulation of skeletogenic differentiation in cranial dermal bone." Development 134(17): 3133-3144.

Akiyama, H., M. C. Chaboissier, et al. (2002). "The transcription factor Sox9 has essential roles in successive steps of the chondrocyte differentiation pathway and is required for expression of Sox5 and Sox6." Genes Dev 16(21): 2813-2828.

Algar, E. M., T. Khromykh, et al. (1996). "A WT1 antisense oligonucleotide inhibits proliferation and induces apoptosis in myeloid leukaemia cell lines." Oncogene 12(5): 1005-1014.

Amiel, J. and S. Lyonnet (2001). "Hirschsprung disease, associated syndromes, and genetics: a review." J Med Genet 38(11): 729-739.

Andermann, P. and E. S. Weinberg (2001). "Expression of zTlxA, a Hox11-like gene, in early differentiating embryonic neurons and cranial sensory ganglia of the zebrafish embryo." Developmental dynamics : an official publication of the American Association of Anatomists 222(4): 595-610.

Anderson, R. B., A. L. Stewart, et al. (2006). "Phenotypes of neural-crest-derived cells in vagal and sacral pathways." Cell Tissue Res 323(1): 11-25.

Argos, P., A. Landy, et al. (1986). "The integrase family of site-specific recombinases: regional similarities and global diversity." EMBO J 5(2): 433-440.

Armstrong, J. F., K. Pritchard-Jones, et al. (1993). "The expression of the Wilms' tumour gene, WT1, in the developing mammalian embryo." Mech Dev 40(1-2): 85-97.

Bagheri-Fam, S., C. Ferraz, et al. (2001). "Comparative genomics of the SOX9 region in human and Fugu rubripes: conservation of short regulatory sequence elements within large intergenic regions." Genomics 78(1-2): 73-82.

Baird, P. N. and P. J. Simmons (1997). "Expression of the Wilms' tumor gene (WT1) in normal hemopoiesis." Exp Hematol 25(4): 312-320.

Barlow, A. J., A. S. Wallace, et al. (2008). "Critical numbers of neural crest cells are required in the pathways from the neural tube to the foregut to ensure complete enteric nervous system formation." Development 135(9): 1681-1691.

Bartkowska, K., K. Turlejski, et al. (2010). "Neurotrophins and their receptors in early development of the mammalian nervous system." Acta neurobiologiae experimentalis 70(4): 454-467.

Baynash, A. G., K. Hosoda, et al. (1994). "Interaction of endothelin-3 with endothelin-B receptor is essential for development of epidermal melanocytes and enteric neurons." Cell 79(7): 1277-1285.

Bernard, O. A., M. Busson-LeConiat, et al. (2001). "A new recurrent and specific cryptic translocation, t(5;14)(q35;q32), is associated with expression of the Hox11L2 gene in T acute lymphoblastic leukemia." Leukemia : official journal of the Leukemia Society of America, Leukemia Research Fund, U.K 15(10): 1495-1504.

Betancur, P., M. Bronner-Fraser, et al. (2010). "Genomic code for Sox10 activation reveals a key regulatory enhancer for cranial neural crest." Proceedings of the National Academy of Sciences of the United States of America 107(8): 3570-3575.

Bickmore, W. A., K. Oghene, et al. (1992). "Modulation of DNA binding specificity by alternative splicing of the Wilms tumor wt1 gene transcript." Science 257(5067): 235-237.

Bixby, S., G. M. Kruger, et al. (2002). "Cell-intrinsic differences between stem cells from different regions of the peripheral nervous system regulate the generation of neural diversity." Neuron 35(4): 643-656.

Brady, J. (1965). "A simple technique for making very fine, durable dissecting needles by sharpening tungsten wire electrolytically." Bull World Health Organ 32(1): 143-144.

Bronner-Fraser, M. (1996). "Manipulations of neural crest cells or their migratory pathways." Methods Cell Biol 51: 61-79.

Burns, A. J., D. Champeval, et al. (2000). "Sacral neural crest cells colonise aganglionic hindgut in vivo but fail to compensate for lack of enteric ganglia." Dev Biol 219(1): 30-43.

Burns, A. J. and N. M. Douarin (1998). "The sacral neural crest contributes neurons and glia to the post-umbilical gut: spatiotemporal analysis of the development of the enteric nervous system." Development 125(21): 4335-4347.

Burns, A. J. and N. M. Le Douarin (2001). "Enteric nervous system development: analysis of the selective developmental potentialities of vagal and sacral neural crest cells using quail-chick chimeras." Anat Rec 262(1): 16-28.

Call, K. M., T. Glaser, et al. (1990). "Isolation and characterization of a zinc finger polypeptide gene at the human chromosome 11 Wilms' tumor locus." Cell 60(3): 509-520.

Cano, A., M. A. Perez-Moreno, et al. (2000). "The transcription factor snail controls epithelial-mesenchymal transitions by repressing E-cadherin expression." Nat Cell Biol 2(2): 76-83.

Carmona, R., M. Gonzalez-Iriarte, et al. (2001). "Localization of the Wilm's tumour protein WT1 in avian embryos." Cell Tissue Res 303(2): 173-186.

Chaffer, C. L., E. W. Thompson, et al. (2007). "Mesenchymal to epithelial transition in development and disease." Cells Tissues Organs 185(1-3): 7-19.

Chalazonitis, A. (2004). "Neurotrophin-3 in the development of the enteric nervous system." Progress in brain research 146: 243-263.

Chalazonitis, A., F. D'Autreaux, et al. (2004). "Bone morphogenetic protein-2 and -4 limit the number of enteric neurons but promote development of a TrkC-expressing neurotrophin-3-dependent subset." The Journal of neuroscience : the official journal of the Society for Neuroscience 24(17): 4266-4282.

Chalazonitis, A., T. P. Rothman, et al. (1998). "Age-dependent differences in the effects of GDNF and NT-3 on the development of neurons and glia from neural crest-derived precursors immunoselected from the fetal rat gut: expression of GFRalpha-1 in vitro and in vivo." Dev Biol 204(2): 385-406.

Coppes, M. J., C. E. Campbell, et al. (1993). "The role of WT1 in Wilms tumorigenesis." FASEB J 7(10): 886-895.

Couly, G., A. Grapin-Botton, et al. (1996). "The regeneration of the cephalic neural crest, a problem revisited: the regenerating cells originate from the contralateral or from the anterior and posterior neural fold." Development 122(11): 3393-3407.

Dai, Y. S. and P. Cserjesi (2002). "The basic helix-loop-helix factor, HAND2, functions as a transcriptional activator by binding to E-boxes as a heterodimer." The Journal of biological chemistry 277(15): 12604-12612.

Dallosso, A. R., A. L. Hancock, et al. (2004). "Genomic imprinting at the WT1 gene involves a novel coding transcript (AWT1) that shows deregulation in Wilms' tumours." Hum Mol Genet 13(4): 405-415.

Danielian, P. S., D. Muccino, et al. (1998). "Modification of gene activity in mouse embryos in utero by a tamoxifen-inducible form of Cre recombinase." Curr Biol 8(24): 1323-1326.

Davies, J. A., M. Ladomery, et al. (2004). "Development of an siRNA-based method for repressing specific genes in renal organ culture and its use to show that the Wt1 tumour suppressor is required for nephron differentiation." Hum Mol Genet 13(2): 235-246.

Dettman, R. W., W. Denetclaw, Jr., et al. (1998). "Common epicardial origin of coronary vascular smooth muscle, perivascular fibroblasts, and intermyocardial fibroblasts in the avian heart." Dev Biol 193(2): 169-181.

Dressler, G. R. (2006). "The cellular basis of kidney development." Annu Rev Cell Dev Biol 22: 509-529.

Duband, J. L., F. Monier, et al. (1995). "Epithelium-mesenchyme transition during neural crest development." Acta Anat (Basel) 154(1): 63-78.

Dudnakova, T., L. Spraggon, et al. (2010). "Actin: a novel interaction partner of WT1 influencing its cell dynamic properties." Oncogene 29(7): 1085-1092.

Elbashir, S. M., J. Harborth, et al. (2001). "Duplexes of 21-nucleotide RNAs mediate RNA interference in cultured mammalian cells." Nature 411(6836): 494-498.

Erlebacher, A., E. H. Filvaroff, et al. (1995). "Toward a molecular understanding of skeletal development." Cell 80(3): 371-378.

Essafi, A. and N. D. Hastie (2010). "WT1 the oncogene: a tale of death and HtrA." Mol Cell 37(2): 153-155.

Foster, J. W., M. A. Dominguez-Steglich, et al. (1994). "Campomelic dysplasia and autosomal sex reversal caused by mutations in an SRY-related gene." Nature 372(6506): 525-530.

Francke, U., L. B. Holmes, et al. (1979). "Aniridia-Wilms' tumor association: evidence for specific deletion of 11p13." Cytogenet Cell Genet 24(3): 185-192.

Fuente Mora, C., E. Ranghini, et al. (2011). "Differentiation of Podocyte and Proximal Tubule-Like Cells from a Mouse Kidney-Derived Stem Cell Line." Stem Cells Dev.

Furness, J. B. (2006). The Enteric Nervous System. Oxford, UK, Blackwell Publishing.

Gammill, L. S. and J. Roffers-Agarwal (2010). "Division of labor during trunk neural crest development." Developmental biology 344(2): 555-565.

Gans, C. and R. G. Northcutt (1983). "Neural crest and the origin of vertebrates: a new head." Science 220(4594): 268-273.

Gao, F., S. Maiti, et al. (2006). "The Wilms tumor gene, Wt1, is required for Sox9 expression and maintenance of tubular architecture in the developing testis." Proc Natl Acad Sci U S A 103(32): 11987-11992.

Gershon, M. D. (2010). "Developmental determinants of the independence and complexity of the enteric nervous system." Trends Neurosci 33(10): 446-456.

Gessler, M., A. Poustka, et al. (1990). "Homozygous deletion in Wilms tumours of a zinc-finger gene identified by chromosome jumping." Nature 343(6260): 774-778.

Gubbay, J., J. Collignon, et al. (1990). "A gene mapping to the sex-determining region of the mouse Y chromosome is a member of a novel family of embryonically expressed genes." Nature 346(6281): 245-250.

Haber, D. A., S. Park, et al. (1993). "WT1-mediated growth suppression of Wilms tumor cells expressing a WT1 splicing variant." Science 262(5142): 2057-2059.

Haber, D. A., H. T. Timmers, et al. (1992). "A dominant mutation in the Wilms tumor gene WT1 cooperates with the viral oncogene E1A in transformation of primary kidney cells." Proc Natl Acad Sci U S A 89(13): 6010-6014.

Hammes, A., J. K. Guo, et al. (2001). "Two splice variants of the Wilms' tumor 1 gene have distinct functions during sex determination and nephron formation." Cell 106(3): 319-329.

Harborth, J., S. M. Elbashir, et al. (2001). "Identification of essential genes in cultured mammalian cells using small interfering RNAs." J Cell Sci 114(Pt 24): 4557-4565.

Hashimoto, Y., R. Myojin, et al. (2009). "The bHLH transcription factor Hand2 regulates the expression of nanog in ANS differentiation." Biochemical and biophysical research communications 390(2): 223-229.

Hastie, N. D. (1994). "The genetics of Wilms' tumor--a case of disrupted development." Annu Rev Genet 28: 523-558.

Hastie, N. D. (2001). "Life, sex, and WT1 isoforms--three amino acids can make all the difference." Cell 106(4): 391-394.

Hay, E. D. (1995). "An overview of epithelio-mesenchymal transformation." Acta Anat (Basel) 154(1): 8-20.

Hayashi, S. and A. P. McMahon (2002). "Efficient recombination in diverse tissues by a tamoxifen-inducible form of Cre: a tool for temporally regulated gene activation/inactivation in the mouse." Dev Biol 244(2): 305-318.

Heanue, T. A. and V. Pachnis (2006). "Expression profiling the developing mammalian enteric nervous system identifies marker and candidate Hirschsprung disease genes." Proc Natl Acad Sci U S A 103(18): 6919-6924.

Heanue, T. A. and V. Pachnis (2007). "Enteric nervous system development and Hirschsprung's disease: advances in genetic and stem cell studies." Nat Rev Neurosci 8(6): 466-479.

Hearn, C. J., M. Murphy, et al. (1998). "GDNF and ET-3 differentially modulate the numbers of avian enteric neural crest cells and enteric neurons in vitro." Dev Biol 197(1): 93-105.

Herbarth, B., V. Pingault, et al. (1998). "Mutation of the Sry-related Sox10 gene in Dominant megacolon, a mouse model for human Hirschsprung disease." Proc Natl Acad Sci U S A 95(9): 5161-5165.

Hoess, R. H., M. Ziese, et al. (1982). "P1 site-specific recombination: nucleotide sequence of the recombining sites." Proc Natl Acad Sci U S A 79(11): 3398-3402.

Hohenstein, P. and N. D. Hastie (2006). "The many facets of the Wilms' tumour gene, WT1." Hum Mol Genet 15 Spec No 2: R196-201.

Hong, C. S. and J. P. Saint-Jeannet (2005). "Sox proteins and neural crest development." Semin Cell Dev Biol 16(6): 694-703.
Hong, C. S. and J. P. Saint-Jeannet (2005). "Sox proteins and neural crest development." Seminars in cell & developmental biology 16(6): 694-703.
Hosoda, K., R. E. Hammer, et al. (1994). "Targeted and natural (piebald-lethal) mutations of endothelin-B receptor gene produce megacolon associated with spotted coat color in mice." Cell 79(7): 1267-1276.
Hugo, H., M. L. Ackland, et al. (2007). "Epithelial--mesenchymal and mesenchymal--epithelial transitions in carcinoma progression." J Cell Physiol 213(2): 374-383.
Ito, K. and T. Takeuchi (1984). "The differentiation in vitro of the neural crest cells of the mouse embryo." J Embryol Exp Morphol 84: 49-62.
Jaenisch, R. (1985). "Mammalian neural crest cells participate in normal embryonic development on microinjection into post-implantation mouse embryos." Nature 318(6042): 181-183.
Jessen, K. R. and R. Mirsky (2005). "The origin and development of glial cells in peripheral nerves." Nat Rev Neurosci 6(9): 671-682.
Jomgeow, T., Y. Oji, et al. (2006). "Wilms' tumor gene WT1 17AA(-)/KTS(-) isoform induces morphological changes and promotes cell migration and invasion in vitro." Cancer Sci 97(4): 259-270.
Kalcheim, C. and T. Burstyn-Cohen (2005). "Early stages of neural crest ontogeny: formation and regulation of cell delamination." Int J Dev Biol 49(2-3): 105-116.
Kanai, Y., R. Hiramatsu, et al. (2005). "From SRY to SOX9: mammalian testis differentiation." J Biochem 138(1): 13-19.
Kapur, R. P. (1999). "Early death of neural crest cells is responsible for total enteric aganglionosis in Sox10(Dom)/Sox10(Dom) mouse embryos." Pediatr Dev Pathol 2(6): 559-569.
Kapur, R. P. (2000). "Colonization of the murine hindgut by sacral crest-derived neural precursors: experimental support for an evolutionarily conserved model." Dev Biol 227(1): 146-155.
Kapur, R. P., C. Yost, et al. (1992). "A transgenic model for studying development of the enteric nervous system in normal and aganglionic mice." Development 116(1): 167-175.
Kaufmann, M. (1992). The atlas of mouse development, Elsevier
Kawaguchi, A., T. Miyata, et al. (2001). "Nestin-EGFP transgenic mice: visualization of the self-renewal and multipotency of CNS stem cells." Molecular and cellular neurosciences 17(2): 259-273.
Kent, J., S. C. Wheatley, et al. (1996). "A male-specific role for SOX9 in vertebrate sex determination." Development 122(9): 2813-2822.
Kirby, M. L., T. F. Gale, et al. (1983). "Neural crest cells contribute to normal aorticopulmonary septation." Science 220(4601): 1059-1061.
Kirby, M. L., K. L. Turnage, 3rd, et al. (1985). "Characterization of conotruncal malformations following ablation of "cardiac" neural crest." Anat Rec 213(1): 87-93.
Kirby, M. L. and K. L. Waldo (1995). "Neural crest and cardiovascular patterning." Circ Res 77(2): 211-215.
Kist, R., H. Schrewe, et al. (2002). "Conditional inactivation of Sox9: a mouse model for campomelic dysplasia." Genesis 32(2): 121-123.

Knudson, A. G., Jr. (1971). "Mutation and cancer: statistical study of retinoblastoma." Proc Natl Acad Sci U S A 68(4): 820-823.
Knudson, A. G., Jr. and L. C. Strong (1972). "Mutation and cancer: a model for Wilms' tumor of the kidney." J Natl Cancer Inst 48(2): 313-324.
Kobayashi, A., H. Chang, et al. (2005). "Sox9 in testis determination." Ann N Y Acad Sci 1061: 9-17.
Koesters, R., M. Linnebacher, et al. (2004). "WT1 is a tumor-associated antigen in colon cancer that can be recognized by in vitro stimulated cytotoxic T cells." Int J Cancer 109(3): 385-392.
Koopman, P., J. Gubbay, et al. (1991). "Male development of chromosomally female mice transgenic for Sry." Nature 351(6322): 117-121.
Kreidberg, J. A., H. Sariola, et al. (1993). "WT-1 is required for early kidney development." Cell 74(4): 679-691.
Kruger, G. M., J. T. Mosher, et al. (2002). "Neural crest stem cells persist in the adult gut but undergo changes in self-renewal, neuronal subtype potential, and factor responsiveness." Neuron 35(4): 657-669.
Kulesa, P. M. and L. S. Gammill (2010). "Neural crest migration: patterns, phases and signals." Developmental biology 344(2): 566-568.
Kuo, B. R. and C. A. Erickson (2010). "Regional differences in neural crest morphogenesis." Cell Adh Migr 4(4): 567-585.
Kuratani, S. C. and M. L. Kirby (1991). "Initial migration and distribution of the cardiac neural crest in the avian embryo: an introduction to the concept of the circumpharyngeal crest." Am J Anat 191(3): 215-227.
Le Douarin, N. M. (2004). "The avian embryo as a model to study the development of the neural crest: a long and still ongoing story." Mech Dev 121(9): 1089-1102.
Le Douarin, N. M. and M. A. Teillet (1973). "The migration of neural crest cells to the wall of the digestive tract in avian embryo." J Embryol Exp Morphol 30(1): 31-48.
Le Lievre, C. S. and N. M. Le Douarin (1975). "Mesenchymal derivatives of the neural crest: analysis of chimaeric quail and chick embryos." J Embryol Exp Morphol 34(1): 125-154.
Levanti, M. B., I. Esteban, et al. (2009). "Enteric glial cells express full-length TrkB and depend on TrkB expression for normal development." Neuroscience letters 454(1): 16-21.
Levy, E. M. (1980). "The ability of horse serum to support an in vitro antibody response." J Immunol Methods 36(2): 181-183.
Li, Z., M. G. Caron, et al. (2010). "Dependence of serotonergic and other nonadrenergic enteric neurons on norepinephrine transporter expression." The Journal of neuroscience : the official journal of the Society for Neuroscience 30(49): 16730-16740.
Lo, L., F. Guillemot, et al. (1994). "MASH-1: a marker and a mutation for mammalian neural crest development." Perspect Dev Neurobiol 2(2): 191-201.
Loeb, D. M., E. Evron, et al. (2001). "Wilms' tumor suppressor gene (WT1) is expressed in primary breast tumors despite tumor-specific promoter methylation." Cancer Res 61(3): 921-925.
Lucini, C., B. Facello, et al. (2010). "Distribution of glial cell line-derived neurotrophic factor receptor alpha-1 in the brain of adult zebrafish." Journal of anatomy 217(2): 174-185.

Lui, V. C., W. W. Cheng, et al. (2008). "Perturbation of hoxb5 signaling in vagal neural crests down-regulates ret leading to intestinal hypoganglionosis in mice." Gastroenterology 134(4): 1104-1115.
Martinez-Estrada, O. M., L. A. Lettice, et al. (2010). "Wt1 is required for cardiovascular progenitor cell formation through transcriptional control of Snail and E-cadherin." Nat Genet 42(1): 89-93.
Masu, Y., E. Wolf, et al. (1993). "Disruption of the CNTF gene results in motor neuron degeneration." Nature 365(6441): 27-32.
Matsunaga, E. (1981). "Genetics of Wilms' tumor." Hum Genet 57(3): 231-246.
Mikawa, T. and R. G. Gourdie (1996). "Pericardial mesoderm generates a population of coronary smooth muscle cells migrating into the heart along with ingrowth of the epicardial organ." Dev Biol 174(2): 221-232.
Moore, A. W., L. McInnes, et al. (1999). "YAC complementation shows a requirement for Wt1 in the development of epicardium, adrenal gland and throughout nephrogenesis." Development 126(9): 1845-1857.
Moore, A. W., A. Schedl, et al. (1998). "YAC transgenic analysis reveals Wilms' tumour 1 gene activity in the proliferating coelomic epithelium, developing diaphragm and limb." Mech Dev 79(1-2): 169-184.
Moore, M. W., R. D. Klein, et al. (1996). "Renal and neuronal abnormalities in mice lacking GDNF." Nature 382(6586): 76-79.
Morris, J. F., S. L. Madden, et al. (1991). "Characterization of the zinc finger protein encoded by the WT1 Wilms' tumor locus." Oncogene 6(12): 2339-2348.
Murray, S. A. and T. Gridley (2006). "Snail1 gene function during early embryo patterning in mice." Cell Cycle 5(22): 2566-2570.
Mutsaers, S. E. (2002). "Mesothelial cells: their structure, function and role in serosal repair." Respirology 7(3): 171-191.
Mutsaers, S. E. (2004). "The mesothelial cell." Int J Biochem Cell Biol 36(1): 9-16.
Nachtigal, M. W., Y. Hirokawa, et al. (1998). "Wilms' tumor 1 and Dax-1 modulate the orphan nuclear receptor SF-1 in sex-specific gene expression." Cell 93(3): 445-454.
Nelms, B. L., E. R. Pfaltzgraff, et al. (2011). "Functional interaction between Foxd3 and Pax3 in cardiac neural crest development." Genesis 49(1): 10-23.
Nieto, M. A., M. G. Sargent, et al. (1994). "Control of cell behavior during vertebrate development by Slug, a zinc finger gene." Science 264(5160): 835-839.
Niksic, M., J. Slight, et al. (2004). "The Wilms' tumour protein (WT1) shuttles between nucleus and cytoplasm and is present in functional polysomes." Hum Mol Genet 13(4): 463-471.
Nishida, S., N. Hosen, et al. (2006). "AML1-ETO rapidly induces acute myeloblastic leukemia in cooperation with the Wilms tumor gene, WT1." Blood 107(8): 3303-3312.
Okamura, Y. and Y. Saga (2008). "Notch signaling is required for the maintenance of enteric neural crest progenitors." Development 135(21): 3555-3565.
Park, S., M. Schalling, et al. (1993). "The Wilms tumour gene WT1 is expressed in murine mesoderm-derived tissues and mutated in a human mesothelioma." Nat Genet 4(4): 415-420.

Pattyn, A., X. Morin, et al. (1999). "The homeobox gene Phox2b is essential for the development of autonomic neural crest derivatives." Nature 399(6734): 366-370.

Pelletier, J., M. Schalling, et al. (1991). "Expression of the Wilms' tumor gene WT1 in the murine urogenital system." Genes Dev 5(8): 1345-1356.

Pomeranz, H. D. and M. D. Gershon (1990). "Colonization of the avian hindgut by cells derived from the sacral neural crest." Dev Biol 137(2): 378-394.

Pritchard-Jones, K., S. Fleming, et al. (1990). "The candidate Wilms' tumour gene is involved in genitourinary development." Nature 346(6280): 194-197.

Puig, I., D. Champeval, et al. (2009). "Deletion of Pten in the mouse enteric nervous system induces ganglioneuromatosis and mimics intestinal pseudoobstruction." The Journal of clinical investigation 119(12): 3586-3596.

Que, J., B. Wilm, et al. (2008). "Mesothelium contributes to vascular smooth muscle and mesenchyme during lung development." Proc Natl Acad Sci U S A 105(43): 16626-16630.

Rajewsky, K., H. Gu, et al. (1996). "Conditional gene targeting." J Clin Invest 98(3): 600-603.

Rauscher, F. J., 3rd (1993). "The WT1 Wilms tumor gene product: a developmentally regulated transcription factor in the kidney that functions as a tumor suppressor." FASEB J 7(10): 896-903.

Rauscher, F. J., 3rd, J. F. Morris, et al. (1990). "Binding of the Wilms' tumor locus zinc finger protein to the EGR-1 consensus sequence." Science 250(4985): 1259-1262.

Rhee, K. D. and X. J. Yang (2010). "Function and Mechanism of CNTF/LIF Signaling in Retinogenesis." Advances in experimental medicine and biology 664: 647-654.

Riccardi, V. M., E. Sujansky, et al. (1978). "Chromosomal imbalance in the Aniridia-Wilms' tumor association: 11p interstitial deletion." Pediatrics 61(4): 604-610.

Rivera, M. N. and D. A. Haber (2005). "Wilms' tumour: connecting tumorigenesis and organ development in the kidney." Nat Rev Cancer 5(9): 699-712.

Rupp, P. A. and P. M. Kulesa (2007). "A role for RhoA in the two-phase migratory pattern of post-otic neural crest cells." Dev Biol 311(1): 159-171.

Sakai, D. and Y. Wakamatsu (2005). "Regulatory mechanisms for neural crest formation." Cells Tissues Organs 179(1-2): 24-35.

Sauka-Spengler, T. and M. Bronner-Fraser (2008). "A gene regulatory network orchestrates neural crest formation." Nat Rev Mol Cell Biol 9(7): 557-568.

Schedl, A., Z. Larin, et al. (1993). "A method for the generation of YAC transgenic mice by pronuclear microinjection." Nucleic Acids Res 21(20): 4783-4787.

Schepers, G. E., R. D. Teasdale, et al. (2002). "Twenty pairs of sox: extent, homology, and nomenclature of the mouse and human sox transcription factor gene families." Dev Cell 3(2): 167-170.

Schiltz, C. A., J. Benjamin, et al. (1999). "Expression of the GDNF receptors ret and GFRalpha1 in the developing avian enteric nervous system." J Comp Neurol 414(2): 193-211.

Schuchardt, A., V. D'Agati, et al. (1994). "Defects in the kidney and enteric nervous system of mice lacking the tyrosine kinase receptor Ret." Nature 367(6461): 380-383.

Shum, A. S. and A. J. Copp (1996). "Regional differences in morphogenesis of the neuroepithelium suggest multiple mechanisms of spinal neurulation in the mouse." Anat Embryol (Berl) 194(1): 65-73.

Sinclair, A. H., P. Berta, et al. (1990). "A gene from the human sex-determining region encodes a protein with homology to a conserved DNA-binding motif." Nature 346(6281): 240-244.

Sommer, L. (2011). "Generation of melanocytes from neural crest cells." Pigment cell & melanoma research.

Soriano, P. (1999). "Generalized lacZ expression with the ROSA26 Cre reporter strain." Nat Genet 21(1): 70-71.

Southard-Smith, E. M., L. Kos, et al. (1998). "Sox10 mutation disrupts neural crest development in Dom Hirschsprung mouse model." Nat Genet 18(1): 60-64.

Stanchina, L., V. Baral, et al. (2006). "Interactions between Sox10, Edn3 and Ednrb during enteric nervous system and melanocyte development." Dev Biol 295(1): 232-249.

Stemple, D. L. and D. J. Anderson (1992). "Isolation of a stem cell for neurons and glia from the mammalian neural crest." Cell 71(6): 973-985.

Sugiyama, H. (2005). "Cancer immunotherapy targeting Wilms' tumor gene WT1 product." Expert Rev Vaccines 4(4): 503-512.

Svedberg, H., K. Chylicki, et al. (1998). "Constitutive expression of the Wilms' tumor gene (WT1) in the leukemic cell line U937 blocks parts of the differentiation program." Oncogene 16(7): 925-932.

Taraviras, S., C. V. Marcos-Gutierrez, et al. (1999). "Signalling by the RET receptor tyrosine kinase and its role in the development of the mammalian enteric nervous system." Development 126(12): 2785-2797.

Tatsumi, N., Y. Oji, et al. (2008). "Wilms' tumor gene WT1-shRNA as a potent apoptosis-inducing agent for solid tumors." Int J Oncol 32(3): 701-711.

Teng, L., N. A. Mundell, et al. (2008). "Requirement for Foxd3 in the maintenance of neural crest progenitors." Development 135(9): 1615-1624.

Vainio, S. and Y. Lin (2002). "Coordinating early kidney development: lessons from gene targeting." Nat Rev Genet 3(7): 533-543.

Vitalis, T., C. Alvarez, et al. (2003). "Developmental expression pattern of monoamine oxidases in sensory organs and neural crest derivatives." The Journal of comparative neurology 464(3): 392-403.

Vize, P. D., A. S. Woolf, et al. (2003). The Kidney: From normal development to congenital disease, Academic press Inc.

Wagner, T., J. Wirth, et al. (1994). "Autosomal sex reversal and campomelic dysplasia are caused by mutations in and around the SRY-related gene SOX9." Cell 79(6): 1111-1120.

Wegner, M. (1999). "From head to toes: the multiple facets of Sox proteins." Nucleic Acids Res 27(6): 1409-1420.

Whitehouse, F. R. and J. W. Kernohan (1948). "Myenteric plexus in congenital megacolon; study of 11 cases." Arch Intern Med (Chic) 82(1): 75-111.

Wiese, C., A. Rolletschek, et al. (2004). "Nestin expression--a property of multi-lineage progenitor cells?" Cellular and molecular life sciences : CMLS 61(19-20): 2510-2522.

Wilm, B., A. Ipenberg, et al. (2005). "The serosal mesothelium is a major source of smooth muscle cells of the gut vasculature." Development 132(23): 5317-5328.

Winnik, S., M. Klinkert, et al. (2009). "HoxB5 induces endothelial sprouting in vitro and modifies intussusceptive angiogenesis in vivo involving angiopoietin-2." Cardiovascular research 83(3): 558-565.

Wong, C. E., C. Paratore, et al. (2006). "Neural crest-derived cells with stem cell features can be traced back to multiple lineages in the adult skin." J Cell Biol 175(6): 1005-1015.

Wu, Y., M. Moser, et al. (2003). "HoxB5 is an upstream transcriptional switch for differentiation of the vascular endothelium from precursor cells." Molecular and cellular biology 23(16): 5680-5691.

Yntema, C. L. and W. S. Hammond (1954). "The origin of intrinsic ganglia of trunk viscera from vagal neural crest in the chick embryo." J Comp Neurol 101(2): 515-541.

Young, H. M., A. J. Bergner, et al. (2004). "Dynamics of neural crest-derived cell migration in the embryonic mouse gut." Dev Biol 270(2): 455-473.

Young, H. M., K. N. Cane, et al. (2010). "Development of the autonomic nervous system: A comparative view." Auton Neurosci.

Young, H. M., D. Ciampoli, et al. (1999). "Expression of Ret-, p75(NTR)-, Phox2a-, Phox2b-, and tyrosine hydroxylase-immunoreactivity by undifferentiated neural crest-derived cells and different classes of enteric neurons in the embryonic mouse gut." Dev Dyn 216(2): 137-152.

Young, H. M., C. J. Hearn, et al. (1998). "A single rostrocaudal colonization of the rodent intestine by enteric neuron precursors is revealed by the expression of Phox2b, Ret, and p75 and by explants grown under the kidney capsule or in organ culture." Dev Biol 202(1): 67-84.

Young, H. M., C. J. Hearn, et al. (2000). "Embryology and development of the enteric nervous system." Gut 47 Suppl 4: iv12-14; discussion iv26.

Young, H. M. and D. Newgreen (2001). "Enteric neural crest-derived cells: origin, identification, migration, and differentiation." Anat Rec 262(1): 1-15.